Alma Mater Studiorum – Università di Bologna

DOTTORATO DI RICERCA IN

Scienze farmacologiche e tossicologiche, dello sviluppo e del movimento umano

Ciclo XXVI

Settore Concorsuale di afferenza: 05/G1

Settore Scientifico disciplinare: BIO14

STUDY OF NOVEL NATURAL COMPOUNDS AS POTENTIAL DRUGS IN THE TREATMENT OF ACUTE LEUKEMIAS

Presentata da: **Dott. Lorenzo Ferruzzi**

Coordinatore Dottorato

Chiar.mo Prof.
Giorgio Cantelli-Forti

Relatore

Chiar.ma Prof.ssa
Carmela Fimognari

Esame finale anno 2014

INDEX

Abstract

Introduction: Cancer is the second leading cause of death in the USA after heart diseases in both man and woman. Among all cancer types leukemia represents the leading cause of cancer death in man younger than 40 years. Single-target drug therapy has generally been highly ineffective in treating complex diseases such as cancer, endowed with the deregulation of multiple, redundant and aberrant signaling pathways. Based on the complexity that characterizes cancer, a growing interest has been directed toward multi-target drugs able to hit multiple targets. In the context of multi-target strategy, plant products, based on their intrinsic complexity, could represent an interesting and promising approach. Aim of the research followed during my PhD was to indentify and study novel natural compounds for the treatment of acute leukemias. Two potential multi-target drugs were identified in *Hemidesmus indicus* and piperlongumine.

Materials and Methods: The decoction of *Hemidesmus indicus* was characterized by HPLC to quantify its main phytomarkers. The study was conducted on different cell types. Induction of apoptosis, cell-cycle analysis, levels of specific proteins involved in the regulation of apoptosis, cell-cycle progression, angiogenesis and membrane differentiation markers were evaluated by flow cytometry. The mRNA levels of some proteins involved in the anti-leukemic activity of *Hemidesmus* were evaluated using TaqMan realtime PCR. The analysis of cell differentiation by nitroblue tetrazolium (NBT) reducing activity, adherence to the plastic substrate, α-napthyl acetate esterase activity and morphological analysis were performed through light microscopy (LM) and transmission electron microscopy (TEM). The effects of *Hemidesmus* on angiogenesis were studied in normoxic and hypoxic conditions through the use of an *in vitro* assay and LM. The capacity of *Hemidesmus* and piperlongumine to selectively kill leukemic stem cells (LSCs) was tested on the CD34+ cell fraction sorted from acute myeloid leukemia (AML) patient samples and on their healthy counterpart.

Results: We have demonstrated that *Hemidesmus* modulates many components of intracellular signaling pathways involved in cell viability and proliferation and alters gene and protein expression, eventually leading to tumor cell death, mediated by a loss of mitochondrial transmembrane potential, inhibition of Mcl-1, increase in Bax/Bcl-2 ratio, and ROS formation. *Hemidesmus* induced a significant $[Ca^{2+}]_i$ raise through the mobilization of intracellular Ca^{2+} stores and significantly enhanced the antitumor activity of three commonly used chemotherapeutic drugs (methotrexate, 6-thioguanine, cytarabine). Moreover, the decoction caused differentiation of HL-60 cells as shown by NBT reducing activity, adherence to the plastic substrate, α-naphtyl acetate

esterase activity, and increasing expression of CD14 and CD15. The morphological analysis by LM and TEM clearly showed the presence of granulocytes and macrophages after *Hemidesmus indicus* treatment. Furthermore, we showed that *Hemidesmus* regulates angiogenesis of HUVECs in hypoxia and normoxia, by the inhibition of new vessel formation and the processes of migration/invasion. It is indeed able to inhibit key proteins and genes involved in neoangiogenesis such as HIF-1α, VEGF, and VEGFR-2. Clinically relevant observations are that its cytotoxic activity was also recorded in primary cells from AML patients. Moreover, both *Hemidesmus* and piperlongumine showed a selective action toward LSC.

Conclusions: Our results identified the molecular basis of the anti-leukemic effects of *Hemidesmus indicus* and indentify the mitochondrial pathways, $[Ca^{2+}]_i$, cytodifferentiation and angiogenesis inhibition as crucial actors in its anticancer activity. The ability to hit selectively LSC exerted by *Hemidesmus* and piperlongumine enriched the knowledge of their anti-leukemic activity. On these bases, we conclude that *Hemidesmus* and piperlongumine can represent a valuable strategy in the anticancer pharmacology.

Abbreviations

2H4MBAC	2-hydroxy 4-methoxybenzoic acid
2H4MBAL	2-hydroxy 4- methoxybenzaldehyde
3H4MBAL	3-hydroxy 4- methoxybenzaldehyde
7-AAD	7-amino-actinomycin D
ALL	acute lymphoblastic leukemia
AML	acute myeloblastic leukemia
APL	acute promyelocytic leukemia
BA	bongkrekic acid
BFU-E	burst forming unit erythroid
BM	bone marrow
CATR	carboxyatractyloside
CFU	colony-forming unit
CFU	colony-forming unit
CFU-GEMM	colony forming units of granulocytes, erythrocytes, macrophages and megakaryocytes progenitor
CFU-GM	colony forming units of granulocyte-macrophage progenitor
CI	combination index
CLP	committed lymphoid progenitor
CMEP	common myeloid–erythroid progenitor
CMLP	common myelo–lymphoid progenitor
CMP	committed myeloid progenitor
CNS	central nervous system
CR	complete remission
CSC	cancer stem cell
Cyc A	ocyclosporine A
DEVD	aspartic acid-glutamic acid-valineaspartic acid
DHF	dichlorofluorescein
DMSO	dimethyl sulfoxide
ECM	extracellular matrix
EHS	Engelbreth Holm-Swarm
E-MK	erythroid and megakaryocyte
ETP	earliest thymic progenitors
FAM	6-carboxyfluorescein
FBS	fetal bovine serum
FDA	Food and Drug Administration
FITC	fluorescein isothiocyanate
FMK	fluoromethylketone
GMP	granulocytic myeloid progenitor
H_2DCFDA	2′,7′-dichlorofluorescin diacetate
HIF	hypoxia-inducible factor
HPLC	high-throughput liquid chromatography
HSC	hematopoietic stem cell
HUVEC	human umbilical vein endothelial cell
IND	investigational new drug
JC-1	5,59,6,69- tetrachloro-1,19,3,39-tetraethylbenzimidazol-carbocyanine iodide
LETD	leucine-glutamic acid-threonine-aspartic acid
LMPP	lymphoid-primed multipotent progenitors
LSC	leukemic stem cell
MEP	megakaryocytic/erythroid progenitor

MPP	multipotent progenitors
NAC	N-acetyl-L-cysteine
NAE	α-naphthyl acetate
NBT	nitroblue tetrazolium
NOD/SCID	non-obese diabetic/severe combined immunodeficiency
PB	peripheral blood
PBS	phosphate buffer saline
PCR	polymerase chain reaction
PE	phycoerythrin
Pgp	glycoprotein P
Q	quencher
qRT-PCR	quantitative real time PCR
R	reporter
RIN	RNA integrity number
ROS	reactive oxygen species
RPMI	Roswell Park Memorial Institute
SCF	stem cell factor
TPA	12-O–tetradecanoylphorbol 13-acetate
VEGF	vascular endothelial growth factor

Chapter 1

Introduction

Cancer is the second leading cause of death in the USA after heart diseases in both man and woman. It is estimated that 1.6 million of new cases of cancer will be diagnosed in the United States in 2014, with a number of death estimated in 585,720. Among all cancer types, leukemia represents the leading cause of cancer death in man younger than 40 years. Moreover, it accounts for almost one-third of all cancers diagnosed in children aged 0 to 14 years. The amount of estimated death correlated to leukemia for 2014 in the USA is 24,090[1].

Leukemia is a cancer concerning the hematopoietic system and in particular blood and bone marrow (BM). It is characterized by an abnormal proliferation of immature white blood cells called "blasts". Leukemias are classified either acute or chronic and, according to the type of blood cell affected, as either myelogenous or lymphocytic. Acute leukemia is characterized by a rapid proliferation of hematopoietic progenitor cells, which lose the ability to differentiate normally leading to an accumulation of cells at various stage of incomplete maturation and to a reduction in the production of healthy hematopoietic elements[2]. Chronic leukemia is characterized by a dysfunctional production of relatively mature, but abnormal, white blood cells. The progression of the pathology is slow and can takes months or years. The combination between these characteristics is used to define the four main categories of leukemia: acute myelogenous, acute lymphocytic, chronic myelogenous, and chronic lymphocytic leukemia[3].

It is not possible to indentify one single cause that leads to the development of leukemia, but most likely different leukemias have different causes. For most cases, the cause of leukemia is unknown. It is now clear that leukemia is a complex disease derived from multiple DNA mutations that lead to the activation of oncogenes or the deactivation of tumor suppressor genes. Many chemical substances such as solvents, alkylating chemotherapy agents, ionizing radiation or virus such as the human T-lymphotropic virus, represent, nowadays few known causes of leukemia's development[3].

Leukemia is usually diagnosed trough the complete blood count and the examination after a complete evaluation of the patient's clinical picture. A physical examination often reveals a swollen spleen and liver[3].

1.1 Hematopoiesis

Despite the complexity that characterizes the blood, it is probably the best understood human system. Blood is a highly regenerative tissue, with approximately one trillion (10^{12}) cells arising daily in adult human BM from a hematopoietic stem cell (HSC). Nowadays, there are two models that describe the complexity of the blood organization: the classical model and the myeloid-based model[4] (Fig. 1).

The classical model of hematopoiesis

The classical model classifies blood cells in two fundamental branches: lymphoid and myeloid. In the lymphoid category are included T, B, and natural killer cells, which carry out adaptive and innate immune responses. Otherwise, myeloid branch consists of a number of distinct, fully differentiated, short-lived cell types including granulocytes (neutrophils, eosinophils, mast cells, and basophils), monocytes, erythrocytes, and megakaryocytes. At the apex of hematopoietic hierarchy are placed the multipotent HSCs and their connection to mature cells is determined by a complex roadmap of specific lineage relationships between stem cells, progenitors, and mature cells[4].

The isolation of committed mouse progenitors of the myeloid (CMP) and lymphoid (CLP) lineages led to the formulation of the first comprehensive classical model of hematopoiesis[5-7]. The first principle of this model is that loss of self-renewal ability during differentiation precedes lineage commitment. This was deduced from the existence of multipotent progenitors (MPPs) that remain multipotent, but possess only transient repopulation ability[8, 9]. Another key postulate of the classical model is that the earliest commitment decision (downstream of MPPs) segregates lymphoid and myeloid lineages, inferred from the existence of CLPs and CMPs. Lastly, the classical model predicts that lineage decisions occur through several bifurcations. The first myelo-lymphoid split originates CMPs and CLPs and each of these undergo further commitment steps. CMPs give rise to granulocytic myeloid progenitors (GMPs), which become committed to the granulocyte-monocyte fate, and megakaryocytic/erythroid progenitors (MEPs), which only produce erythroid and megakaryocyte (E-MK) cells. On the lymphoid side, CLPs give rise to B cell precursors and the earliest thymic progenitors (ETPs) committed to the T and NK lineages. The classical model represents a simple yet powerful template for understanding hematopoiesis[4].

The myeloid-based model of hematopoiesis

The myeloid-based model of hematopoiesis postulates that the HSC first bifurcation is into a common myeloid–erythroid progenitor (CMEP) and a common myelo–lymphoid progenitor (CMLP); this model does not contemplate the presence of CLP[10-12]. CMLPs generate T and B cell progenitors through a bipotential myeloid–T progenitor and a myeloid–B progenitor stage, respectively. In this model, instead of splitting early in differentiation, lymphoid and myeloid fates remain coupled[13]. One postulate of this model is the existence of progenitors with myelo-lymphoid, but not E-MK, potential. This was confirmed with the isolation of lymphoid-primed multipotent progenitors (LMPPs) from adult mouse marrow[14]. A key principle of this model, supported by the balance of available evidence, is that lymphoid specification is not a single lineage bifurcation, but a gradual and possibly parallel process with many intermediate states. By contrast, myeloid development more closely adheres to the classical model[15, 16].

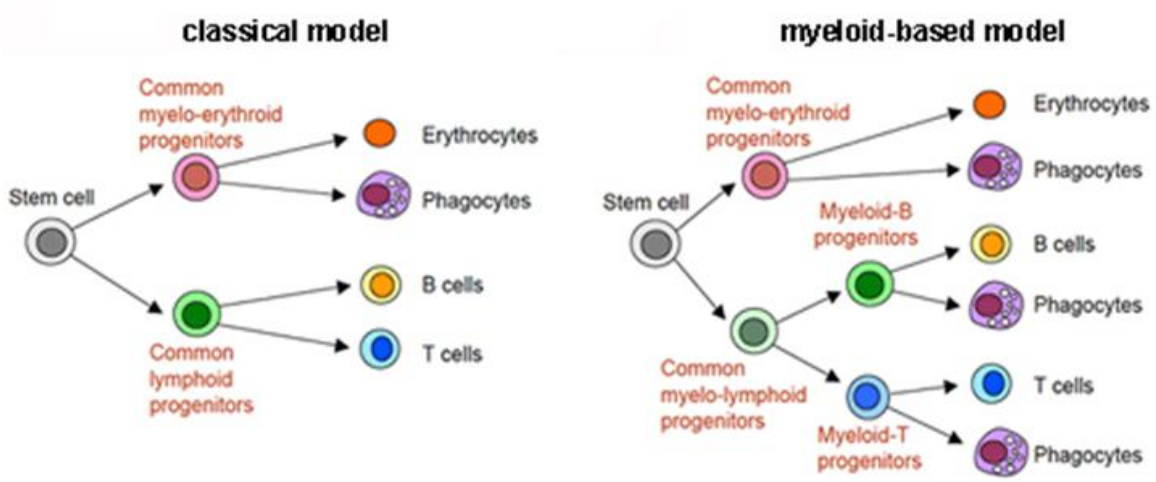

Figure 1: Current human hematopoiesis models.

Stem cell concept

Stem cells are highly undifferentiated cells characterized by self-renewal and differentiating capability. The regenerative potential is an essential property of stem cells that are present in different mammalian tissues[17]. Stem cells can generate either one or both daughter cells with the same stemness potential but uncommitted differentiation options (self-renewal division). On the other hand, they may generate progeny that exits the stem cell state to begin the stepwise process of differentiation into mature and specialized cells that usually lack in proliferative ability and intend to undergo in senescence (differentiation division). Regeneration requires conditions that favor self-renewal divisions, whereas homeostasis requires that the outcomes of self-renewal and differentiation divisions are balanced. Stem cells constitute a reservoir of cells with active

mechanisms for self-renewal. For these reasons, stem cells obviously represent candidates for accruing the events that can generate a fully malignant cell population, and are the basis of the original concept of cancer stem cells (CSCs)[18].

Normal hematopoietic stem cells

Hematopoiesis depend on the division of HSCs that are responsible for the formation of both new HSCs through self-renewal and differentiating progeny. Currently, non-obese diabetic/severe combined immunodeficiency (NOD/SCID) mice are used to assay human hematopoietic stem and progenitor cells[19]. Only those cells that are able to repopulate the hematopoietic system of these immunodeficient mice, as well as of secondary recipients, are thought to be HSCs. A common strategy adopted for the isolation of candidate repopulating cells consists first in the sorting of cell fractions according to the expression of some membrane antigens and then in the transplant of these sorted cells into NOD/SCID mice. According to several studies, the majority of normal HSCs are present among the CD34+/ CD38− cell fractions[20, 21]; some HSCs are also observed among CD34−/Lin− cells that possess a long-term repopulating ability[22, 23]; CD34+/CD38+ cell fractions contain some HSCs but endowed with short-term repopulating activity[24, 25].

According to their capability of repopulating hematopoiesis, the HSC pool can be subdivided into three groups: short-term HSCs, capable of generating clones of differentiating cells for only 4–6 weeks; intermediate-term HSCs, capable of sustaining a differentiating cell progeny for 6–8 months before becoming extinct; and long-term HSCs, capable of maintaining hematopoiesis indefinitely[26]. The classical model and the myeloid-based model of hematopoietic hierarchy imply that all mature cells of the peripheral blood (PB) are the progeny of a single long-term HSC. Recent studies of stem cell purification, based on canonical HSC markers in combination with Hoechst dye efflux, provided evidence about the existence of myeloid-biased HSCs and lymphoid-biased HSCs, differentially responding to TGF-β1: the first ones are triggered to proliferate; the last ones are inhibited in their proliferation. These observations are compatible with the view that the hematopoietic system is maintained by a continuum of HSC subtypes rather than a functional uniform stem cell pool[27]. According to their differentiation stage, HSCs and progenitors are localized in specific tissue microdomains termed “niches”. These specific microenvironments play a crucial role in controlling HSC fate and regulate whether these cells remain quiescent, cycle to self-renew and/or to differentiate, or undergo apoptosis. A particularly important role within the niche is exerted by some reticular cells responsible for the production of a chemokine, the stromal-derived factor 1 (fundamental for HSC homing), and a hematopoietic growth factor, the stem cell factor

(SCF) (essential for the survival of HSCs). Of note, stem cells present at the level of the BM niches possess not only the potentiality for hematopoietic differentiation but also an adipogenic and osteogenic differentiation potential. The maintenance of this adipogenic and osteogenic differentiation capacities is essential to maintain optimal microenvironmental conditions for HSC survival and maintenance in an undifferentiated state within the BM[28]. Within the HSC niche, the interaction between the receptors (i.e., cytokine receptors present on HSCs) and ligands (i.e., membrane-anchored receptors present on stromal cells) is essential for the maintenance of HSC survival, self-renewal, and differentiation and therefore essential for ensuring the homeostasis of the hematopoietic system. Studies carried out in recent years have led to the identification of some growth factors/cytokines that are essential for stem cell survival and/or self-renewal, such as SCF, thromboplastin, notch ligands, angiopoietin-1, angiopoietin-like proteins, and prostaglandin E2. In addition, recent studies have shown that pleiotrophin, a heparin-binding protein that is mitogenic for neurons, is a potent regulator for HSC expansion and regeneration both in mouse and man[29]. The ability of HSCs within the niche to self-renew and maintain multipotency depends on the balance of complex signals in their microenvironment. Among the various factors, low oxygen tension (hypoxia) plays a key role in maintaining undifferentiated states of HSCs[30]. Recent studies have in part clarified the role of hypoxia signaling at the level of the HSC compartment. The cellular responses to hypoxia are mediated by the hypoxia-inducible factors (HIFs) which regulate gene expression in a way that permits a cellular adaption to the hypoxic condition. It was shown that HIF-1α deficiency at the level of the HSC compartment causes an increased cell cycling rate and progressive loss of long-term repopulating activity[31]. Under steady-state conditions, the large majority of HSCs are quiescent, slowly cycling cell populations; however, in response to environmental cues, these cells are capable of intensive cycling activity, with dramatic expansion to ensure the proper homeostatic reconstitution of blood elements. The quiescence status of HSCs is considered as a very important protective mechanism, capable of reducing risks related to DNA replication and cellular oxidative metabolism[32]. HSCs possess an efficient cell-intrinsic mechanism to survive following exposure to DNA-damaging agents such as ionizing irradiation, characterized at the molecular level by the enhanced expression of pro-survival genes and strong p53 induction, which mediates, in turn, growth arrest and DNA repair; in contrast, the majority of myeloid-committed progenitors undergo apoptosis following genotoxic exposure[33]. However, intriguingly, the HSC quiescence is a double-edged sword since, on one hand, it protects HSCs against potential endogenous stresses but, on the other hand, it renders HSCs intrinsically vulnerable to mutagenesis following DNA damage[33].

1.2 Acute myeloid leukemia

Acute myeloid leukemia (AML) is a clonal disorder of HSCs characterized by the inhibition of differentiation and the subsequent accumulation of cells at various stages of incomplete maturation, and by reduced production of healthy hematopoietic elements. AML can occur in people of all ages, but is most common in older patients (older than 65 years). It can be caused by the exposure to ionizing radiations and drugs that damage DNA. Two types of chemotherapy-related AML exist. Drugs that target topoisomerase II, such as anthracyclines and epipodophyllotoxins, can cause patients to develop rapidly proliferative diseases, within 2 years of treatment[34]. More common is the so-called alkylator agent-induced disease occurring 5–6 years after exposure, characterized by a myelodysplastic prodrome with complex karyotypes and deletions in chromosomes 5 and 7[35]. *In vitro* and preclinical models have shown that the development of AML requires a multistep series of mutations. Leukemogenesis requires, at a least, activating mutations in class I genes that stimulate signal transduction pathways and induce cell to proliferate, in association with mutations in class II genes that affect transcription factors and compromise normal differentiation[36]. Mutations that lead to the activation of the receptor tyrosine kinase KIT, FLT3, and RAS signaling pathway belong to class I mutations. Examples of class II mutations are, *RUNX1/ETO*, *CBFB/MYH11*, and *PML/RARα*, which are fusion transcripts generated by recurring chromosomal abnormalities such as t(8;21), inv(16), and t(15;17), respectively[37].

AML is a biologically and clinically heterogeneous disease, characterized by distinct clinical presentations in different morphological and cytogenetic subtypes. Many mutations have been identified in patients with normal karyotypes (the majority of patients with AML) through molecular biology techniques (Tab. 1), and mutations in the *NPM1*[38] and *FLT3* genes are the most common and now routinely tested for. Although patients with *NPM1* mutations have an improved outcome with chemotherapy alone, mutations in *FLT3*, which lead to constitutive receptor activation, dysregulation of FLT3 signal transduction pathways, and stimulation of cell proliferation, are associated with a worse prognosis, with a larger negative effect if the mutations are homozygous[39-42]. If these two mutations are present in combination, *FLT3* mutations cancel out the better effects of *NPM1* and the outcome becomes poorer than when *NPM1* is mutated and *FLT3* is germline[43-45]. Several other mutations have been identified (Tab. 1); however, the prognostic effect of many of these findings is uncertain, with discrepant results reported by different groups.

	Approximate frequency in de-novo AML	Frequency in CN AML	Strong associations	Not recorded with	Outlook
NPM1	35%	50%	CN AML, *FLT3*-ITD, *FLT3*-TKD, *DNMT3A*, *IDH1*, *IDH2*	*CEBPA* double mutant	Favourable in patients with CN AML and in elderly patients
CEBPA	7%	8–19%	CN AML, *FLT3*-ITD	*NPM1*	Favourable in patients with CN AML (if biallelic)
FLT3-ITD	20–25%	30–35%	CN AML, APL, t(6;9), *NPM1*	--	Adverse in patients with CN AML; could vary with allelic burden; no clear effect in patients with APL
FLT3-TKD	5%	14%	CN AML, *NPM1*	--	Controversial
KIT	--	25%	Core binding factor leukaemias	Most other karyotypes	Adverse in adult patients with core binding factor leukaemias
TET2	8–12%	23%	Possibly CN AML	*IDH1*, *IDH2*	Controversial
DNMT3A	14–22%	20–33%	CN AML, *NPM1*, *FLT3*	Core binding factor leukaemias, *CEBPA*, *MLL* translocations	Possibly adverse in patients with CN AML
IDH1, *IDH2*	8–16%	30%	CN AML, *NPM1*, *FLT3*	*TET2*, *WT1*	Controversial
ASXL1	5–30%	About 10%	Uncommon with *NPM1* and *FLT3*	Possibly *CEBPA*	Adverse in patients with CN AML and older patients; more common in older patients

Table 1: Molecular markers in AML. Copyright Ferrara and Schiffer 2013.

Treatment of AML

AML is conventionally treated in two steps: an induction phase followed by a consolidation, which includes stem cell transplantation (Tab. 2). The aim of induction is to achieve a complete remission (CR), whereas consolidation is designed to eliminate residual leukemia cells that persist after induction. CR is reached when in the BM there is less than 5% of leukemic blasts compared to a normocellular BM, absence of extramedullary leukemia, neutrophil count greater than 1,000/µL, and a platelet count greater than 100,000/µL[46].

	Treatment	Comment
Induction	Daunorubicin (or idarubicin) plus cytarabine	3+7 regimen remains the standard treatment for adults of all ages; analyses of the possible benefit of the addition of gemtuzumab ozogamicin in AML subgroups, including young patients with CBF leukaemia and older* patients with intermediate karyotype are in progress
Consolidation	High-dose or intermediate-dose cytarabine	Intermediate or high dose cytarabine for patients who are candidates for stem-cell transplantation; high-dose cytarabine of most benefit for patients with CBF AML
Allogeneic stem-cell transplantation	Consider for patients with intermediate karyotype, except those with *NPM1* mutation in the absence of *FLT3* internal tandem duplication and in all patients with unfavourable karyotypes	Consider reduced intensity conditioning for selected older patients
Autologous stem-cell transplantation	Consider for patients with CBF AML and *NPM1* mutated/*FLT3* germline	Useful discipline for investigation of new conditioning regimens; no proven benefit compared with high-dose cytarabine in randomised trials; might be interesting to assess in patients without evidence of minimal residual disease.

3+7=anthracycline for 3 days with continuous infusion of cytarabine for 7 days. AML=acute myeloid leukaemia. CBF AML=core binding factor acute myeloid leukaemia.
*Older than 60 years of age.

Table 2: Treatments of AML. Copyright Ferrara and Schiffer 2013.

More than 30 years after its introduction[47], the combination of an anthracycline, usually daunorubicin given for 3 days, with continuous infusion of cytarabine for 7 days (3+7) is still the standard induction regimen (Fig. 2). CR rates of patients treated with the 3+7 regimen are about 70% in patients younger than 60 years. Numerous trials have been done to improve the rate and quality of CR, including the use of anthracyclines other than daunorubicin (eg, idarubicin hydrochloride and mitoxantrone)[48-50], the addition of a third drug (usually etoposide), the use of high-dose instead of conventional dose of cytarabine[51], the combination of anthracyclines with fludarabine phosphate [52] or cladribine[53], and the use of hematopoietic growth factors such as granulocyte colony-stimulating factor and granulocyte-macrophage colony-stimulating factor[54]. Overall, results have been disappointing, the alternative treatments tested for AML failed to show improvements in outcome. Many groups have shown that it is feasible to select specific induction treatment for patients according to molecular subtyping, which could become the standard for future clinical trials. So far, the only mutation that can be pharmacologically targeted is *FLT3*. Inhibitors such as midostaurin and lestaurtinib used in combination with the conventional chemotherapy are currently tested in newly diagnosed patients[55].

The achievement of CR regards only the first phase of treatment.Patients could eventually relapse[56] and thus consolidation treatment is essential (with the ultimate goal of cure) (Fig. 2). Number of cycles and optimum dose are not established, although three cycles of intermediate doses of cytarabine (1.5 g/m^2) reduce toxicity without worsening treatment outcome[57, 58], suggesting that this dose is reasonable for routine practice. Clinical trials and registry data strongly suggest that much lower relapse rates occur after allogeneic stem cell transplantation (stem cells obtained directly from the patient) than autologous stem cell transplantation (stem cells from a matched donor related

or unrelated with the patient) or chemotherapy, because of the graft-versus-leukemia effect. However, the main drawback that limits allogeneic stem cell transplantation is the significant treatment-related mortality of 10–25% because of graft-versus-host disease. Randomized trials have not shown a survival benefit from allogeneic stem cell transplantation compared with chemotherapy in the overall population of AML patients[59-61].

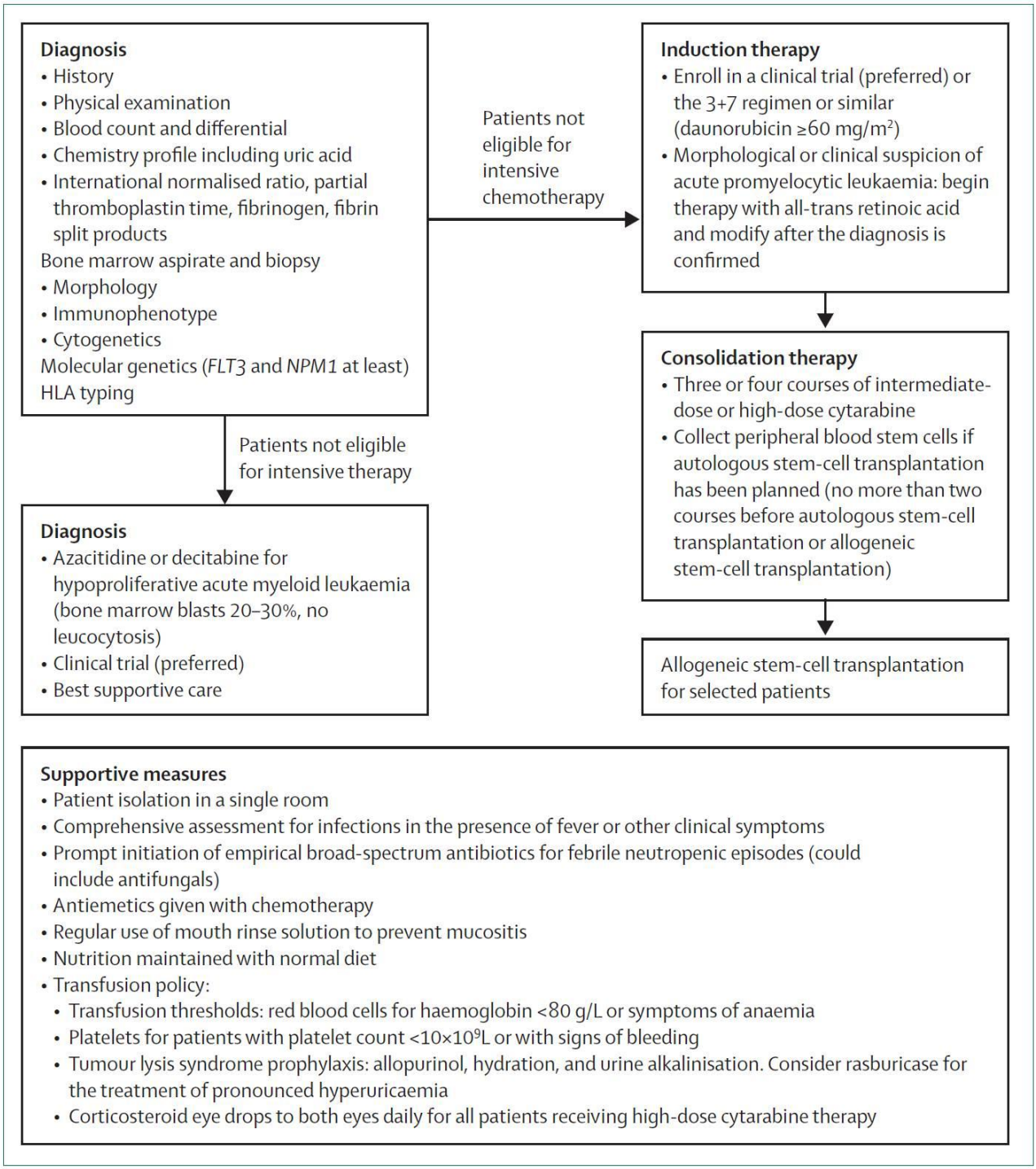

Figure 2: Practical approaches to management of AML. Copyright Ferrara and Schiffer 2013.

Acute promyelocytic leukemia

Acute promyelocytic leukemia (APL) is a distinct subtype of AML with a unique morphology characterized by hypergranulated promyelocytes and the presence of a t(15;17) translocation that results in an abnormal fusion protein termed PML/RARα. It is clinically characterized by a severe hemorrhagic diathesis. As AML, APL is sensitive to anthracyclines, and studies reported that the association between anthracyclines and all-trans retinoic acid represents the best induction approach, able to achieve CR rates of over 90% and, with various consolidation approaches, cure rates of roughly 80%[62]. All-trans retinoic acid was the first, and perhaps the only, example of remission induction caused by the overcome of the inability of leukemic cells to differentiate into functional mature cells. Arsenic trioxide is perhaps now the most effective single agent drug[63] and small trials without any chemotherapy, with combinations of all-trans retinoic acid and arsenic trioxide[64] or arsenic trioxide alone[65], have shown very promising results and are being assessed in large multicentre studies. The biggest challenge that remains now is to increase the diagnostic awareness about this highly curable disease, in order to reduce early mortality from hemorrhage by prompt initiation of all-trans retinoic acid treatment.

Leukemic stem cells (LSCs) in acute leukemias

The discovery that the large majority of AML blasts do not proliferate and only a minority of them (≈1%) is capable of forming colonies (colony-forming units, AML-CFU) when plated in a semisolid medium, brought to the discovery of LSCs in AMLs. Immunodeficient mice have been used to assay sorted fractions of AML cells. LSCs represent the leukemic counterpart of normal HSCs and are capable of inducing a leukemic graft when transplanted into immunodeficient mice. Initial studies have shown that the leukemia-initiating cells, as assayed in the NOD/SCID assay model, are detected only within the CD34+/CD38− fraction of the majority of AML samples[66-69]. However, some recent studies have shown that LSCs are present also in the CD34+/CD38+ fraction. In fact, it was shown that, in a significant proportion of AMLs, cells contained in the CD34+/CD38+ fraction are capable of initiating and maintaining the leukemic process when grafted in NOD/SCID mice[70]. These observations further reinforce the concept that the membrane phenotype of leukemia-initiating cells is heterogeneous in various AMLs. The extreme heterogeneity characteristic of leukemia cells in individual patients has many implications for the use and development of treatments that specifically affect the products of these gene mutations. The heterogeneity of LSCs limits the use of specific antibodies or drugs that target these progenitors[71].

Another important factor that characterizes LSCs is their interactions with the BM microenvironment. Several key receptors and their ligands control the homing of leukemic stem cells to the microenvironment that plays a fundamental role in supporting AML LSC survival. These receptors and ligands such as VLA-4, CD44, CXCR4, IL-3Rα, CD47, represent crucial factors in the maintenance of the survival and self-renewing capability of LSC. Therefore, several promising pharmacological strategies were develop toward them (Tab. 3).

	Description	Pharmacology strategy
VLA-4	Control of AML bone marrow homing, sensitivity of leukemic blast to chemotherapy	
CD44	Homing and engraftment of AML stem cells	anti-CD44 mAb led to failed engraftment of leukemic cells
CXCR4	Homing, survival and response to chemotherapy of AML stem cells. Elevated levels of CXCR4 are related with poor prognosis.	
Interleukin-3 receptor alpha (IL-3Rα) CD123	Homing, survival of AML stem cells. Overexpressed in AML cells but not on HSCs	anti-CD123 inhibits the IL3 mediated survival of LSC in vitro and homing, engraftment, expansion and serial transplantation of AML in NOD/SCID mice. Less effects on HSC. A humanized version of anti-CD123 is in a phase I clinical trial.
CD47	Transmembrane ligand for the signal regulatory protein α (SIRPα) found on macrophage and dendritic cells. Their interaction results in an inhibitory effect on macrophage phagocytosis. Upregulated in AML LSC and it is associated with poor prognosis.	Inhibition of CD-47-SIRPα complex by a mAb induce an increase of AML LSCs phagocytosis, a reduction of engraftment and serial transplantation in NOD/SCID mice. No effects on HSC.

Table 3: List of receptors and ligands that control the homing of LSC and pharmacological strategies.

Concerning APL, many efforts, without success, have been made to grow APL cells in NOD/SCID mice. Anyway, a recent study proved that PML-RARα mediates the acquisition of a self-renewing capability in the promyelocyte compartment as an initiating step in the pathogenesis of APL[72]. Another study demonstrated that a sub-fraction of myeloid-committed cells isolated from PML-RARα transgenic mice was capable of developing leukemia in recipient mice. According to these data, Guibal et al. suggested that myeloid-committed progenitors represent APL cancer-initiating cells[73].

1.3 Acute lymphoblastic leukemia

An estimated 6000 new cases of acute lymphoblastic leukemia (ALL) are diagnosed yearly in the USA. Patients are mainly children and roughly 60% of cases occur in people younger than 20 years. Survival in childhood ALL is approaching 90%[74, 75]. Established causes for childhood ALL are the exposure to ionizing radiation, as evidenced by the effects of the 1945 atomic bombs in Japan[76], and the significantly increased risks associated with x-ray pelvimetry during pregnancy[77]. Anyhow, the first and most certain causal exposure for childhood ALL is infection. The illness is probably promoted indirectly by an abnormal or dysregulated immune response to one or more common infections (viral or bacterial) in susceptible individuals. Influenza viruses are plausible candidates[78]. Furthermore, the constitutive presence of trisomy 21 in infants represents an increased risk factor for the development of ALL (roughly 40 fold at age 0–4 years) and AML[79]. So far, common allelic variants in *IKZF1*, *ARID5B*, *CEBPE*, and *CDKN2A* have been significantly and consistently associated with childhood ALL[80-82]. The overall conclusion from these observations is that co-inheritance of several low-risk variants affects the risk of ALL. The four genes represent key regulators of blood cell development, proliferation, and differentiation. Acquired or somatic mutations of each of these genes have been detected in ALL, suggesting that the inherited gene variants contribute to the intrinsic vulnerability of stem or precursor blood cells to transforming events either in uterus at initiation or with subsequent postnatal promotion and clonal evolution, or both[83]. It is possible to ascribe to these factors an incidence of ALL in 1 every 2,000 disease in childhood (0–15 years)[84]. Due to the rarity of the illness and the presence of different subtypes, the characterization of the epidemiology is complicated[85].

ALL is classified based on the phenotype of leukemic cells. Through molecular biology tests is possible to divide ALL into groups based on the immunophenotype of the leukemia, which takes into account the type of lymphocyte (B cell or T cell) the leukemia cells come from and how mature these leukemia cells are. Therefore, ALL is divided in B-cell disease that is subclassified in early pre-B ALL (pro-B ALL) (10% of cases), common ALL (50% of cases), pre-B ALL (10% of cases) and mature B-cell ALL (Burkitt leukemia) (4% of cases); and T-cell ALL that is sub-classified in pre-T ALL (5-10% of cases) and mature T-cell ALL (15-20% of cases)[86].

The pathobiology of ALL is extremely complex and characterized by several genetic alterations. In B lymphoblastic leukemia, these alterations include high hyperdiploidy with non-random gain of at least five chromosomes (including X, 4, 6, 10, 14, 17, 18, and 21); hypodiploidy with fewer than 44 chromosomes; and recurring translocations including t(12;21)(p13;q22) encoding *ETV6–RUNX1*, t(1;19)(q23;p13) encoding *TCF3–PBX1*, t(9;22)(q34;q11) encoding *BCR–ABL1*, rearrangement of

MLL at 11q23 with a wide range of partner genes, and rearrangement of *MYC* into antigen receptor gene loci. The dysregulation of *TAL1*, *TLX1*, *TLX3*, and *LYL1*, particularly by rearrangement into T-cell antigen receptor loci, often occurs in T lymphoblastic leukemia. These changes are of key importance in both pathogenesis and clinical management[83] (Fig. 3).

More than 50 recurring regions of DNA copy number alteration have been identified in ALL[87, 88]. The most common mutations are focal deletion and often implicate only one gene. The cell lineage and cytogenetic disease subtype influence the nature and frequency of these alterations. Notably, *MLL*-rearranged ALL, which is typically aggressive and arises early in life, harbors, on average, roughly one additional genetic alteration per case, whereas diseases associated with *ETV6–RUNX1* and *BCR–ABL1* translocations manifest later in childhood and typically harbor between at least six and eight additional genetic alterations (Fig. 4A). Many of the implicated genes encode regulators of lymphoid development or cell cycle, tumor suppressors, or lymphoid signaling molecules[83] (Fig. 4B).

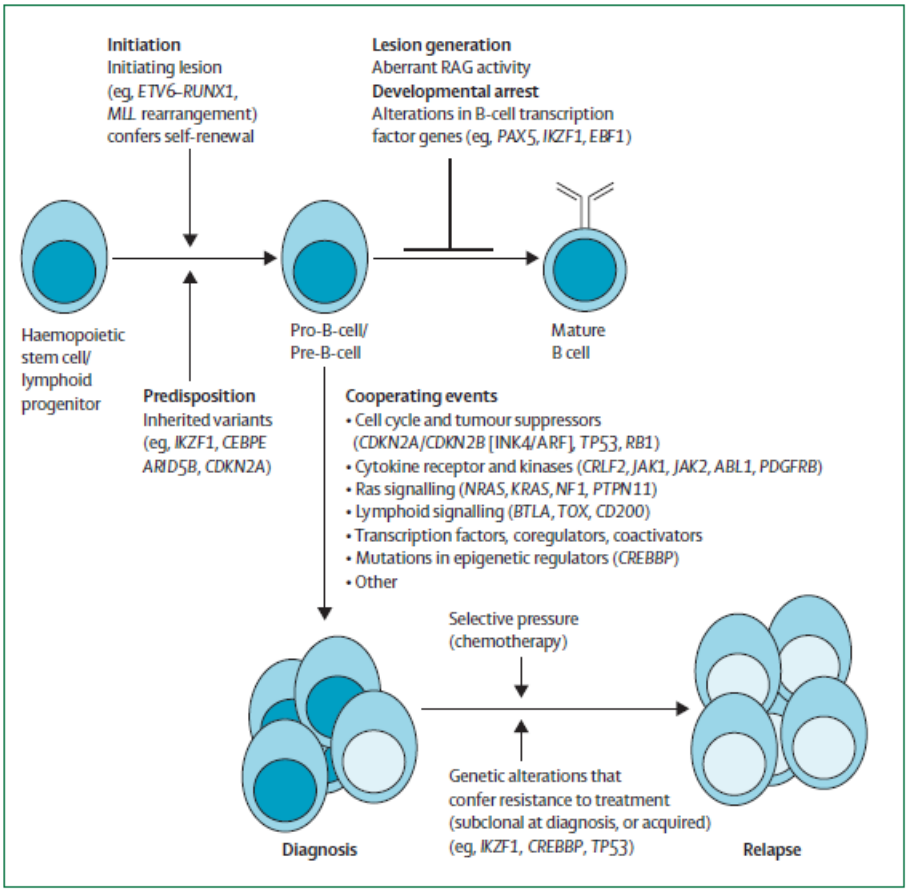

Figure 3: Genetic pathogenesis of B lymphoblastic leukemia at diagnosis and relapse. Copyright Inaba and Mullighan 2013.

A

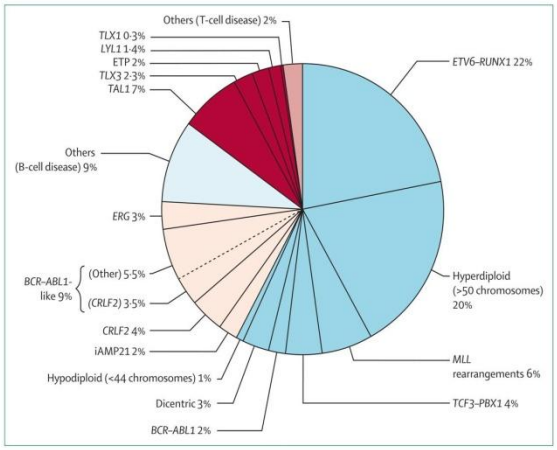

B

	Frequency	Pathway and consequences	Clinical relevance
PAX5			
Focal deletions, translocations, sequence mutations	31·7%	Transcription factor needed for B-lymphoid development; mutations impair DNA binding and transcriptional activation	Not associated with adverse outcome
IKZF1			
Focal deletions, sequence mutations	15% of paediatric cases More than 80% of *BCR–ABL1* cases and 66% of cases of chronic myeloid leukaemia in lymphoid blast crisis A third of cases of high-risk *BCR–ABL1*-negative disease	Transcription factor needed for development of haemopoietic stem cells to lymphoid precursors; deletions and mutations result in loss of function or dominant negative isoforms	Associated with poor outcomes Tripling of cumulative incidence of relapse
Inherited variants	..	..	Increased risk of developing disease
JAK1, JAK2			
Pseudokinase and kinase domain mutations	18–35% of Down's-syndrome-associated cases, 11% of high-risk *BCR–ABL1*-negative cases	Mutations cause constitutive JAK-STAT activation; transforms mouse Ba/F3-EpoR haemopoietic cell line	..
CRLF2			
Rearrangement as *IGH@–CRLF2* or *P2RY8–CRLF2* resulting in overexpression	5–16% of paediatric and adult cases and >50% of cases associated with Down's syndrome 14% of paediatric high-risk cases of B lymphoblastic leukaemia	Associated with mutant *JAK* in as much as 50% of cases; *CRLF2* and *JAK* mutations cotransform in Ba/F3 cells, causing constitutive STAT activation Associated with *IKZF1* alteration and *JAK* mutations	.. Associated with poor outcome
CREBBP			
Focal deletion and sequence mutations	19% of relapsed cases of B lymphoblastic leukaemia*	Impaired histone acetylation and transcriptional regulation	Mutations selected for at relapse and associated with glucocorticoid resistance

A referenced version of this table is in the appendix. *Also mutated in non-Hodgkin lymphoma.

Figure 4: Cytogenetic and molecular genetic abnormalities in childhood ALL (A) and key genetic alterations in B lymphoblastic leukemia, by gene (B). Copyright Inaba and Mullighan 2013.

The diagnosis of ALL is essentially done through the morphological identification of lymphoblasts by microscopy and immunophenotypic assessment of lineage commitment and developmental stage by flow cytometry[75].

Adolescents and adults have a lower incidence of favorable ALL (eg, *ETV6–RUNX1*, hyperdiploidy), greater prevalence of biologically high-risk subtypes (eg, *BCR–ABL1*, *MLL* rearrangement), and poorer adherence to, and tolerance of, treatment than do pre-adolescent children. The old age (≥60 years) and the high leukocyte count are poor prognostic factors in adults[89].

Treatment of ALL

Treatment typically requires from 2 to 2.5 years, and is constituted by three phases: induction of remission, intensification (or consolidation), and continuation (or maintenance)[75]. The prevalence of drugs used in therapy was developed before 1970. However, doses and uses in combination chemotherapy have been optimized on the basis of leukemic-cell biological features, response to treatment, and pharmacodynamic and pharmacogenomic findings in patients, resulting in a high survival rate. Allogeneic HSC transplantation can be performed for patients at very high risk.

The induction therapy takes 4–6 weeks in which the initial leukemic cell burden is eradicated and normal hematopoiesis is restored in 96–99% of children and 78–92% of adults with ALL[74, 75, 90]. Chemotherapy generally includes a glucocorticoid (prednisone or dexamethasone), vincristine, and

asparaginase, with or without anthracycline. Prednisone (or prednisolone) has traditionally been used, but dexamethasone is increasingly used[91]. The dose of dexamethasone is 7 times lower than that required forprednisone. Moreover, dexamethasone yielded better event-free survival, especially in children with T-cell disease who responded well to prednisone prephase treatment and children younger than 10 years with B-cell disease. The use of glucocorticoids is associated with infection, osteonecrosis, fracture, psychosis, and myopathy; these side effects appear generally more frequently with dexamethasone than with prednisone. Patients with *BCR–ABL1*-positive disease have poor prognosis but benefit from early treatment with tyrosine-kinase inhibitors (eg, imatinib, dasatinib). The association of tyrosine-kinase inhibitors with conventional chemotherapy conduces to CR in more than 90% of patients, with an event-free survival superior to historical results with chemotherapy alone[92].

The second phase of ALL treatment is represented by the consolidation therapy and its function is to eradicate residual leukemic cells[75, 90]. This goal is achieved with the use of high-dose (ie, 1–8 g/m2) methotrexate with mercaptopurine, intensified by adding vincristine and glucocorticoids, uninterrupted asparaginase for 20–30 weeks, and reinduction therapy with drugs similar to those used during induction therapy. Intensified reinduction therapy with vincristine and asparaginase improved the outcome of patients with high-risk disease[93]. The main side effect associated with reinduction therapy is osteonecrosis, especially in children aged 10 years or older. Administration of dexamethasone in an alternating week schedule (10 mg/m2 per day on days 0–6 and 14–20) rather than continuous (10 mg/m2 per day on days 0–20) significantly reduced osteonecrosis despite delivering a higher cumulative dose[94].

Last step of ALL treatment is the so-called continuation therapy. It lasts 2 years or even longer and consists in the daily mercaptopurine and weekly methotrexate administration with or without pulses of vincristine and dexamethasone. Adherence of less than 95% to planned mercaptopurine doses is associated with relapse[95]. Therefore, uninterrupted, pharmacogenetics-based mercaptopurine dosing is important. In this phase an allogeneic HSC transplantation can be performed. It remains an option just for children with very high-risk or persistent disease[96].

LSCs in ALL

The nature and the frequencies of stem cells in ALLs have been controversial. Several studies reported the identification of ALL LSC in different cellular sub-fractions. Hong et al. proposed that CD34+CD38^{low}CD19+ leukemic blasts could represent a candidate for LSCs in ALL, due to their ability to re-initiate and sustain leukemic growth in immunodeficient NOD/SCID mice[97]. Recently,

Cox et al. have provided evidence that, in pediatric ALLs, there is a minority (i.e., <1%) of CD133+CD19− cells that are capable of initiating and maintaining long-term *in vitro* cultures of B-ALL cells and of engrafting serial NOD/SCID recipient mice, with development of a B-ALL process[98]. Another study showed that sorted CD34+CD19−, CD34+ CD19+, and CD34−CD19+ populations all contain leukemia-initiating cells, although with different frequencies[99]. Importantly, it was proved that each fraction re-establishes the complete immunophenotype of the original leukemia and is able to self-renew: this observation demonstrates the ability of B-ALL blasts to move back and forth between the different populations[99]. As mentioned before, the Philadelphia chromosome t(9;22) leading to the *BCR/ABL* fusion oncogene and the translocation t(4;11) with formation of the *MLL/AF4* fusion oncogene have been associated with a particular poor outcome. Cell fractionation studies have shown that both childhood high-risk ALL t(9;22) and t(4;11) originate in a primitive CD34+CD19− progenitor/stem cell population, without a myelo-erythroid differentiation potential[84].

1.4 Limits of traditional anticancer therapy

The traditional use of anticancer drugs is essentially based on their ability to act on cellular target involved in mechanisms of DNA duplication and repair. The ultimate goal of their activity is to inhibit the uncontrolled replication and induce the death of cancer cells (Fig. 5). Nevertheless, the major part of those drugs is not able to discriminate between healthy and cancer cells[100].

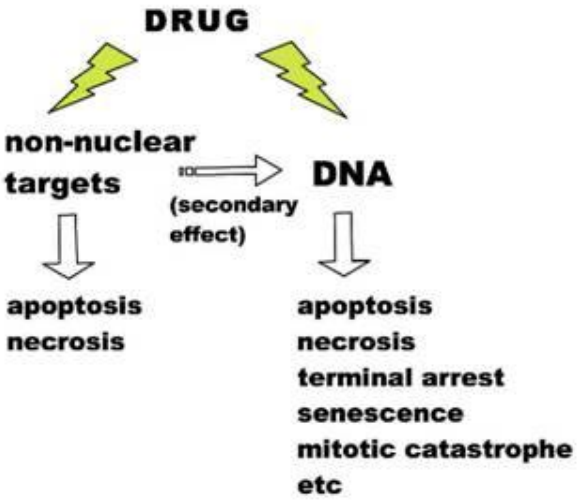

Figure 5: Main targets of traditional anticancer chemotherapy.

Nowadays, several new anticancer approaches are based on the induction of cytotoxic effects on cancer cells targeting key factors of the programmed cell death process. This purpose is reached using agents able to selectively induce apoptosis in mutated cells[101].

Furthermore, most of the drugs used in clinic for the treatment of cancer, characterized by a mechanism of action that exploits the high proliferation of tumor cells, are toxic for cells in rapid proliferation (i.e. healthy cells in replicative state). For this reason, during anticancer treatment toxic events occur and bring to the induction of severe side effects like liver, kidneys or BM damages. Another frequent consequence, that can occur using chemotherapeutic agents with a wide range of action, is the development of secondary cancer sites, despite the treatment of the first cancer[101].

The low selectivity of many anticancer drugs is closely related to their low molecular weight. Indeed after intravenous administration, they distribute throughout most tissues of the body[102].

Drug resistance is one of the most critical problems that characterize anticancer therapy (Fig. 6). Some cancers (i.e. lung or colon) show an intrinsic drug resistance that appears since the first contact with chemotherapy agents. In this model of drug resistance both the stem cells and the

variably differentiated cells are inherently drug resistant, thus therapies have little or no effect, resulting in tumor growth (Fig. 6d). One of the main studied mechanisms of resistance is the efflux of drug from cancer cells. This event appears to be determined by several membrane proteins like ABC-transporter (ATP-binding-cassette). Within this family of proteins, the glycoprotein P (Pgp) is the best known. In most cases, the expression of Pgp is low, but high levels have been reported in kidneys, liver, pancreas, colon, small intestine and adrenals. The development of intrinsic resistance characteristic of adenocarcinomas in these tissues has been attributed to its high expression. Moreover, recent studies of imatinib resistance in patient with leukemias provide an example of how ABC-transporter-mediated efflux in stem cells could facilitate, but not be the solely responsible for, the acquisition of mechanisms of drug resistance[103-105].

An alternative model of drug resistance is the acquired one, where a tumor, originally sensible to drug treatment, becomes insensible to multiple anticancer drugs[106]. The acquisition of drug resistance can occur by a range of mechanisms, including the mutation or over-expression of the drug target, the inactivation of the drug, or the excretion of the drug from the cell. During anticancer treatment, cancer cells undergo an evolutionary pressure. This fact associated with a genomic instability brings to a selection of the most resistant cells to chemotherapy agents[106] (Fig. 6a). Another fundamental mechanism for the acquisition of drug resistance has been attributed to the lost or alteration of the p53 gene. Functional alterations of p53 have been reported in most of cancers. These alterations can be originated by a gene mutation followed by its inactivation, or by an indirect inactivation through the binding with viral proteins or alterations of genes that interact and modulate p53. The inactivation of the p53 gene is essentially caused by small missense mutations or nucleotide insertions and deletions that led, in the 90% of cases, to the production of an aberrant protein. These mutations make the p53 protein unable to bind to the specific recognition sequences on the DNA, and bring to the miss transcription of target genes[107].

CSCs play a pivotal role in the mechanism of resistance. While chemotherapy kills most cells in a tumor, CSCs seem to be naturally resistant through their quiescence, their capability for DNA repair, and ABC transporter expression. As a result, LSCs that survive from anti-leukemic chemotherapy can support the regrowth and the relapse of the leukemia[7] (Fig. 6b).

In a forth model of resistance, the tumor stem cells, which express drug transporters, survive the therapy, whereas the committed but variably differentiated cells are killed. Those resistant stem cells originate a population of multidrug-resistant tumor cells that can be found in many patients who have recurrence of their cancer following chemotherapy (Fig. 6c). The same mechanisms that allow stem cells to accumulate mutations over time, producing the long-term consequences of

exposure to irradiation or carcinogens, would then allow CSCs to accumulate mutations that confer drug resistance to their abnormally developing offspring. As an example, genetic alterations such as those that up-regulate *ABCB1* gene expression in human leukemia and lymphoma cells could have originated in the stem cell[108].

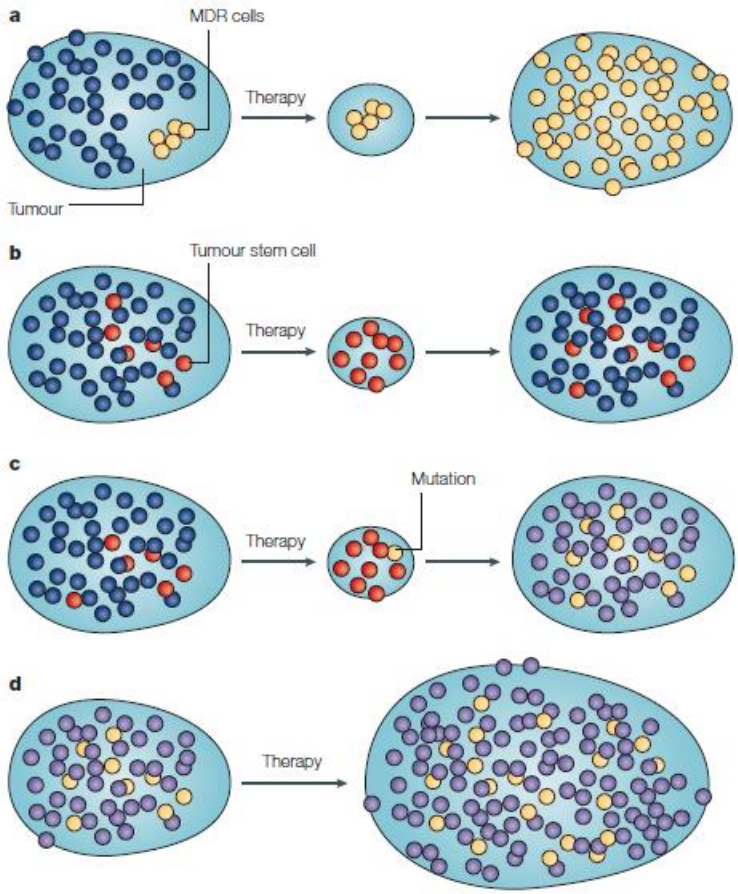

Figure 6: Models of tumor drug resistance. (a) In the conventional model of tumor-cell drug resistance, rare cells with genetic alterations that confer multidrug resistance form a drug resistant clone (yellow). Following chemotherapy, these cells survive and proliferate, forming a recurrent tumor that is composed of offspring of the drug-resistant clone. (b) In the cancer-stem cell model, drug resistance can be mediated by stem cells. In this model, tumors contain a small population of tumor stem cells (red) and their differentiated offspring, which are committed to a particular lineage (blue). Following chemotherapy, the committed cells are killed, but the stem cells, which express drug transporters, survive. These cells repopulate the tumor, resulting in a heterogeneous tumor composed of stem cells and committed but variably differentiated offspring. (c) In the "acquired resistance" stem-cell model, the tumor stem cells (red), which express drug transporters, survive the therapy, whereas the committed but variably differentiated cells are killed. Mutation(s)

*in the surviving tumor stem cells (yellow) and their descendants (purple) can arise (by mechanisms such as point mutations, gene activation or gene amplification), conferring a drug-resistant phenotype. As in model **a**, the stem cell with the acquired mutations could be present in the population before therapy. (d) In the 'intrinsic resistance' model, both the stem cells (yellow) and the variably differentiated cells (purple) are inherently drug resistant, so therapies have little or no effect, resulting in tumor growth. Copyright Dean et al., 2005.*

1.5 Multi-target and botanical drugs as a new anticancer strategy

In the last years, the anticancer therapy strategy has been focused on the selective inhibition of key targets of cancer development. Even if chemotherapy brought a major contribution to the treatment of cancer, so far its results are not as good as prevented. One of the main causes of its partial failure is the development of resistance and relapse[100]. Most of the anticancer drugs used in therapy were designed to hit a single intracellular target. An example is cetuximab that binds an epidermal growth factor receptor, or infliximab that counteracts tumor necrosis factor. A target is a single gene, a gene product or a signaling pathway that has been identified based on genetic analyses or specific biological observations. In theory, a selective modulation of a single molecular mechanism should be sufficient to achieve a significant therapeutic effect with ideally less toxic effects than traditional treatments. However, single-target drug therapy has generally been highly ineffective in treating complex diseases such as cancer, endowed with the deregulation of multiple, redundant and aberrant signaling pathways. Any given cancer carries mutations in an estimated 300 genes and deregulation of more than 500 protein kinases[109]. The genetic plasticity and the advent of secondary mutations in cancer cells complicate the development of targeted therapy and may bring to the failure of targeted agents. Various cell signaling network models indicate that the partial inhibition of many targets is more effective than the complete inhibition of a single target[110].

Based on the complexity that characterizes a cancer, a growing interest has been directed toward multi-target drugs able to hit multiple targets. Aim of this strategy is to counteract the biological complexity of cancer with the association of more pharmacologically active agents[111]. In the context of multi-target strategy, plant products, based on their intrinsic complexity, could represent an interesting and promising approach. They are able to interact with numerous molecular targets, thus perturbing biological networks rather than individual targets[112]. They are also relatively safe and affordable in most cases. This evidence has been supported by the fact that the 70% of the anticancer drugs on the market are related to substances of natural origin. In recent years, the interest in further development of botanical drug products has been increasing steadily.

Botanical drugs represent a complex mixture of constituents. Through their intrinsic complexity they are able to exhibit pharmacological effects by the interaction of many phytochemicals with multiple targets[113]. Multiple interactions may lead to a multi-target effect, which can results in the modification of transport across biological membranes, protection of an active compound from degradation, reversion of multidrug resistance mechanisms, activation of pro-drugs or deactivation of active compounds, and action of synergistic partners at different points of the same signaling or

different signaling pathways. However, the intrinsic complexity that characterizes botanical drugs can pose a number of problems, among which metabolic interactions with antineoplastic drugs and genotoxic potential are the most relevant[114].

Recently, the Food and Drug Administration (FDA) approved the first two botanical drugs for prescription use; Veregen®, a water extract of green tea leaves, for perianal and genital condyloma, and Fulyzq™, an extract of the red sap of the *Croton lechleri plant*, indicated for the symptomatic relief of noninfectious diarrhea in adult patients with HIV/AIDS on antiretroviral therapy. Unlike most small molecule drugs that are comprised of a single chemical compound, the FDA approved drugs contain a mixture of known and possibly active compounds[115]. Of note, as specified in the FDA's guidelines, the term botanicals does not include highly purified substances derived from botanical sources[116]. However, the approval of the first botanical drugs show that new therapies from natural complex mixtures can be developed to meet current FDA standards of quality control and clinical testing.

Before marketing, botanical drugs should satisfy some legal requirements in order to prove their safety and efficacy as new drugs in reference to the Food, Drug & Cosmetic Act. Moreover, the procedure for the production has to guarantee the quality of the product. Essentially, the requirements for the quality, efficacy and safety of the product do not differ from the ones requested for any new drug approval. Concerning the quality of the product, it should be emphasized that natural products are usually constituted by complex mixtures where the active principle could be unknown. Anyhow, the main problem ascribable to botanical drugs is the therapeutic consistency of the different commercialized batches. Since the growing and the composition of the plant can be conditioned by culture methods, weather, seasonal changes and geographic location, the differences between batches can be a serius problem. Even if the quality control of botanical drugs is more complex than that for high purified drugs, a reasonable guarantees of quality shoud be made. Useful strategies include the control of raw material on field, chromatographic anlyses of commercial compounds and the development of biological assays relevant for the quantificaiton of their activity[115]. Of note, FDA determined that the therapeutic consistency of the commercial batches of simple botanical preparations (single part of single plant) can be assured. Although the chemical constituents of a botanical drug are not always well defined and in many cases the active constituent is not identified nor is its biological activity characterized[116], variations in raw material quality can be minimized by restricting the cultivars and the composition of the preparation can be equivalent by robust chemistry, manufacturing and control measures, "fingerprinting", conducting chromatographic analyses of marker compounds[115].

In the last few years, interest in developing botanical drugs escalated. The number of submissions increased rapidly from 5–10 per year in 1990–1998 to an average of 22 per year in 1999–2002 and nearly 40 per year in 2003–2007[115]. Currently, in USA, there are about 10 to 20 botanical drugs that take place in clinical trials[117]. Among the therapeutic areas, the number of botanical products submitted to the FDA was particularly high for cancer and related conditions. Between 1982 and 2007, more than 350 botanical investigational new drug (IND) applications and pre-IND consultation requests were submitted to the agency. These data indicate a growing interest in several therapeutic areas towards a rigorous clinical evaluation of botanical drugs, with a focus on indications where there is a clear medical need for new treatments[115] (Fig. 7).

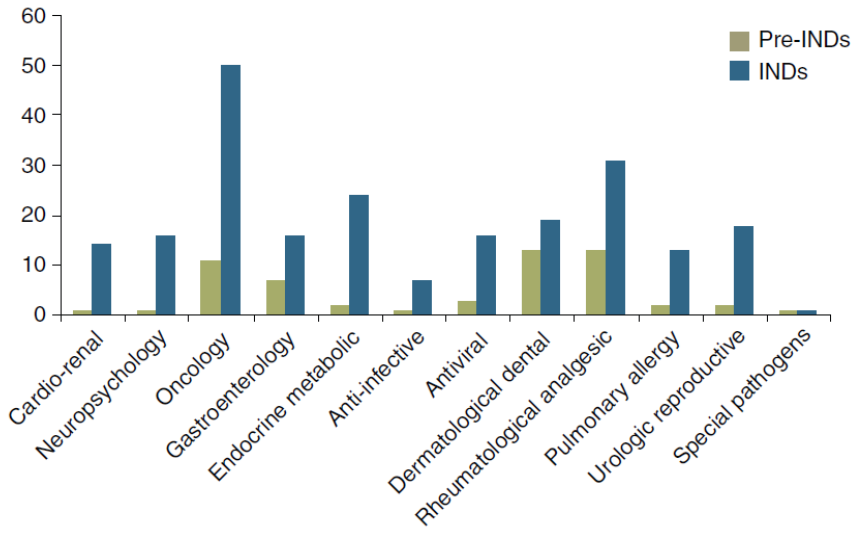

Figure 7: Distribution of botanical drugs pre-INDs and IND submitted to FDA from 1999 and 2007, categorized by therapeutic areas. Copyright Chen et al., 2008.

Although, Veregen® and Fulyzq™ are relatively simple botanical drugs, as they derive from a single part of a single plant, their commercialization prove the usefulness of FDA guidelines and guarantee the possibility to launch botanical drugs endowed with the same standards of highly purified drugs.

1.6 *Hemidesmus Indicus*

***Hemidesmus indicus* R. Br.**

Hemidesmus var. indicus

Hemidesmus var. pubescens

Common name: *Sarsaparilla indiana, Anantumul*

Scientific name: *Hemidesmus Indicus R.Br*

Classification

Family: *Apocynacea*

Subfamily: *Asclepiadoideae*

Type: *Hemidesmus*

Species: *Hemidesmus indicus /Hemidesmus pubescens*

Identification: is a common weed found all over India.

Description: It is a perennial bush, woody, with thick and brown bark, that presents longitudinal grooves and transverse slits. It has numerous stems that become enlarged at the nodes. The leaves are opposite and petiolate, with different shapes, bright green with white streaks on the surface, gray-white on the underside, and smooth to the touch. The flowers present a tubular corolla and can be yellow or purple, based on the species. The fruits are two follicles, curved and sometimes apart. The seeds are flat, dark-gray with a white stripe.

Uses: It is widely used in the Indian traditional medicine and has been extensively investigated for its pharmacological effects. It owns a variety of ethno-medicinal uses, the most important is probably the treatment of dysentery and diarrhea. It is also used for the treatment of infections, skin disease, menorrhagia, post-partum recovery, stomach ulcer and gastric ailments, fever, headache, pain and inflammation, sore mouth, venereal disease including gonorrhea and syphilis, impotence, as a blood purifier, cooling tonic, appetite stimulant, and to neutralize snake bite and scorpion sting[118]. The first pharmacological study was conducted in 1962 on the diuretic activity of the

root[119], and since then, several studies have been published on *Hemidesmus* pharmacological properties[120-122].

Phytochemistry

There are two variants of *Hemidesmus* in nature, *indicus* and *pubescens*. The roots are the part of the plant with the highest amount of active constituents. The components are similar between the two variants, although var. *pubescens* has been found to have a higher content of β-sitosterol and tannins whereas var. *indicus* has a higher content of phenols and free amino acids[121]. The major constituent found in the steam distillation product (yield, 0.25 %) is 2-hydroxy 4-methoxy benzoic acid (2H4MBAC, 91%), along with 40 minor constituents[123]. The aqueous extract of *Hemidesmus* root has been analyzed in order to quantitatively estimate its chemical constituents. The analysis reported the following constituents: saponins (12.55%), tannins (3.06%), flavonoids (1.12%), phenols (1.1%), alkaloids (1.23%), coumarins (0.91%), and terpenoids (0.79%)[124]. Several studies reported a wide variety of biologically active compounds in *Hemidesmus* roots (Tab. 4), including hemidesmins, a series of novel coumarino-lignans[125], and steroidal glycosides known as hemidesmosides A-C[126], which are thought to contribute to the therapeutic activity.

Class of compound	Compound	Activity found
Terpenoids	Ledol, nerolidol, cis-caryophyllene, isocaryophyllene, camphor, β-selinene, borneol, dehydrolupanyl-3 acetate, dehydrolupeol acetate, lupeol, lupeol octacosanoate, lupeol acetate, tetracyclic triterpene alcohols	Anti-snake venom, antimicrobial, anti-inflammatory, antioxidant.
Aromatic aldehydes and acids	2-Hydroxy 4-methoxy benzaldehyde, 2-hydroxy 4-methoxy benzoic acid (HMBA), 4-hydroxy 3-methoxy benzaldehyde (vanillin), 3-hydroxy 4-methoxy benzaldehyde	Anti-snake venom, antidiabetic, anti-inflammatory, antipyretic, antioxidant.
Lignans	Hemidesminin, hemidesmin-1 and 2	Antioxidant, cytotoxic, anti-inflammatory, cardioprotective.
Phytosterols	α-Amyrin, β-amyrin, sitosterols, β-amyrin acetate, 16-dehydropregnenolone	Antimicrobial, lipid and hormone regulatory, immunomodulatory.
Glycosides	Hindicusine, hemidesmosides A-C	Anti-adhesive, antioxidant and anti-dyslipidemic.
Tannins	Unspecified	Mucoprotective, antidiarrhoeal.
Flavonoids	Rutin	Antioxidant, anti-inflammatory, vasodilatory, antiedema and antiplatelet aggregation activity.
Saponins	Unspecified	Antioxidant, cytotoxic, anti-inflammatory, cardioprotective.
Aliphatic acids	Dodecanoic acid, hexadecanoic acid, linalyl acetate, dihydrocarvyl acetate, hexatriacontane	Not specified

Table 4: List of actives contained in Hemidesmus indicus. Copyright Das and Bisht, 2012.

In vivo pharmacological studies

Several beneficial effects has been reported in a wide range of *in vivo* animal studies of *Hemidesmus* root. Nowadays, there are no clinical trial reports available for *Hemidesmus* for any of its traditional uses, and many of the *in vivo* studies are of poor quality. However, from the sum of all the studies, a clear biological activity of *Hemidesmus* results and suggests that this plant has a high potential for therapeutic use in some of its traditional indications. Some of the beneficial

effects include cancer chemoprevention and antitumour activity, hepatoprotection, free radical scavenging and antioxidant activity, cardioprotection, neuroprotection, antithrombotic and hypolipidaemic effects, renal protection, antiulcer activity, anti-infective and anti-inflammatory activity[127] (Tab. 5).

Table 2. Summary of *in vivo* animal studies on *Hemidesmus indicus* root

Type of activity	Experiment	Animal model
Chemoprevention/ antitumour activity	The ethanolic extract (1.5 and 3.0 mg/kg) applied prior to 12-*O*-tetradecanoylphorbol 13-acetate (TPA)/cumene hydroperoxide treatment significantly inhibited cutaneous oxidative stress, epidermal ornithine decarboxylase activity and enhanced DNA synthesis, and prevented tumourigenesis	Mouse
	The aqueous extract of *H. indicus* (root) with *Nigella sativa* (seed), and *Smilax glabra* (rhizome) (6 g/kg/day) inhibited diethylenitrosamine mediated carcinogenic changes in rat liver in the short term (10 weeks) and longer term (16 months), and prevented DMBA-initiated and TPA-promoted murine skin carcinogenesis.	Rat
Hepatoprotection	Oral treatment with the ethanol extract (100 mg/kg × 15 days) significantly prevented rifampicin and isoniazid-induced hepatotoxicity in male Wistar rat.	Rat
	A 50% aqueous ethanolic extract (200, 400mg/kg × 6 days) showed antioxidant and antihepatotoxic activities in a CCl_4 induced hepatic damage model, possibly due to free radical scavenging effects.	Rat
	The methanolic extract (100, 250, 500 mg/kg × 7 days) showed antihepatotoxic effects in paracetamol and CCl_4 models of liver damage.	Rat
	The ethanolic extract (500 mg/kg × 30 days) protected against free radical-mediated oxidative stress in plasma, erythrocytes and liver of animals with ethanol-induced liver injury.	Rat
	HMBA, extracted from *H. indicus* (200 μg/kg x 30 days) significantly inhibited liver injury caused by ethanol administration, reducing the severity of liver damage in terms of body weight, hepatic marker enzymes, oxidative stress, antioxidant status and histological changes.	Rat
	The aqueous extract, 100 mg/kg, administered prior to bromobenzene, showed significant beneficial effects including respiratory stimulation, prevention of the rise in lipid peroxides and protein carbonyls, and increased the level of sulphydryl groups back to control levels.	Rat
	The hepatoprotective activity of the methanol extract (500 mg/kg × 30 days) in acute experimental liver injury induced by paracetamol was reported to be comparable to that of the standard drug, *silymarin* (100 mg/kg, p.o.).	Rat
Cardioprotection	The cardioprotective effects were evaluated in salt water-induced ventricular hypertrophy: the aqueous and methanolic extracts (100, 200 and 400 mg/kg) showed inhibitory effects on microalbuminuria, serum urea, calcium and creatinine levels, myocyte diameter, and retention of Na^+ and water.	Rat
	An extract (0.09g/L for 15min) protected the myocardium against contractile dysfunction and arrhythmias, and reduced tissue damage, following ischemia.	Rat
	The extract (90, 180, 360 μg/kg for 15 min) reduced infarction size, number of ectopic beats, and duration of ventricular tachycardia in the mouse heart, resulting in vasodilation, positive inotropic effects and cardioprotection.	Mouse
Neuroprotection	The ethanolic extract (30, 100, 300 mg/kg × 7 days) increased the discrimination index in the object recognition test and reduced the reaction time in the hot plate test; it potentiated haloperidol-induced catalepsy and delayed the onset of death in sodium nitrite induced respiratory arrest in both acute and chronic studies.	Mouse
	The n-butanol fraction of ethanolic extract (3, 10, 30 mg/kg × 7 days) significantly improved learning and memory in a mouse model.	Mouse
	The ethanolic extract (100, 200 mg/kg) showed anticonvulsant activity by reducing the duration of the tonic extensor phase and the duration of clonus in the maximal electro shock and pentylenetetrazol models.	Rat
	The methanol extract (200, 400 mg/kg) was investigated on cerebral infarct by the four vessel occlusion method: it improved vestibulomotor and neuromuscular functions, increased brain antioxidant enzymes, dopamine and serotonin, and decreased acetylcholine esterase, glutamate and monoamine oxidase.	Rat
Antisnake venom effects	Lupeol acetate, isolated from *H. indicus* (50–100 μg/kg) neutralized *Daboia russellii* venom-induced pathophysiological changes, and the methanolic extract neutralized viper venom-induced lethality and haemorrhagic activity.	Rat, Mouse
	HMBA (200 μg/kg) and lupeol acetate (1–160 μg/kg) neutralized viper and cobra venom-induced lethality, inflammation, hemorrhage, defibrinogenation, cardiotoxicity, neurotoxicity and potentiated antiserum activity.	Rat
Antihyperlipidaemic activity	HMBA (200 μg/kg) showed antihyperlipidaemic activity in ethanol (5 g/kg p.o.) induced hyperlipidaemia, significantly decreasing plasma and hepatic lipids, and increasing plasma Low-density lipoprotein (LPL) concentrations.	Rat
Renoprotective	The root powder showed efficacy in the management of gentamicin-induced nephrotoxicity in albino rats.	Rat
	The antioxidant effect of the ethanolic extract (500 mg/kg × 30 days) offered protection against free radical-mediated oxidative stress in kidney of animals with ethanol-induced nephrotoxicity.	Rat
	The extracts of *H. indicus* (250, 500 mg/kg) and *Acorus calamus* L. protected renal tissue from cisplatin-induced oxidative damage, reducing levels of lipid peroxidation.	Rat
	The nephroprotective activity of the ethanolic extract (250, 500 mg/kg) produced a dose-dependent reduction in the elevated blood urea and serum creatinine, and inhibition of lipid peroxidation, in cisplatin-induced renal injury.	Rat
Antiulcerogenic effects	The ethanolic extract (150, 300, 450 mg/kg) showed antiulcerogenic properties in the modified pyloric ligated, cysteamine-induced and aspirin- induced ulcer models. The effects were thought to be mainly due to mucoprotective activity and a selective increase in prostaglandin content.	Rat
	The ethanol extract (200, 400 mg/kg) showed ulcer protection comparable to that of omeprazole in the indomethacin (20 mg/kg) induced ulcer model, possibly due to cytoprotective action or strengthening of vgastric mucosa.	Rat
	A polyherbal formulation (500 mg/kg) {*Glycyrrhizia glabra* rhizome 200 mg, *Aegle marmelos* leaf 150 mg, *H. indicus* root 75 mg, *Cuminum cyminum* seed 75 mg} reduced gastric lesions in an ethanol-induced gastric ulcer model, comparable to omeprazole and possibly due to the antisecretory activity.	Rat
Antileprotic activity	The extract delayed multiplication of *Mycobacterium leprae* in infected mice.	Mouse

Table 5: Summary of in vivo animal studies on Hemidesmus indicus root. Copyright Das and Bisht, 2012.

In vitro pharmacological studies

Most *in vitro* studies support the evidences reported by *in vivo* studies[127] (Tab. 6). In particular, the anti-inflammatory and antioxidant activities of *Hemidesmus* were confirmed. The antimicrobic activity has been extensively studied *in vitro* and several mechanisms of action have been suggested to be related with the traditional use of *Hemidesmus* as antidiarrheal[128, 129].

Type of activity	Experiment	*In vitro/Ex vivo* model
Cytotoxicity	The aqueous and ethanolic extracts (300–4800 μg/ml) were shown to be cyotoxic to HepG2 cells using 3-(4, 5-dimethylthiazol-2-yl)-2,5-diphenyl tetrazolium bromide (MTT) and sulphorhodamine B assays. The aqueous extract was more active than the ethanolic extract.	HepG2
	The cytotoxic activity of the methanolic extract (12.5–1000 μg/ml) was reported in the MCF7 breast cancer cell line, with an IC_{50} value of 48 ± 0.02 μg/ml.	MCF7
	The methanolic extract (100–1.5 μg/ml) was also shown to be cytotoxic in the human colon cancer cell line HT29, using the MTT assay, with an IC_{50} value of 1.89 μg/ml.	HT29
	The extract (1–100 μg/ml) modulated components of intracellular signaling pathways involved in cell viability and proliferation, altering protein expression and leading to tumour cell death. It also enhanced the antitumour activity of methotrexate, 6-thioguanine and cytarabine.	Leukemic cells
Anti-inflammatory effects	Polymorphonuclear leukocytes (PMNL) and monocytes treated with *Propionibacterium acnes* in the presence or absence of *H. indicus* (5–50 μg/ml) showed a significant suppression of ROS and pro-inflammatory cytokines, two inflammatory mediators in acne pathogenesis.	PMNL, monocytes
Antioxidant/Antithrombotic effects	The *in vitro* and *ex vivo* antioxidant activity of the extract (4–500 μg/ml) was evaluated using free radical scavenging activity in various systems, and inhibition of lipid peroxidation induced by different agents.	Erythrocyte, liver homogenate
	The methanolic extract (50–250 μg/ml) inhibited ADP-induced platelet aggregation *in vitro*, which was comparable to commercial heparin.	Platelet
	The antioxidant and radioprotective effects of the extract (10–100 μg/ml) were demonstrated using inhibition of lipid peroxidation in liver microsomes and plasmid DNA, where it protected from radiation-induced strand breaks.	Rat liver microsome
	Using an *in vitro* thrombolytic model, the extract (10 mg/ml) showed a weak effect on clot lysis.	Whole blood
	The *in vitro* free radical scavenging potential of the terpenoidal fraction (25–100 mg/ml) was demonstrated in antioxidant assays. It also had antibacterial properties against *P. acnes* and *Staphylococcus epidermidis*.	Bacteria
	Phenolics and flavonoids extracted from *H. indicus* showed highest OH^- radical scavenging activity.	Chemical colourimetric
	Antioxidant activity was reported for hindicusine (200μg/ml).	Chemical colourimetric
	Aqueous and alcoholic extract of *H. indicus* (100–500 μg/ml) showed significant antioxidant activity.	Chemical colourimetric
	The phenolic compounds of *H. indicus* (2–25 μg/ml) inhibited lipid peroxidation and supplemented DNA and cytoprotective activities.	Rat liver, calf DNA, human erythrocyte
Antimicrobial activity	The methanolic extract (500–1000 μg/ml) showed antimicrobial activity against *Salmonella typhimurium, Escherichia coli* and *Shigella flexneri*, *in vitro*.	Enterobacteria
	The extract (5 μl/disc) was active against *Helicobacter pylori* with an effect comparable to standard antibiotics.	*Helicobacter pylori*
	The chloroform and methanol extracts (500–1000 μg/ml) were effective against *S. flexneri* and other enterobacterial strains, except for *Shigella dysenteriae*.	Enterobacteria
	The glycoside fraction of the extract (100μg/ml) inhibited *S. typhimurium* induced pathogenesis in the human intestinal (Int 407) and murine macrophage (P388D1) cell lines, thought to be by reducing bacterial surface hydrophobicity and mimicking host cell receptors, blocking attachment to host cells in local and systemic infections.	*S. typhimurium*
	The effect of the sterol and fatty acid fraction (100μg/ml) was studied on *Salmonella typhimurium*-mediated apoptosis in murine macrophages (P388D1) and human intestinal epithelial cells (Int 407). Treated bacteria were found to be defective and smaller than the wild bacteria.	*S. typhimurium*
	The methanolic extract (500–1000 μg/ml) reduced bacterial adherence, multiplication and pathogenesis, and inhibited the secretory proteins encoded by *Salmonella* Pathogenicity Island −1 (SPI-1; relevant to invasion and enteritis) as well as SPI-2 (relevant to intracellular survival and multiplication). Prophylactic or therapeutic activity against *S. typhimurium*-induced pathogenesis occurred *in vitro* and *in vivo* and depended on the composition of the extract.	*S. typhimurium* Rat colon
	The ethanolic extract (100 mg/ml) had strong inhibitory effects against the causative agents of acne vulgaris, *P. acnes* and *S. epidermidis*.	Acne bacteria
	The saponin fraction (10 mg/ml) exhibited antimicrobial activity against *Staphylococcus aureus, Salmonella typhi, Klebsiella pneumoniae* and antifungal activity against *Aspergillus flavus, Aspergillus fumigatus* and *Aspergillus niger*.	Bacteria, fungi
	The aqueous extract (1 mg/ml) was found to be antibacterial to *S. aureus, K. pneumoniae* and *Pseudomonas aeruginosa*, in that order of potency.	Bacteria
	The antimicrobial and anthelmintic activity of the steam distilled essential oil, alone and in combination with cow urine (a traditional formula), were evaluated, and the pure distillate found to be more potent than the cow urine combination.	Bacteria, fungi, helminths
	The extract (1 mg/ml) was tested against 12 bacterial species, with *E. coli, P. mirabilis* and *S. typhimurium* found to be the most susceptible.	Bacteria
Genotoxic and antigenotoxic activity	A reduction in cisplatin-induced sister chromatid exchanges and micronucleated or binucleate cells was observed at lower concentrations (4 and 8 μg/ml) of the ethanolic extract (2–32 μg/ml), whereas an increase in chromosome aberrations was found at higher concentrations.	Human Lymphocyte
Immunomodulatory effects	*H. indicus* extract (1mg/ml) stimulated the proliferation and viability of peripheral blood lymphocytes (PBLs), increased IgG production and adenosine deaminase activity, and suppressed both cell-mediated and humoral components of the immune system.	PBLs
Otoprotection	Co-administration of the extract (25, 50 μg/ml) significantly counteracted the toxic effect of gentamicin on hair cells, and inhibited gentamicin-induced apoptosis.	Hair cell

Table 6: Summary of in vitro/in vivo studies on Hemidesmus indicus root. Copyright Das and Bisht, 2012.

Safety and toxicity of *Hemidesmus indicus*

The toxicity of the plant for the liver and the kidney has been reviewed by Austin et al.[121]. The samples of *Hemidesmus* collected during the vegetative season presented a lower concentration of active constituents and higher value of the lethal dose 50 (DL50) compared to the once collected in the blossoming season. The DL50 of the 50% alcoholic extract of the *Hemidesmus* root was 915,21 mg/kg b.w. in the vegetative season and 853,17 mg/kg b.w. in the blossoming season. The powder suspension of the root has been tested for its acute toxicity in albino Swiss mice. None death or behavioral alteration has been observed up to 5g/kg b.w.[130] and 12 g/kg b.w.[131]. Das and colleagues showed that *Hemidesmus* 600 and 800 µg/mL was able to reduce the vitality of embryonic interstitial cells and lymphoid cells by 50% (CD50), respectively. The CD50 of the chloroformic fraction was 500 µg/mL in both cell lines[118, 127-129]. Among the most important therapeutic indications of *Hemidesmus*, there are diarrhea and dysentery, but for these uses the method for the preparation of the root is crucial. The alcoholic extract inhibits the absorption of water and electrolytes from the intestine, and this would be a risk for patients affected by diarrhea and dysentery, while the water extract has the opposite effect, stimulating the absorption of water and electrolytes[131]. This indicates that the plant contains one or more components that are toxic in defined conditions[127].

1.7 Piperlongumine

Piperlongumine (piperlongumine, 5,6-dihydro-1-[(2E)-1-oxo-3-(3,4,5-trimethoxyphenyl)-2-propenyl]-2(1H)-pyridinone) is a biologically active component derived from *Piper* species (*Piperaceae*). Interestingly, piper seeds are used in traditional medicine, including the Indian Ayurvedic system of medicine and the folk medicine of Latin America. In particular, piperlongumine is the principal alkaloid from long pepper (*Piper longum L.*)[132]. *P. longum* root is traditionally used to induce expulsion of the placenta after birth, or for treatment of tumors, diseases of the spleen, malaria, viral hepatitis, bronchitis, cough, asthma, respiratory infections, stomachache, and gonorrhea[133]. The main pharmacological activities reported for piperlongumine include cytotoxic[132, 134-143], anti-angiogenic[142], antimetastatic[142], antiplatelet aggregation[143-148], anti-atherosclerotic[149], antidiabetic[150], antifungal[151], and schistosomicidal[152, 153] activities.

Chemical structure of piperlongumine

Piperlongumine was isolated and characterized as a new amide alkaloid for the first time in 1961 by Atal and Banga, a pair of Indian chemists working with *P. longum* (Fig. 8.1). After several reports from different groups, in 1968 Kamat and Saksena published the correct structure of piperlongumine. Further studies in the 1980s allowed comparison of the X-ray crystallographic data of piperlongumine obtained from an improved synthetic route, and of piperlongumine isolated from *P. longum*, definitively establishing the accuracy of structure[132] (Fig . 8.2).

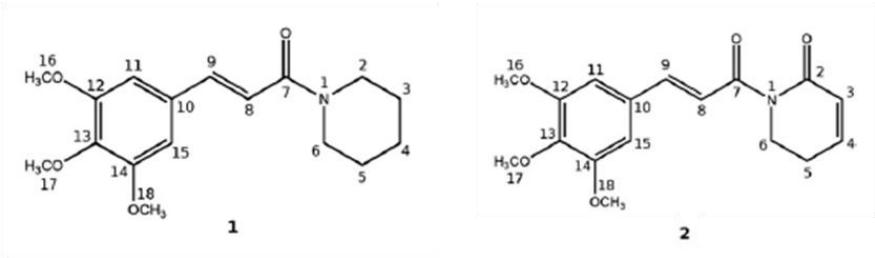

Figure 8: Proposed chemical structure (1). Correct structure of piperlongumine (2) (5,6-dihydro-1-[(2E)-1-oxo-3-(3,4,5-trimethoxyphenyl)-2-propenyl]-2(1H)- pyridinone). Copyright Bezerra et al, 2012.

Biological effects of piperlongumine

Piperlongumine shows multiple *in vitro* and *in vivo* pharmacological activities (Tab. 7). These activities include antiplatelet aggregation, anxiolytic, antidepressant, antinociceptive, anti-atherosclerotic, antidiabetic, antibacterial, antifungal, leishmanicidal, trypanocidal, and schistosomicidal properties[131-152].

Effect	Models
Cytotoxic and antitumor activities	Selective cytotoxicity over cancer cells presents only a weak activity in normal cells
	Cell cycle arrest in G_1 or G_2/M phase
	Induction of apoptotic cell death
	Induction of oxidative stress by inhibition of GSTp1 and CRB1
	In vivo antitumor effects against Sarcoma 180 (murine tumor), B16-F10 (murine melanoma), EJ (human bladder carcinoma), MDAMB436 (human breast carcinoma), A549 (human lung carcinoma), and MMTV-PyVT (transgenic mouse model of spontaneous breast cancer)
	Enhancement of 5-fluorouracil activity in tumor cells in culture and in animal models
Genotoxicity	Genotoxicity in Chinese hamster fibroblast lung-cultured cells (V79) using comet assay
	Mutagenecity in yeast *Saccharomyces cerevisiae*
	Negative results in *Salmonella typhimurium* TA 97a, TA 100, and TA 102 with and without metabolic activation (Ames test)
	Positive results in the *in vitro* micronuclei and chromosomal aberration assays using V79 cells
	Clastogenecity in mice using the bone-marrow micronucleus test
Antiangiogenic effect	*In vivo* inhibition of the formation of blood vessels in tumors observed by the reduction of the expression of VEGF and CD31
Antimetastatic effect	*In vitro* inhibition of the expression of Twist and N-cadherin, and disruption of the p120-ctn/vimentin/N-cadherin complex
	In vivo inhibition of the spontaneous metastasis to lungs in a transgenic mouse model
Antiplatelet aggregation action	*In vitro* studies using collagen-, arachidonic acid-, platelet-activating factor-, and thrombin-induced platelet aggregation
	In vivo study using collagen-induced platelet aggregation
Antinociceptive effect	Acetic acid-induced abdominal constriction model in mice
Anxiolytic and antidepressant action	Elevated plus maze, open field, and forced swimming tests in mice
Anti-atherosclerotic effect	*In vivo* inhibition of atherosclerosis plaque formation
	In vitro inhibition of platelet-derived growth factor receptor pathways
Antidiabetic effect	*In vitro* inhibition of the recombinant human aldose reductase
Antibacterial	*In vitro* antibacterial activity against clinical strains of *Pseudomonas aeruginosa*, *Klebsiella pneumonia*, and *Staphylococcus aureus*
Antifungal	*In vitro* antifungal activity against *Cladosporium sphaerospermun* and *Cladosporium cladosporioides*
Leishmanidal	*In vitro* antileishmanial activity against *Leishmania donovani*
	In vivo antileishmanial activity in a hamster model of visceral leishmaniasis
Trypanocidal	*In vitro* trypanocidal activity against *Trypanosoma cruzi*
Schistosomicidal	*In vitro* schistosomicidal activity against *Schistosoma mansoni*

Table 7: Summary of the reported pharmacological effects of piperlongumine. Copyright Bezerra et al., 2012.

Anticancer effects of piperlongumine

Beyond the several pharmacological activities attributed to piperlongumine, different research groups have extensively investigated its anticancer potential. Therefore, a patent that provides methods for the treatment of cancer using piperlongumine and/or its analogs has been published[154].

Cytotoxicity studies

Several studies concerning the cytotoxic activity of piperlongumine against tumor cell lines have been performed (Tab. 8). Piperlongumine is able to kill several types of cancer cells, including hematological, colon, melanocyte, lung, breast, central nervous system (CNS), pancreatic, nasopharyngeal, osseous, bladder, renal, and prostate cells. The IC_{50} values reported in the different cancer cell lines were in the micromolar range. This compound showed a selectivity of action against cancer cells and presented only a weak activity in normal cells [132, 134-143].

A common strategy to reduce chemoresistance is the use of drugs in combination. Interestingly, piperlongumine increased the cytotoxicity of 5-fluorouracil (5-FU) in several cell lines, as observed by the lower IC_{50} value and increase in the maximum response achieved[155]. As well, the association of piperlongumine with diferuloylmethane (curcumin), an anti-inflammatory and anticancer agent, enhanced piperlongumine induced cytotoxicity[140].

Cell lines	Histotype	Origin	IC_{50} (μM)
P-388	Leukemia lymphocytic	Mouse	2.8
HL-60	Leukemia promyelocytic	Human	5.3
CEM	Leukemia lymphocytic	Human	4.4
K-562	Leukemia myeloid	Human	5.7
JUKART	Leukemia lymphocytic	Human	5.3
MOLT-4	Leukemia lymphoblastic	Human	1.7
HT-29	Colon carcinoma	Human	1.4
HCT-8	Colon carcinoma	Human	2.2
HCT116	Colon carcinoma	Human	~7
SW620	Colon carcinoma	Human	~7
DLD-1	Colon adenocarcinoma	Human	~7
B16	Melanoma	Mouse	5.3
MDA-MB-435	Melanoma	Human	~7
A-549	Lung carcinoma	Human	1.9
H1975	Lung carcinoma	Human	~7
BT-474	Breast carcinoma	Human	~7
MDA-MB-231	Breast carcinoma	Human	~7
SF-295	Glioblastoma	Human	~7
IMR32	Neuroblastoma	Human	>25
Panc-1	Pancreatic carcinoma	Human	~7
Mia PaCa-2	Pancreatic carcinoma	Human	~7
U2OS	Osteosarcoma	Human	~7
SaoS-2	Osteosarcoma	Human	~7
J774	Macrophages	Mouse	>25
P388D1	Macrophages	Mouse	~5
EJ	Bladder carcinoma	Human	~7
PC-3	Prostate carcinoma	Human	~10
LNCaP	Prostate carcinoma	Human	>30
786-0	Renal carcinoma	Human	61.4
BC-8	Histiocytoma	Rat	~5
PCC4	Embryonal carcinoma	Mouse	~5
KB	Nasopharyngeal	Human	5.6
V79	Normal lung fibroblast	Hamster	~60
PBMC	Normal lymphocytes	Human	>31.5
PAE	Normal aortic endothelial	Human	>15
76N	Normal breast epithelial	Human	>15
HKC	Normal keratinocytes	Human	>15
HDF	Normal skin fibroblasts	Human	>15
184B5	Immortalized breast epithelial	Human	>15
MCF 10A	Immortalized breast epithelial	Human	>15
Melan-a	Immortalized melanocyte	Mouse	~10

Table 8: In vitro cytotoxic effects of piperlongumine against normal and tumor cell lines. Copyright Bezerra et al., 2012.

Cytotoxic mechanisms

Understanding the molecular mechanism of drugs is vital for predicting their potential therapeutic and side effects. For this purpose, several studies investigated the molecular and cellular mechanism by which piperlongumine induces cytotoxicity (Fig. 9). Bezerra et al. in 2007 studied the activity of piperlongumine on human leukemia cells (HL-60 and K-562). Piperlongumine showed the ability to suppress leukemia growth and reduce cell survival, triggering cell death by both caspase-dependent apoptosis and/or necrosis. However, only a weak cytotoxicity was observed in normal lymphocytes. Later studies, by the same group, reported the effects of piperlongumine in the inhibition of cell-cycle progression in G_2/M phase followed by mitochondrial dependent apoptosis[156]. This result was confirmed in other cell lines. In particular, in PC-3 cells (androgenin-dependent prostate carcinoma), the G_2/M arrest was associate with a dose-dependent decrease in CDK-2 expression[157]. The pro-apoptotic activity exerted by piperlongumine was mainly correlated to a down-regulation of Bcl-2 and to the activation of caspase-3. Piperlongumine effects on cell death, cell cycle and signal transduction pathways were also evaluated in a mouse embryonal carcinoma cell line (PCC4). In contrast to previous works, piperlongumine induced a significant increase of cells in the G_1 phase of the cell cycle. A decrease in CDK2 and cyclin D1 (two G_1 cell-cycle regulators) was found[140]. Additionally, piperlongumine showed the ability to inhibit HIF-2 transcription activities in a renal carcinoma cell line (786-0)[137]. Raj et al. in 2011 demonstrated that piperlongumine exerted its cytotoxic activity toward cancer cells through the induction of p53 expression and acetylation. Additionally, piperlongumine showed the ability to repress the expression of several pro-survival proteins, including Bcl-2, survivin, and Xiap. Moreover, Raj et al. reported that piperlongumine was able to up-regulate members of the pro-apoptotic BH3 only family, like Bim, Puma and Noxa[142]. A crucial role for piperlongumine's induction of apoptosis was attributed to its ability to stimulate the production of reactive oxygen species (ROS), like hydrogen peroxide and nitric oxide, in cancer cells. Moreover, the combination of piperlongumine with N-acetyl-L-cysteine (NAC), an antioxidant agent, prevented ROS production and cell death. In contrast, the induction of ROS was not reported in normal cells[142].

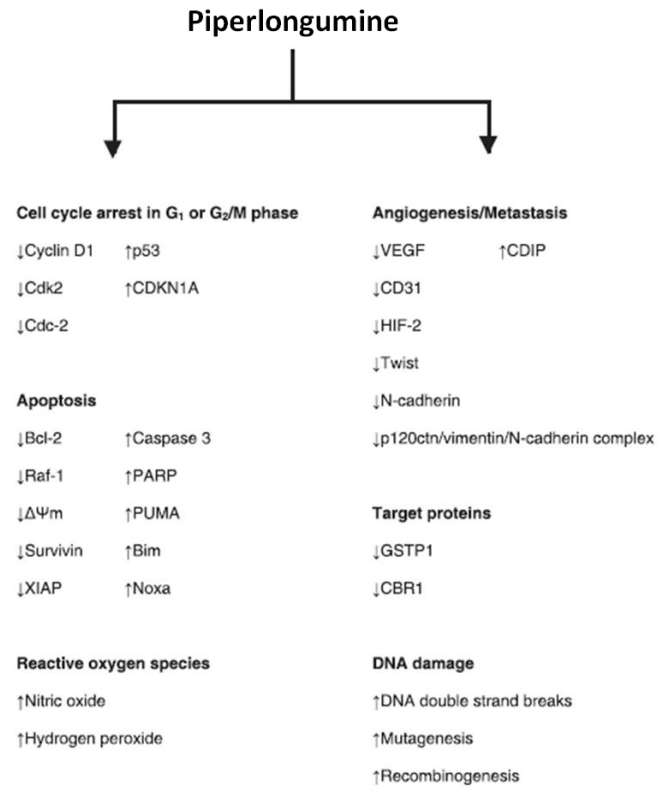

Figure 9: Summary of the anticancer mechanisms of piperlongumine. Copyright Bezerra et al. 2012.

Toxicological profile of piperlongumine

Several toxicology studies on piperlongumine are found in literature. As genotoxic compounds are potentially mutagenic or carcinogenic, the genotoxic potential of piperlongumine has been investigated in many models. Piperlongumine induced DNA strand breaks in V79 cells (Chinese hamster fibroblast cell line)[155].Subsequent studies in the same cell line reported that piperlongumine is able to induce significant chromatid and chromosomal aberrations, and to increase the incidence of micronuclei[158]. In mouse BM micronucleus assay, piperlongumine at 50 mg/kg b.w. does not induce micronucleus formation, but at 100 mg/kg it increased the levels of micronucleated immature polychromatic erythrocytes. Hematological, biochemical, histopathological and morphological analyses of the piperlongumine-treated animals were also performed on healthy Swiss mice after 7 days of treatment at a dose of 50 mg/kg. Neither the enzymatic activity of transaminases nor the urea levels were significantly modified when compared with the control group; hematological parameters also remained unchanged[156].

Chapter 2

Research aim

My research project aims to indentify and study novel natural compounds for the treatment of acute leukemias. Single-target drug therapy has generally been highly ineffective in treating complex diseases such as cancer, characterized by the deregulation of multiple, redundant and aberrant signaling pathways. On these bases, a growing interest has been directed toward multi-target drugs able to hit multiple targets. Aim of this strategy is to counteract the biological complexity of cancer with the association of more pharmacologically active agents[111]. In the context of multi-target strategy, plant products, based on their intrinsic complexity, could represent an interesting and promising approach. They are able to interact with numerous molecular targets, thus perturbing biological networks rather than individual targets[112]. Two potential multi-target drugs were identified in *Hemidesmus indicus* and in piperlongumine. In the first two years of my PhD I investigated the multi-target activity of *Hemidesmus indicus decoction*; in the last year, I explored the ability of piperlongumine of selectively hitting LSC.

From preliminary studies conducted in our lab, *Hemidesmus* showed the ability to induce cytostatic and cytotoxic effects on a T-lymphoblastoid cell line. Starting from these results the cellular and molecular mechanisms by which *Hemidesmus* exerts its anti-leukemic activity were investigated. The first part of the research was conducted on Jurkat cells examining the effect of *Hemidesmus* in the modulation of key factors involved in the regulation of apoptosis and cell-cycle. We thus evaluated the ability of *Hemidesmus* to induce apoptosis, regulate the activation of caspase-3, and the cleave one of its essential substrates, PARP. Afterwards, it was investigated whether the pro-apoptotic effect of *Hemidesmus* was induced through the extrinsic or the intrinsic pathway. To this purpose, the modulation of caspase-8 activity and of the mitochondrial transmembrane potential were studied. Therefore, the ability of *Hemidesmus* to mobilize intracellular levels of Ca^{2+} was investigated. The research continued analyzing the ability of *Hemidesmus* to induce a post-transcriptional and post-translational modulation of proteins involved in the regulation of the intrinsic apoptotic pathway, such as Bax, Bcl-2, Mcl-1, and Noxa. Moreover, the ability of *Hemidesmus* to modulate the 26S proteasome and level of ROS was investigated. In parallel, the expression of proteins involved in the inhibition of cell-cycle progression by *Hemidesmus* was examined.

In the second part of the study, it was investigated the ability of *Hemidesmus* to induce differentiation in a human promyelocytic leukemia cell line and its ability to influence new blood vessels formation.

In the third and final part of the research, a preliminarily exploration of the ability of *Hemidesmus* to induce apoptosis in primary AML cells in culture was performed. Furthermore, due the pivotal role in the process of leukemia initiation and progression of LSCs, the ability of *Hemidesmus* and piperlongumine to selectively target those cells, sorted from AML patient and healthy cord blood samples, was evaluated.

Chapter 3

Materials and methods

Plant decoction preparation

Hemidesmus indicus (voucher #MAPL/20/178) was collected from Ram Bagh (Rajasthan, India), and authenticated by Dr. MR Uniyal, Maharishi Ayurveda Product Ltd., Noida, India. The method described in the Ayurvedic Pharmacopoeia of India[159] was followed for the preparation of *Hemidesmus*. In particular, 10 g of grinded roots were mixed with 300 mL of boiling water, allowing the volume of water to reach 75 mL. The yield of the decoction was 15%. *Hemidesmus* was then filtered, lyophilized, and stored at room temperature. Immediately before the use, the samples were resuspended in water and centrifuged at 2,000 rpm to discard any insoluble material.

HPLC analysis of plant decoction

Hemidesmus was subjected to HPLC analysis to quantify its main phytomarkers, namely 2-hydroxy-4-methoxybenzaldehyde (2H4MBAL), 3-hydroxy-4-methoxybenzaldehyde (3H4MBAL) and 2H4MBAC[127]. The reference compounds (all obtained from Sigma, St. Louis, MO, USA) were used as external standards to set up and calculate appropriate calibration curves. The analyses were performed using a Jasco modular HPLC (Tokyo, Japan, model PU 2089) coupled to a diode array apparatus (MD 2010 Plus) linked to an injection valve with a 20 mL sampler loop. The column used was a Tracer Extrasil ODS2 (2560.46 cm, i.d., 5 mm) with a flow rate of 1.0 mL/min. The mobile phase consisted of solvent solution B (methanol) and A (water/formic acid=95:5). The gradient system adopted was characterized by five steps: 1, isocratic, B/30 for 15 min; 2, B raised progressively from 30% to 40% at 20 min; 3, B then raised to 60% at 50 min; 4, B achieved 80% at 55 min and 5, 100% at 60 min. Injection volume was 40.0 mL. Following chromatogram recording, peaks from *Hemidesmus* samples were identified by comparing their UV spectra and retention time with those from the pure standards. The identity was also confirmed by ^{1}H NMR on the enriched fraction of the compounds obtained by soxhlet extraction in $CHCl_3$/EtOH 1:1. Dedicated Borwin software (Borwin ver. 1.22, JMBS Developments, Grenoble, France) was used to calculate peak area by integration.

Standard solution and calibration procedure

Individual stock solutions of 2H4MBAL, 3H4MBAL and 2H4MBAC were prepared in water. Six different calibration levels were prepared within the following range: 2–20 mg/mL for 2H4MBAL, 1.5–40.0 mg/mL for 3H4MBAL, and 1–100 mg/mL for 2H4MBAC. Each calibration solution was injected into HPLC in triplicate. The calibration graphs were provided by the regression analysis of peak area of the analytes versus the related concentrations. The analysis of *Hemidesmus* (31 mg/mL) was performed under the same experimental conditions. The obtained calibration graphs allowed the determination of the concentration of the three components. Three different batches of *Hemidesmus indicus* were tested.

Cell cultures

Human leukemia Jurkat (acute T lymphoblastic leukemia), CEM (acute T lymphoblastic leukemia), HL-60 (acute promyelocytic leukemia), REH (non-T, non-B lymphoblastic leukemia) and KU812F (chronic myeloblastic leukemia) cell lines, obtained from the Istituto Zooprofilattico of Brescia (Italy), were grown in suspension and propagated in RPMI 1640 supplemented with 10% (Jurkat, CEM, REH, KU812F) or 20% (HL-60) heat inactivated bovine serum, 1% antibiotics (all obtained from Sigma St. Louis, MO, USA). To maintain exponential growth, the cultures were divided every third day by dilution to a final concentration of $1x10^5$ cells/mL. To reduce spontaneous differentiation of HL-60, cells were never allowed to exceed a density of $1.0x10^6$ cells/mL.

Human umbilical vein endothelial cells (HUVECs) were purchased from Lonza (Basel, Switzerland), cultured in EGM complete medium with SingleQuots™ (supplements and growth factors containing hydrocortisone, hEGF, FBS, VEGF, hFGF-B, R3-IGF-1, ascorbic acid, heparin and gentamycin/amphotericin-B, Lonza) at 37°C and 5% CO_2 under normoxic (21% O_2) and hypoxic (2.5% O_2) conditions. To maintain the exponential growth, the cells were divided when they reached the 80% of confluence in a 25 cm^2 dish. HUVECs at passage between 3 and 8 were used for the experiments under normoxic and hypoxic conditions.

Cells were treated with different concentrations of *Hemidesmus* within the following range: 0.0-3.1 mg/mL. The stock solution (31 mg/mL) was diluted to 1/10 and the concentration 3.1 mg/mL was obtained. A series of two-fold dilution was used to obtain the lower concentrations.

Patients

The characteristics of the patients studied are given in Table 9. The diagnosis of leukemia was established by combination of morphological, immunological, cytogenetic and molecular methods,

which were applied to PB samples. The immunological assays were made by fluorochrome-conjugated monoclonal antibodies and analysis by a three-laser (488, 633, 405 nm)-equipped flow cytometer (FacsCanto II, Becton Dickinson, San Jose, CA, USA). A six-color method was applied; therefore the following fluorochrome combination was used: fluorescein isothiocyanate (FITC), phycoerythrin (PE), peridinin chlorophyll protein complex, phycoerythrin-cyanine 7, allophycocyanin, allophycocyanin-cyanine 7. A wide panel of monoclonal antibodies was used that always included: CD45, CD13, CD33, CD34, CD117, HLA-DR, CD4, CD14, CD64, CD38, MPO, CD11b, CD16, CD15, CD56, CD7, CD19 (all from Becton Dickinson). Cytogenetic analysis was made by standard banding methods and by fluorescence in situ hybridization methods. The molecular methods, carried out by PCR, included the following fusion genes: *AML1/ETO*, *CBFb/MYH11*, and *BCR-ABL*. In addition, FLT3/internal tandem duplication (ITD) was also investigated. Patients were studied at the time of diagnosis; one patient was studied during him first relapse.

The AML patient samples BM2985, PB3317, PB2585, PB3924, PB3703, BM2876 and 3 umbilical cord blood specimens from healthy donors (CB10, CB15 and CB19) were provided by the Institute for experimental cancer research, University-Hospital of Ulm, Ulm, Germany.

Preparation of primary cells

PB and BM samples of patients and cord blood samples were collected in tubes containing preservative-free heparin. Briefly, the primary cells were subjected to Ficoll-Paque density gradient separation with Pancoll (PAN Biotech, Aidenbach, Germany) (1,077 g/mL) to isolate mononuclear cells (630 g x 30 min) and maintained in culture in IMDM medium (PAN) containing 15% heat-inactivated bovine serum. The samples always contained >95% blasts.

Preparation of AML patient samples, normal hematopoietic specimens and isolation of LSC and HSC.

In order to isolate CD34+ cells from mononuclear cells, samples obtained from the University-Hospital of Ulm were then stained with CD34-PE antibody (1:100, Becton Dickinson) and the CD34+ population was sorted using FACSAria II cell sorter (Becton Dickinson). Nowadays, the CD34+ subpopulation is considered enriched in LSCs and HSCs[160]. The sorted cells population was treated for 24h with different concentration of *Hemidesmus* (0.00-1.55 mg/mL) and piperlongumine (0-14 µM).

Bio-ID	Sample origin	Sex	Age	Karyotype	Molecular biology
AML-1	PB	M	78	46,XY[20], 47XY	Negative
AML-2	PB	F	66	46,XX[20]	FLT3
AML-3	PB	M	85	46,XY[20]	Negative
AML-4	PB	M	62	46,XY[20]	FLT3-ITD
BM2985	BM	M	25	46,XY[20]	FLT3-ITD
PB3317	PB	F	69	46,XX,del(8)(q13q24)[8], 46,idem,add(17)(p13)[5], 46,idem,+del(11)(q23),-17[3], 46,idem, der(11)t(11;17)(q13;q11)[2]	FLT3-ITD
PB2585	PB	M	44	46,XY[20]	NPM-1, FLT3-ITD
PB3924	PB	M	50	46,XY [20]	FLT3-ITD
PB3703	PB	F	25	54,XX,+4,+8,+10,+12,+13,+14,+21,+22[12], 46, XX[8]	Negative
BM2876	BM	M	60	46,XY,t(3;10)(p11;p14or15), der(7)t(7;8)(p22;q13),inv(16)(p13.1q22)[20]	N-RAS, INV.16

Table 9: Clinical characteristics of AML patients.

Flow cytometry

All flow cytometric analyses were performed by using the easyCyte 5HT flow cytometer (Merck Millipore, Hayward, CA, USA) or LSRFortessa (Becton Dickinson).

Cell viability

Cells were treated with different concentrations of *Hemidesmus* and at different time points. Viability was determined immediately after the end of treatment by flow cytometry. Briefly, cells were mixed with an adequate volume of Guava ViaCount Reagent (containing propidium iodide, Merck Millipore) and allowed to stain 5 min at room temperature. IC_{50} (inhibitory concentration causing cell toxicity by 50% following one cell-cycle exposure) was calculated by interpolation from dose-response curve.

Analysis of apoptosis

After treatment with different concentrations of *Hemidesmus* alone, piperlongumine, or the combination between *Hemidesmus* and methotrexate (0.05– 0.25 mM, Sigma), 6-thioguanine (3.75–30 mM, Sigma), cytarabine (0.10–1.25 mM, Sigma), NAC 10mM aliquots of $2x10^4$ cells were stained with 100 µL of Guava Nexin Reagent (Merck Millipore), a pre-maid cocktail containing Annexin V-PE and 7-amino-actinomycin D (7-AAD) and, after 20 min of incubation at room temperature in the dark, the samples were analyzed by flow cytometry. Camptothecin 2 mM or cytarabine 0.5 µM were used as positive controls. The analysis was also performed on Jurkat cells treated with 2H4MBAL (10 µg/mL), 3H4MBAL (75 µg/mL) or 2H4MBAC (22.0 µg/mL) and their association.

Detection of caspase-8 and caspase-3 activity by flow cytometry

Active caspases' detection employed an affinity label methodology, using the caspase-8-preferred substrate leucine-glutamic acid-threonine-aspartic acid (LETD) or the caspase-3-preferred substrate amino acid sequence aspartic acid-glutamic acid-valineaspartic acid (DEVD) linked to a fluoromethylketone (FMK) moiety, which reacts covalently with the catalytic cysteine residue in the active enzymatic center. A 6-carboxyfluorescein (FAM) group linked to LETD- or DEVD-FMK was used as a reporter. After 24h of treatment with *Hemidesmus* (0.00-0.93 mg/mL), cells were stained with 10 µL of freshly prepared 10X working dilution FAM-LETD-FMK (Merck Millipore) or 10 µL of freshly prepared 30X working dilution FAM-DEVD-FMK solution (CHEMICON International, Temecula, CA, USA) and incubated for 1h at 37°C, protecting tubes from light. After washing, cells were resuspended in 150 µL of 7-AAD diluted 1:200 in 1X working dilution wash buffer (Merck Millipore), incubated for 5 min at room temperature in the dark, and analyzed via flow cytometry. Camptothecin 2 mM was used as positive control.

Measurement of mitochondrial potential

Mitochondrial potential was assessed by using JC-1 (5,59,6,69- tetrachloro-1,19,3,39-tetraethylbenzimidazol-carbocyanine iodide). After 24h of treatment with *Hemidesmus* 0.93 mg/mL, 200 µL of cell suspension were treated with 4 µL of 50X staining solution (Merck Millipore), containing JC-1 and 7-AAD. Cells were incubated for 30 min at 37°C and analyzed via flow cytometry. Valinomycin 0.09 µM was used as positive control. The experiments were also performed in the presence of bongkrekic acid (BA, 20 µM, Sigma) for 2h, carboxyatractyloside (CATR, 20 µmol/L, Sigma) for 90 min, ADP (500 µM) plus oligomycin (20 µg) for 1h, or

cyclosporine A (Cyc A, 1 µM, Sigma) for 1h. The cultures were preincubated with the above reported compounds for the indicated times then cultured with and without *Hemidesmus*.

Analysis of cytochrome c release

Mitochondrial cytochrome c release was monitored during cell death of digitonin-permeabilized cells immunolabeled for cytochrome c. After triggering of apoptosis by *Hemidesmus* treatment, we determined the fraction of cells that have not yet released their mitochondrial cytochrome c and were still highly fluorescent, as well as the fraction of apoptotic cells that have already released their mitochondrial cytochrome c and, therefore, were much less fluorescent. Cells ($1x10^6$) were harvested and treated with 1 mL digitonin (100 µg/mL, Sigma) for 5 min on ice. Cells were fixed in formaldehyde 4% for 20 min at room temperature, washed three times in PBS 1x and incubated in incubation buffer (0.5 g BSA in 100 mL PBS 1X) for 1h. The cells were incubated overnight at 4°C with 1:200 anti-cytochrome c monoclonal antibody (clone 7H8.2C12, Becton Dickinson) in incubation buffer, washed three times and incubated for 1 h at room temperature with FITC-labeled secondary antibody (1:100, Sigma). The cells were then analyzed to quantify FITC binding by flow cytometry. Mean fluorescence intensity values were calculated. Non-specific binding was excluded by gating around those cells which were labeled by the FITC-conjugate isotype control.

Measurement of intracellular Ca^{2+} ($[Ca^{2+}]_i$)

$[Ca^{2+}]_i$ was measured using the cell-permeable Ca^{2+} -sensitive fluorescent dye Fluo-3 acetoxymethyl ester. This dye freely permeates the surface membrane but, following hydrolysis by intracellular esterases, is trapped in cells as Fluo-3. The fluorescence intensity of Fluo-3 is enhanced after it binds to $[Ca^{2+}]_i$ and depends on the free calcium concentration[161]. Cells were incubated for 20 min at room temperature with 4 mM Fluo-3 acetoxymethyl ester diluted in Krebs-Ringer buffer [10 mM Dglucose, 120 mM NaCl, 4.5 mM KCl, 0.7 mM Na_2HPO_4, 1.5 mM NaH_2PO_4, and 0.5 mM $MgCl_2$ (pH 7.4 at 37°C); Sigma]. After washing, the cultures were treated with the indicated concentration of *Hemidesmus*. At the end of incubation, cells were washed in 5 mL of Ca^{2+} -free PBS at 37°C, resuspended in 1 mL of Ca^{2+} -free PBS at 37°C and analyzed immediately by flow cytometry. The experiments were also performed in the presence of nifedipine (10 µmol/L, Sigma), econazole (3 µM, Sigma), thapsigargin (1 µM, Sigma), aristolochic acid (50 µM, Sigma). The cultures were preincubated with the above reported compounds for 10 min then cultured with and

without *Hemidesmus* for 10 min. The experiments were performed in Ca^{2+}-containing medium (RPMI 1640).

Cell proliferation

Carboxyfluorescein diacetate succinimidyl ester diffuses freely into cells where intracellular esterases cleave off the acetate groups, converting it to a fluorescent, membrane-impermeant dye. The dye is equally distributed between daughter cells due to covalent crosslinking to proteins through its succinimidyl groups. The stain is long lived, allowing the resolution of at least three or four cycles of cell division. Propidium iodide is then added to distinguish the live from the dead cells. Through the use of differential staining by the two fluorescent dyes, live and dead proliferated and unproliferated cells can be distinguished. $25x10^6$ cells were incubated with carboxyfluorescein diacetate succinimidyl ester for 15 min at 37°C. After three washes, cell concentration was adjusted to $1x10^6$ cells/mL with complete medium. Cells were treated with different concentrations of *Hemidesmus* for 24h. After incubation, cells were treated with 5 mL of cell growth propidium iodide reagent (Merck Millipore), incubated in the dark at room temperature for 5 min, and analyzed via flow cytometry.

Cell-cycle distribution

Jurkat were treated for 8, 24, 48h and HL-60 for 24, 30 and 48h with different concentrations of *Hemidesmus*, and then fixed with ice-cold ethanol. Samples were then stained with 200 µL of Guava Cell Cycle Reagent (containing propidium iodide, Merck Millipore), incubated at room temperature for 30 min, shielded from light, and analyzed via flow cytometry.

Analysis of protein expression

After treatment for 24h with different concentrations of *Hemidesmus* (0.00-0.93 mg/mL), $1x10^6$ cells were fixed and permeabilized by 4% of paraformaldehyde in PBS 1X and 90% of cold methanol. They were then incubated with FITC-cyclin A (10:100, Beckman Coulter, Brea, CA, USA), p21 (2:100, Abcam, San Francisco, CA, USA), cyclin E (1:100, Abcam), CDK2 (6:100, Abcam), Bax (1:100, Santa Cruz Biotechnology, Santa Cruz, CA, USA), Bcl-2 (1:100, Santa Cruz Biotechnology), PE-conjugated p53 (5:100 BD biosciences, Franklin Lakes, NJ, USA), PSMD11 (1:100 Abcam), FITC 85 kDa fragment of cleaved poly ADP-ribose polymerase (1:100, PARP,

Invitrogen), vascular endothelial growth factor (VEGF) (1:500, Abcam), HIF-1α (1:500, Merck Millipore) antibodies. The staining with Noxa (1:10 Abcam), Mcl-1 (1:10 Abcam) antibodies was performed after 6h treatment with *Hemidesmus* due to their rapid protein turnover[162, 163]. The cells (except those stained with cyclin A, PARP and p53) were washed and incubated with FITC- labeled secondary antibody (1:100, Sigma). Moreover, in order to quantify the expression of membrane proteins, aliquots of $1.0x10^6$ cells treated with *Hemidesmus* were collected, washed twice in ice-cold 1X phosphate buffer (Sigma) and suspended in 20 µL of FITC-conjugated CD15 [3-fucosyl-N-acetyllactosamine (3-FAL)] (Biolegend, San Diego, CA, USA), 20 µL of FITC-conjugated CD14 [glycosylphosphatidilinositol (GPT)- linked] (Biolegend), or VEGFR-2-PE Cy-5.5 (2.5:10, Biolegend) and incubated for 30 min in the dark at 4°C. After incubation, the cells were washed twice and resuspended in 200 µL of phosphate buffer. The mean fluorescence intensity values were calculated. From each sample, 10,000 events were analyzed and non-specific binding was excluded by the isotype negative control antibody [FITC Mouse IgG1, k (FC)] (Biolegend).

RNA isolation

Extraction of total RNA was performed by *mirVana ™ miRNA Isolation Kit* (Life technologies, Waltham, MA, USA) after treatment of cells with different concentrations of *Hemidesmus* (0.00-0.93 mg/mL) for 6h, 12h and 24h. The first step of the procedure consists in the denaturation of the samples with the lysis buffer. Samples were then purified though a liquid-liquid Acid-Phenol:Chloroform extraction which also provides the removal of most DNA[164]. Ethanol was added to samples and then they were passed through a Filter Cartridge containing a glass-fiber filter which immobilizes the RNA. After a series of washing steps finally RNA was eluted with a low ionic strength solution. The RNA collected is stable -20°C for several months.

In order to quantify the amount of extracted RNA was used the NanoVue (GE Healthcare). This instrument is able to measure small volume of highly concentrated nucleic acids at the wave length of 260nm.

Analysis of RNA quality

The quality of the RNA extracted has been quantified by microfluidic capillary electrophoresis with the Agilent 2100 bioanalyzer (Agilent, Santa Clara, CA, USA). The bioanalyzer is an automated bio-analytical device using microfluidics technology that provides electrophoretic separations in an automated and reproducible manner[165]. Small portions of RNA are separated in the different

channels of the microfabricated chips according to their molecular weight and are detected via laser-induced fluorescence detection. The result of the analysis is provided as an electropherogram where the amount of RNA of a given size is correlated to the amount of its measured fluorescence. Though the use of an algorithm, the software is able to calculate a RNA integrity number (RIN). The RIN algorithm is based on a selection of informative features from the electropherograms. For this purpose, each electropherogram is divided into nine adjacent segments: a pre-region, a marker-region, a 5S-region, a fast-region, an 18S-region, an inter-region, a 28S-region, a precursor-region and a post-region. Among these, based on their maximum height and ratios, total RNA ratio and the 28S are the most important features. For classification of RNA integrity, ten categories are defined from ≤1 (totally degraded RNA) to 10 (fully intact RNA)[166].

cDNA synthesis

The cDNA synthesis from the extracted RNA was made with the High Capacity cDNA Reverse Transcription Kit (Life Technologies). The protocol provides that for each sample, in a sterile, nuclease free, thin-walled PCR tube on ice, 10 µL of Master Mix (composition in the table below) should be added to 200 µg of RNA.

RT reaction Mix components	**For each sample µL**
10RT Buffer	2
20x dNTP Mix (100mM	0.08
10x RT Random Primers	2
Multiscibe Reverse Transcriptase	1
RNase Inhibitor	1
Nuclease free water	3.02
Total	10

The thermal cycling conditions were: 25 cycles 10 min at 25°C, 120 min at 37°C, 5 min at 85°C, and finally 4°C forever. The cDNA was stored at -20°C.

Real Time quantitative RT-PCR (real time qRT-PCR)

The real time qRT-PCR is an evolution of the standard PCR (polymerase chain reaction) technique commonly used to quantify DNA or mRNA. The real time qRT-PCR is an amplification and quantification method where the detection of the target sequence occurs in the exponential amplification phase and not at the plateau as occur in the regular PCR. Through the use of specific primers labeled with fluorescent dyes, the relative number of copies of a particular DNA or RNA sequence can be determined. These probes are oligonucleotides from 20 to 30 base pairs length designed to be complementary to the sequence of the target gene that has to be amplified. These probes are equipped in the 5' end sequence with a fluorophore (Reporter or R), usually green, and in 3' with a Quencher (Q), usually red. As long as the probe is inactive, the close gap between the R and the Q delete the fluorescence signal of the R. The process could be described in 4 passages: i) polymerization: R and Q are attached to the 5' and 3' end of a probe; ii) strand displacement, when both dyes are attached to the probe, R dye emission is quenched; iii) cleavage, during each extension cycle: the DNA polymerase system cleaves the R dye from the probe, iv) completion of polymerization: the R dye emits its characteristic fluorescence. The signal is extremely specific because the probes do not interfere and the fluorescent signal is present only when the binding between probes and target DNA is correct.

Analysis of mRNA

TaqMan technology was used to analyze mRNA. The qRT-PCR was performed using ABI 7900 HT (TaqMan^{TM}, Life Technologies).

Components	**For each sample** **µL**
TaqMan Universal Master Mix (2x)	12.5
TaqMan Assay (60x)	1,25
cDNA	2
Water	11,25
Total	26

The thermal cycling conditions were: 10 min at 95°C, 40 cycles: 15 sec at 95°C and 1 min at 60°C.

Gene	TaqMan Gene Expression Assay
18S (Endogenous control)	Hs99999901_s1
GADPH (Endogenous control)	Hs99999905_m1
TP53	Hs01034249_m1
MCL1	Hs01050896_m1
PMAIP1 (Noxa)	Hs00560402_m1
PSMD11 (Proteasome)	Hs00160660_m1
BAX	Hs00180269_m1
BCL2	Hs00608023_m1
VEGF	Hs00900054_m1
HIF (HIF-1α)	Hs00153153_m1
KDR (VEGFR-2)	Hs00176676_m1

Using the data obtained from the real time qRT-PCR analysis has been made a relative quantification of the expression of the genes of interest. This quantification requires an endogenous control 18S, used to normalize the quantity of cDNA, and a calibrator represented by our untreated sample. The relative expression was calculated as described below:

- endogenous control normalization: $Ct_{\text{target gene}} - Ct_{18S} = \Delta Ct$
- normalization on the calibrator: $\Delta Ct_{\text{target gene}} - \Delta Ct_{\text{calibrator}} = \Delta\Delta Ct$
- relative expression of the target gene = $2^{-\Delta\Delta Ct}$

Detection of levels of reactive oxygen species

The formation of ROS in Jurkat cells was quantified after 10 min, 1h, 3h and 6h of treatment with different concentration of *Hemidesmus* (0.00-0.93 mg/mL). Briefly, each sample containing $1x10^6$ cells was treated with 10 µM of 2′,7′-Dichlorofluorescin diacetate (H_2DCFDA) (Sigma), incubated for 20 min at 37°C, 5% CO_2 , in the dark, washed and analyzed by flow cytometry. H2DCFDA is a non polar and a non fluorescent compound that diffuses passively through the cellular membrane. In presence of ROS, the activation of intracellular esterases results in the cleavage of the diacetate

groups and therefore to the formation of the highly fluorescent product dichlorofluorescein (DHF)[167].

Nitro blue tetrazolium (NBT) reduction assay

This assay was used to evaluate the ability of *Hemidesmus* (0.00-0.62 mg/mL) to produce superoxide when challenged with 12-O,–tetradecanoylphorbol 13-acetate (TPA) after treatment of HL-60 for 72h. The assay was performed according to Catino and Miceli[168]. Approximately $1.0x10^6$ cells were treated with *Hemidesmus indicus* and freshly prepared TPA/NBT solution (1X phosphate buffer containing 0.2% NBT and 200 ng/mL TPA) and incubated for 30 min at 37°C. The reaction was stopped by placing the samples on ice for 5 min. Cells were then smeared on glass slides. Positive cells reduced NBT yielding intracellular black–blue formazan deposits and this was determined by microscope examination (10X total magnification) of 500 cells. The results were expressed as percentage of positive cells over total cells. DMSO 1% (v/v) was used as positive control.

Adherence to the plastic substrate

Dish-anchored cells were easily distinguished from the undifferentiated suspended cells. Approximately $1.0x10^6$ cells were grown in normal cell growth conditions. After 72h of treatment with different concentrations of *Hemidesmus* (0.00-0.62 mg/mL), the medium was removed and the remaining non-adherent cells were gently washed away with 1X phosphate buffer. The number of adherent cells was counted on a light microscope. Results were reported as number of attached cells[169]. TPA 50 nM was used as positive control.

α-naphthyl acetate esterase activity

Assay for α-naphthyl acetate esterase was performed using the cytochemical kit from Sigma (91-A). Cellular esterases are ubiquitous, apparently representing a series of different enzymes acting upon select substrates. Under defined reaction conditions, it may be possible to determine hematopoietic cell types, using specific esterase substrates. The assay allows to identify granulocytes from monocytes. HL-60 cells were incubated with *Hemidesmus* (0.00-0.62 mg/mL) and α-naphthyl acetate (NAE) in the presence of freshly formed diazonium salt for 72h. Enzymatic hydrolysis of ester linkages liberates free naphthol compounds. These couple with the diazonium salt, forming

highly colored deposits at sites of enzyme activity[170]. Differentiated cells were assessed by microscopic examination of a minimum of 200 cells (in duplicate) for each experiment.

TEM analysis

After 72h of treatment with *Hemidesmus* (0.00-0.62 mg/mL), cells were washed and fixed with 2.5% glutaraldehyde in 0.1 M phosphate buffer (pH 7.3), post-fixed with 1% OsO_4 in the same buffer, alcohol dehydrated and embedded in araldite[171]. To obtain better direct ultrastructural observations, semithin sections were stained with 1% toluidine blue at 60°C and observed by light microscopy. Thin sections were collected on nickel grids, stained with uranyl acetate and lead citrate, and analyzed with a Philips CM 10 electron microscope.

***In vitro* endothelial cell tube formation assay**

The ability of *Hemidesmus* to influence the endothelial cell tube formation was screened on HUVECs using the *In Vitro* Angiogenesis Assay Kit (Merck Millipore, ECM625). The assay is based on culturing cells in an ECMatrix™, a solid gel of basement proteins prepared from the Engelbreth Holm-Swarm (EHS) mouse tumor. In particular, ECMatrix™ consists of laminin, collagen type IV, heparan sulfate proteoglycans, entactin and nidogen. It also contains various growth factors (TGF-β, FGF) and proteolytic enzymes (plasminogen, tPA, MMPs) that occur normally in tumors. This gel is optimized for maximal tube-formation, endothelial cells can rapidly align and form tube-like structures. Briefly, each well, of a 96-well plate, was coated with 50 µl of cold ECMatrix™ solution and the plate was kept at 37°C for 1h to allow the solidification of the ECMatrix™. Afterwards, $1x10^4$ HUVECs were seeded in each well in a total volume of 150 µL of EGM and treated for 6h in hypoxic or normoxic conditions with various concentrations of *Hemidesmus* (0.00–0.93 mg/mL) and VEGF 10 µg/mL as positive control, and their associations. Pictures from three randomly selected fields were taken using a microscope Eclipse E800 Nikon (Nikon, Tokyo, Japan). The capillary tube branch points formed were counted in four random view-field per well.

Invasion assay

Cell invasion assay was performed with the use of QCM™ 24-well Fluorimetric Cell Invasion Assay Kit (ECM554; Merck Millipore) according to the manufacturer's instructions. In the tumor

metastasis process a crucial role is attributed to the invasion of cancer cells through the extracellular matrix (ECM). Those cells initiate invasion by adhering and spreading along the blood vessel walls. The invasion assay exploits a polycarbonate membrane with an 8 µm pore size coated with a thin layer of ECMatrix™, a reconstituted basement membrane matrix of proteins derived from the EHS mouse tumor (as described above). The gel, simulating the ECM, occludes the membrane pores and physically inhibits the passage of non-invasive cells. Briefly, $1.25x10^5$ HUVECs treated with *Hemidesmus* (0.00-0.93 mg/mL) or untreated were loaded in the upper compartment, while in the lower chamber was used EGM supplemented with 10% FBS as chemoattractant, and the plate was incubated for 24h in hypoxic and normoxic conditions. Cells able to invade through the membrane were detached from the bottom using a Cell Detachment Buffer, and then were fixed and stained with Staining buffer constituted by CYQuant GR Dye. The fluorescence of the invaded cells was evaluated by a fluorescence plate reader (Tecan, Männedorf, Swiss) using 480/520 nm filter set. The invaded cell number was reported as relative fluorescence variation compared to the control.

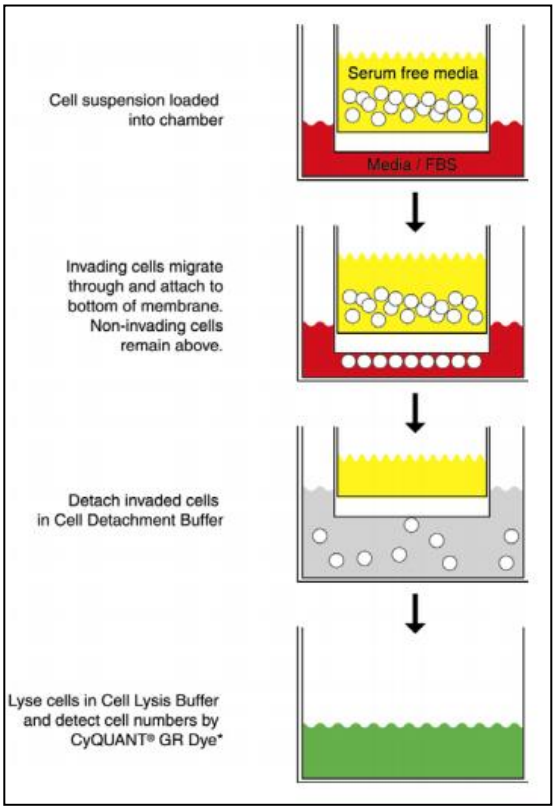

Figure 10: Schematic overview of the invasion and migration assays.

Migration assay

In order to quantify the migration potential of HUVECs treated with *Hemidesmus* (0.00-0.93 mg/mL) in hypoxic and normoxic condition was used the QCM™ 24-well Fluorimetric Cell

Migration Kit (ECM509; Chemicon). Cell migration is a crucial function of normal cellular processes, like embryonic development, angiogenesis, wound healing, immune response, and inflammation. An unregulated cell migration can cause vascular disease and it is considered fundamental for the initiation of the metastatic process[172]. The assay was performed in a migration chamber that includes an 8 µm pore size polycarbonate membrane. This pore size supports optimal migration for most epithelial and fibroblast cells. In particular, $2.00x10^5$ HUVECs cells treated with o without *Hemidesmus* (0.00-0.93 mg/mL) were loaded in the upper compartment, while in the lower chamber was used EGM supplemented with 10% FBS as chemoattractant, and the plate was incubated for 6h. Cells able to migrate through the membrane were detached from the bottom using a Cell Detachment Buffer, and afterwards fixed and stained with Staining buffer constituted by CYQuant GR Dye. The fluorescence of the migrated cells was evaluated by a fluorescence plate reader (Tecan) using 480/520 nm filter set. The migrated cell number was reported as relative fluorescence variation compared to the control.

Colony-forming unit (CFU) assay

This method was used to determine the potential of sorted CD34+ from AML and healthy donor cord blood samples to form colonies in a methylcellulose based medium after 24h treatment with *Hemidesmus* (0.00-1.55 mg/mL) and piperlongumine (0-14 µM). 1×10^5 cells/mL AML cells and $1x10^3$ cells/mL cord blood cells were mixed with MethoCult GF H4434 containing 50 ng/mL stem cell factor, 10 ng/mL GM-CSF, 10 ng/mL IL-3, 50 ng/mL G-CSF, and 3 units/mL erythropoetin (StemCell Technologies) in a poly tube. Then 1 mL mixtures were placed into each of two 35 mm culture dishes using a 3 mL syringe and a 16 gauge blunt-end needle. In order to spread the methylcellulose evenly the dishes were gently rotated and placed in a 100 mm petri dish with a third one full of sterile water. These plates were incubated for 14 days at 37°C and 5% CO_2, and then was evaluated the colony formation capability of the cells through a microscopic analysis (40X magnification, Nikon Instruments Inc, Amsterdam, Netherland). The colonies were counted and separated in 4 groups on the base of their morphological characteristics.

- CFU-GEMM: Colony forming units of granulocytes, erythrocytes, macrophages and megakaryocytes progenitor.
- BFU-E: Burst forming unit erythroid.
- CFU-GM: Colony forming units of granulocyte-macrophage progenitor.
- Cluster: Not yet colonies (<30 cells).

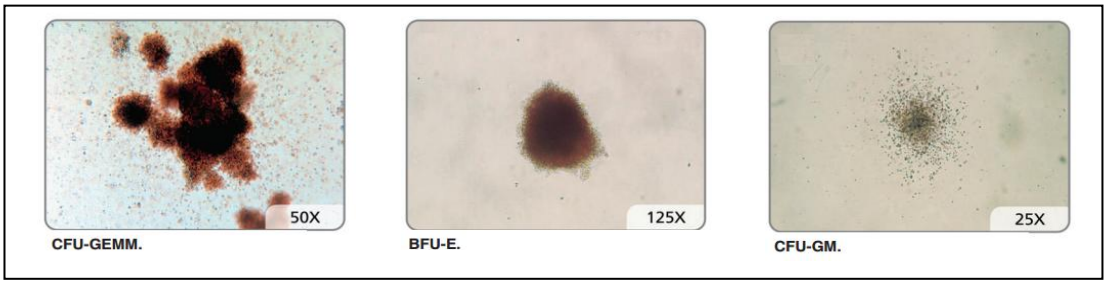

Figure 11: Pictures of three types of colonies.

Statistical analysis

All results are expressed as the mean of at least 3 biological replicates. Differences among treatments were evaluated by one-way or two-way ANOVA, followed by Dunnett or Bonferroni post-test, using GraphPad InStat version 5.00 (Graphpad Prism, San Diego, CA, USA). P,0.05 was considered significant. Interactions between *Hemidesmus* and anticancer drugs were classified using the combination index (CI). CI analysis provides qualitative information on the nature of drug interaction, and CI, a numerical value calculated as described in the following equation, also provides a quantitative measure of the extent of drug interaction[173].

$$CI = \frac{C_{A,x}}{IC_{x,A}} + \frac{C_{B,x}}{IC_{x,B}}$$

CA,x and CB,x are the concentrations of drug A and drug B used in combination to achieve 6% drug effect. ICx,A and ICx,B are the concentrations for single agents to achieve the same effect. A CI of less than, equal to, and more than 1 indicates synergy, additivity, and antagonism, respectively.

Chapter 4

Results

Hemidesmus indicus contains 2H4MBAL, 3H4MBAL and 2H4MBAC

Hemidesmus was found to contain 2H4MBAL, 3H4MBAL and 2H4MBAC (Fig. 12A). NMR data on the decoction and on the enriched fraction are shown in Fig. 12B and 12C. The amounts found in the decoction (31 mg/mL) were: 0.0025±0.001 mg/mL for 2H4MBAL, 0.0018±0.003 mg/mL for 3H4MBAL, 0.0022±0.005 mg/mL for 2H4MBAC. The analyses were performed on the decoction obtained from three different batches. The difference among the batches in the phytomarker content was not significant.

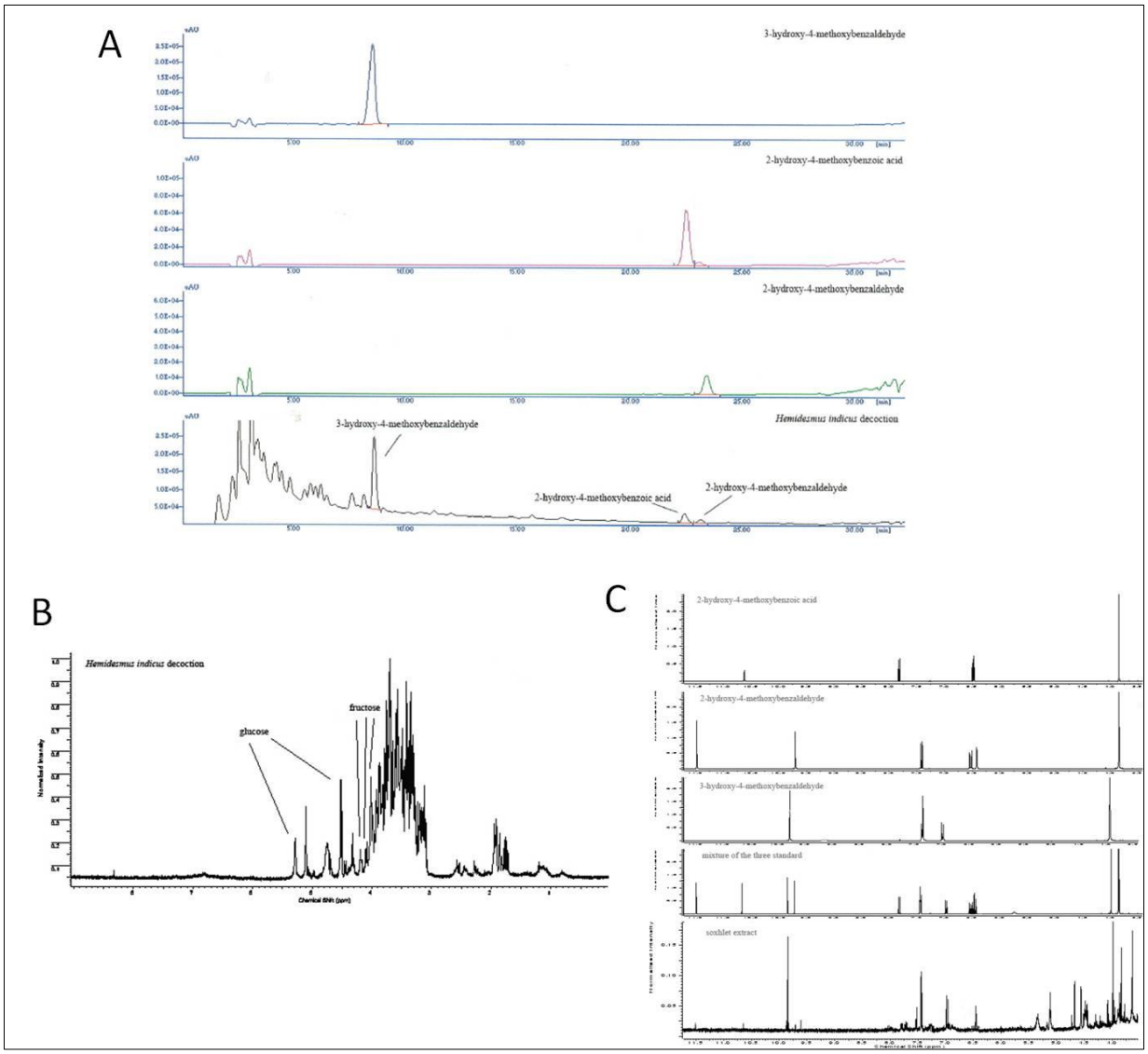

Figure 12: HPLC chromatogram (A), NMR analysis (B) of Hemidesmus and NMR spectrum of an enriched fraction obtained by Soxhlet extraction, compared with ^{1}H NMR evidences of each reference standard (C).

Hemidesmus indicus induces apoptosis in Jurkat cells

Based on the cytotoxicity results (data not shown), cells were treated with concentrations of *Hemidesmus indicus* similar or smaller than the IC_{50} (0.62, 0.93, 1.55 mg/mL) for 24 h. *Hemidesmus* treatment induced apoptosis at all the concentrations tested and in all tested cell lines (Fig. 13A). For example, after treatment of Jurkat cells with 0.93 mg/mL of *Hemidesmus*, the incidence of apoptotic cells was 36.9% (*versus* 4.8% in the control). They increased to 44.8% after treatment with the highest dose studied (Fig. 13B). However, 1.55 mg/mL of *Hemidesmus* induced a significant increase of necrotic cells (Fig. 13B). Similar results were recorded for the other cell lines (Fig. 13A). Since the highest increase in apoptotic cells with respect to the control was seen in Jurkat cells, the study continued on this cell line. For excluding necrotic events, concentrations of up to 0.93 mg/mL were used. No induction of apoptosis was observed in Jurkat cells following treatment with 2H4MBAL, 3H4MBAL or 2H4MBAC. The association between the two aldeydes and the acid induced a significant increase in the apoptotic cell fraction (16% of apoptotic cells *vs* 3% in the untreated sample) (Fig. 13C).

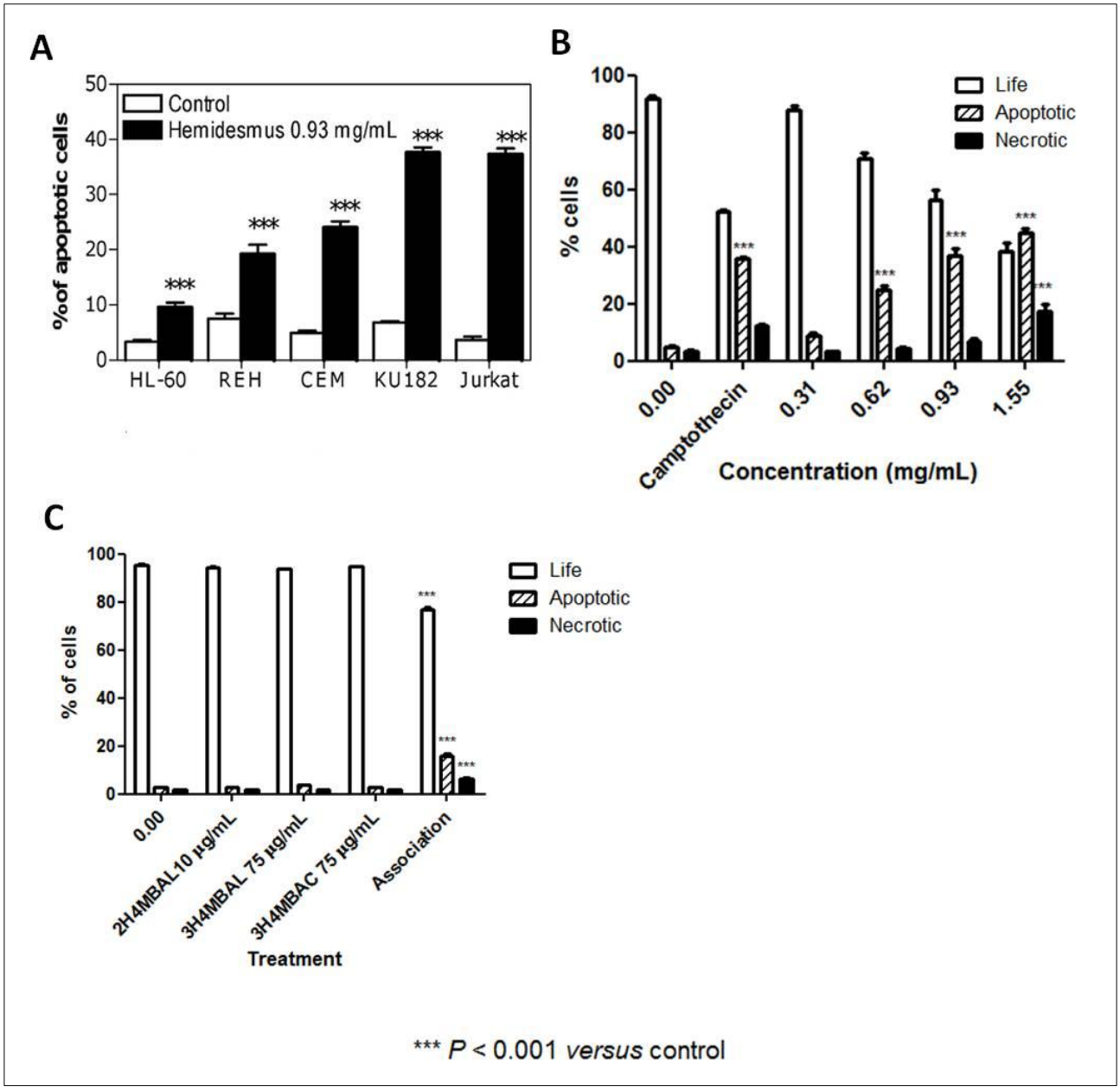

Figure 13: Induction of apoptosis by Hemidesmus indicus. Fraction of viable, apoptotic and necrotic cells in different leukemic cell lines (A) and in Jurkat cells (B). Induction of apoptosis by single phytomarkers and their association in Jurkat cells (C).

Hemidesmus indicus showed the ability to affect caspase-3 but not caspase-8 activity and activate PARP. Caspase-3 activity was significantly increased in cells treated with *Hemidesmus* (0.93 mg/mL). The percentage of cells with caspase-3 activated in non-treated cultures was about 8%, which was increased to 17.4% in cells treated with *Hemidesmus* 0.93 mg/mL (Fig. 14A). An important reporter for caspase-3 activation is PARP. *Hemidesmus* (0.93 mg/mL) induced an increase of PARP cleavage of about 2.7 times compared to the control (Fig. 14B). Figure 14C shows a representative cytogram where two well-defined cell populations are distinguishable in

Hemidesmus-treated cells after labeling with FITC 85 kDa fragment of cleaved PARP. Only one population characterized by a lower fluorescence intensity (white histogram) was recorded in untreated cells. Unstimulated Jurkat T cells incubated with FAM-LETD-FMK generated a low detectable fluorescence signal, indicating that levels of active caspase-8 were low in these cells. Caspase-8 activity increased after treatment with the positive control camptothecin but remained at basal levels after treatment with 0.93 mg/mL of *Hemidesmus* (Fig.14D).

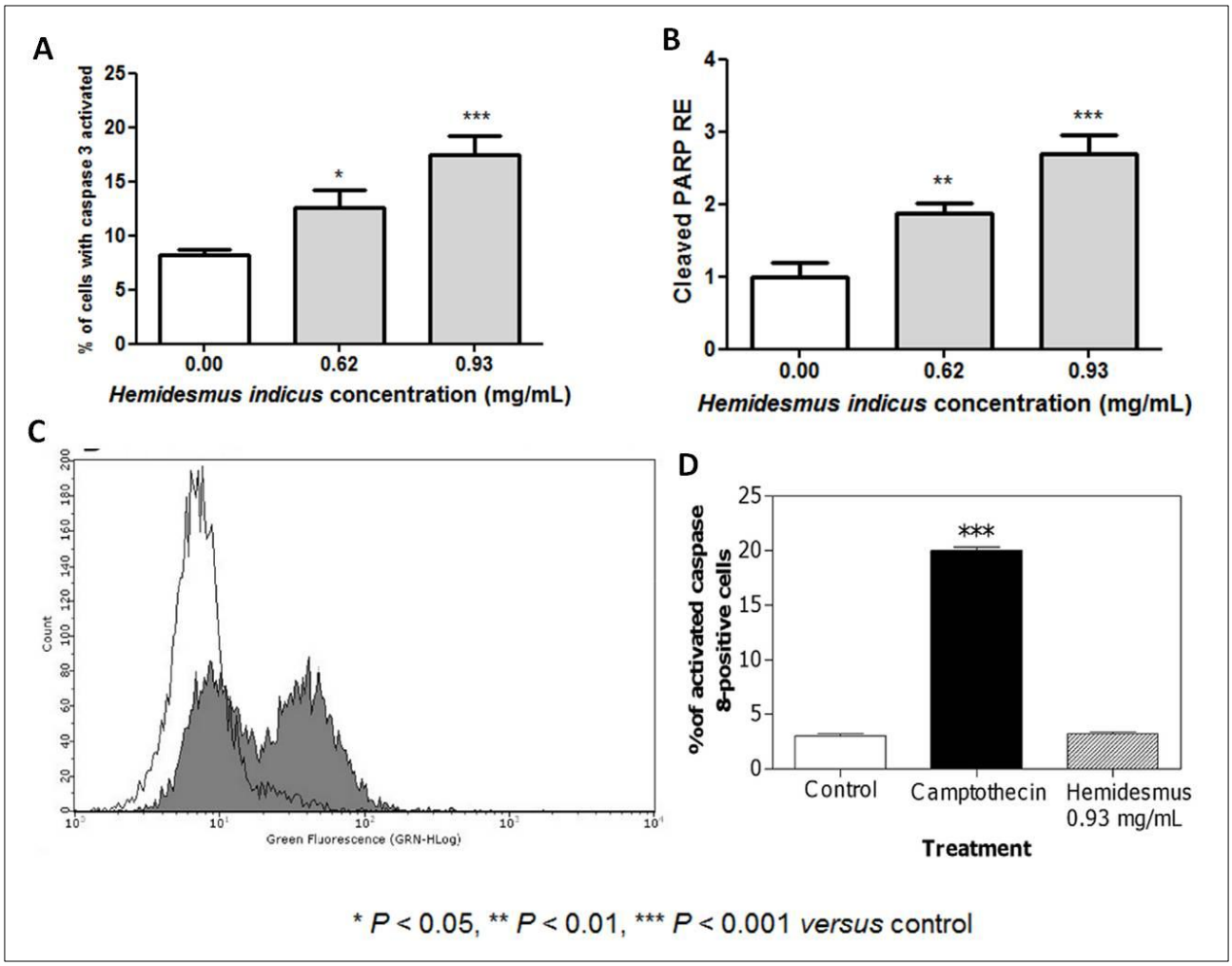

Figure 14: Activation of caspase-3(A), cleavage of PARP (B–C) and activation of caspase-8 (D) following treatment with Hemidesmus for 24h.

In order to determine the ability of *Hemidesmus indicus* to disrupt mitochondrial transmembrane potential, Jurkat cells were treated with 0.93 mg/mL of *Hemidesmus indicus*. The treatment resulted in a significant break-down of the mitochondrial membrane potential. The effect of *Hemidesmus* 0.93 mg/mL resulted even greater than that observed for valinomycin, used as positive control (Figure 15A). Cytochrome c release from mitochondria to cytosol is a hallmark of apoptosis and is used to characterize the mitochondria-dependent pathway of this type of cell death. After treatment

with *Hemidesmus* (0.93 mg/mL), the fraction of cells that retained their mitochondrial cytochrome c, or the highly fluorescent cells, gradually decreased and emerged as a population of low fluorescent cells (Fig. 15E). Since the mitochondrial pathway resulted clearly involved in the pro-apoptotic activity of *Hemidesmus*, we investigated whether classic adenine nucleotide translocator modulators, such as CATR and BA, or Cyc, which targets cyclophilin D in the matrix, could interfere with the action of *Hemidesmus* on mitochondrial depolarization. Mitochondrial depolarization induced by *Hemidesmus* was not specifically inhibited by BA, CATR or Cyc A (Fig. 15B).

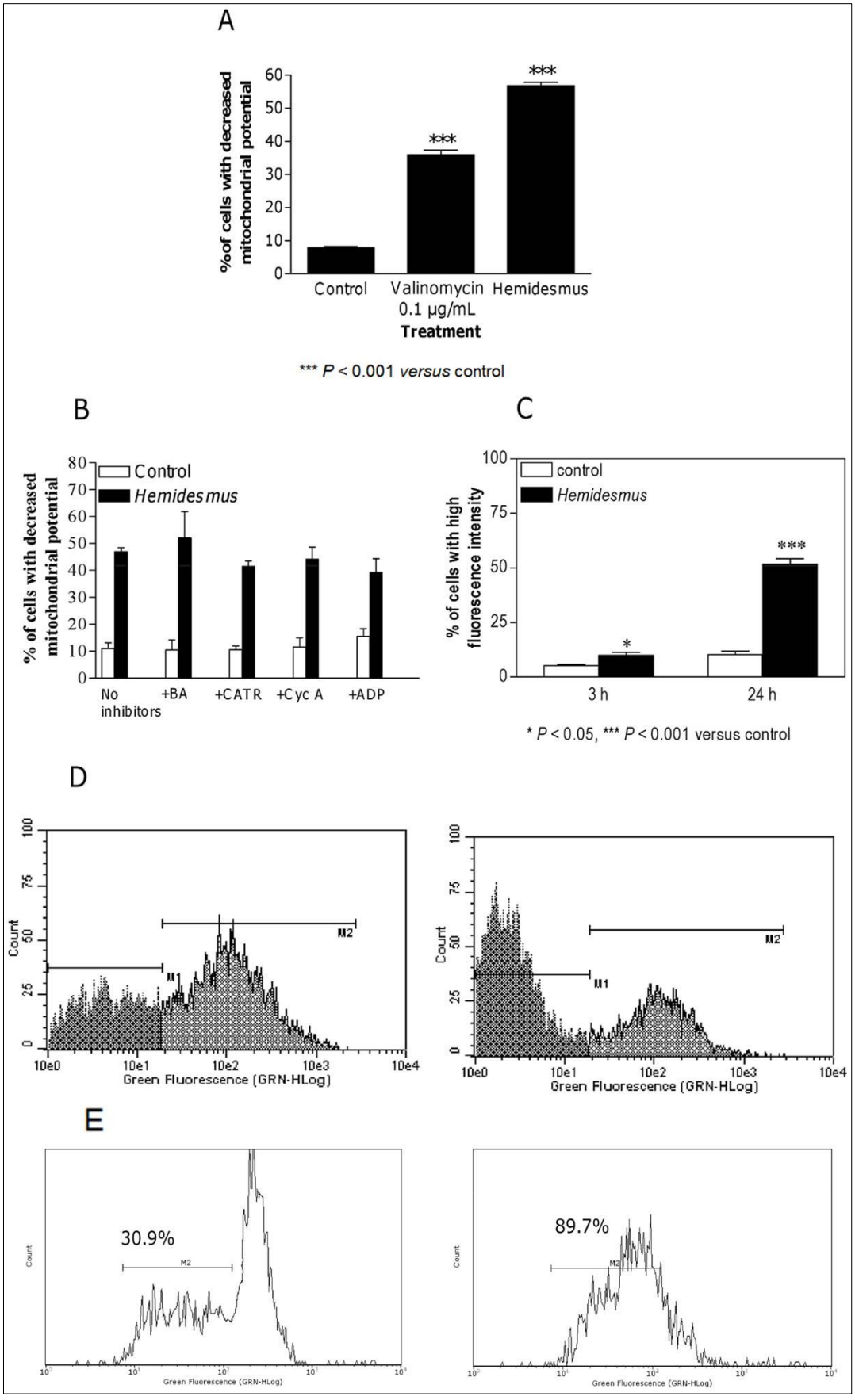
A
%of cells with decreased mitochondrial potential
60
50
40
30
20
10
0
***
***
Control
Valinomycin 0.1 µg/mL
Hemidesmus
Treatment
*** P < 0.001 versus control
B
% of cells with decreased mitochondrial potential
80
70
60
50
40
30
20
10
0
Control
Hemidesmus
No inhibitors
+BA
+CATR
+Cyc A
+ADP
C
% of cells with high fluorescence intensity
100
75
50
25
0
control
Hemidesmus
*
***
3 h
24 h
* P < 0.05, *** P < 0.001 versus control
D
Count
M1
M2
10e0
10e1
10e2
10e3
10e4
Green Fluorescence (GRN-HLog)
E
30.9%
89.7%
M2
Count
Green Fluorescence (GRN-HLog)

Figure 15: Alterations in mitochondrial membrane permeability in absence (A) and presence (B) of inhibitors following treatment with Hemidesmus 0.93 mg/mL. Fraction of cells with increased $[Ca^{2+}]_i$ following 3 or 24h culture in the absence or presence of Hemidesmus (0.93 mg/mL) (C), flow cytometric analysis of $[Ca^{2+}]$(D) and cytochrome c (E) following 24h culture in the absence or presence of Hemidesmus (0.93 mg/mL).

Elevation of cytosolic Ca^{2+} is sufficient to induce mitochondrial permeability transition pore opening and brings to apoptosis in different cell systems[161]. We therefore studied the ability of *Hemidesmus* to modulate $[Ca^{2+}]_i$. Following 24 h-treatment with *Hemidesmus*, $[Ca^{2+}]_i$ was found to be about 5 times higher than that of the controls (Fig. 15C). Short times of exposure (3h) induced a smaller but still significant increase in $[Ca^{2+}]_i$ (Fig. 15C). The recorded mean fluorescence intensity values clearly indicated two defined cell populations with different intracellular calcium levels (Fig. 15D). In *Hemidesmus*-treated cells, the mean fluorescence values were 162.88 and 6.49, respectively (Fig. 15D). Experiments were performed to explore the pathway of *Hemidesmus*-induced $[Ca^{2+}]_i$ raise. The removal of extracellular Ca^{2+} did not abolish the $[Ca^{2+}]_i$ raise induced by *Hemidesmus*. Some Ca^{2+} influx inhibitors, such as nifedipine and econazole, failed to affect *Hemidesmus*-induced $[Ca^{2+}]_i$ rise in Ca^{2+}-containing medium (Fig. 16A and B). In contrast, aristolochic acid and thapsigargin significantly increased *Hemidesmus*-induced $[Ca^{2+}]_i$ rise (Fig. 16C and D).

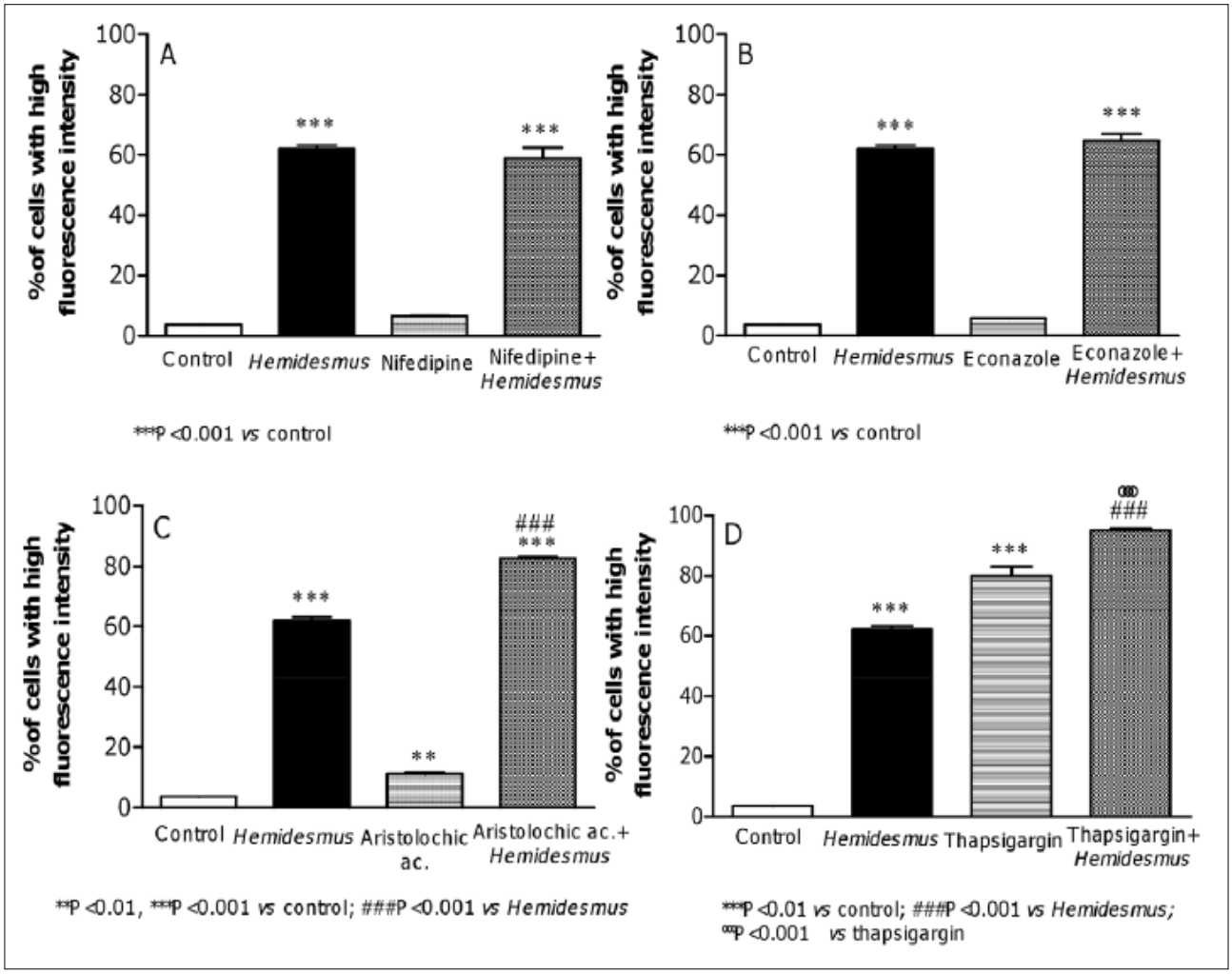

Figure 16: Effect of different inhibitors on Hemidesmus-induced $[Ca^{2+}]_i$ raise. Effects of nifedipine (A), econazole (B), aristolochic acid (C) and thapsigargin (D) on Hemidesmus-induced $[Ca^{2+}]_i$ raise.

Moreover, *Hemidesmus indicus* showed the ability to stymulate the intracellular formation of ROS. We found that Jurkat treated for 10 min, 1h, 3h and 6h with *Hemidesmus* a dose-dendently increased in the formation of ROS (Fig. 17 A-D). In order to prove the role of the ROS formation in the pro-apoptotic activity evoked by *Hemidesmus*, we studied its association with NAC, a well-known antioxidant agent, in terms of induction of apoptosis. The association resulted in a significant reduction of the pro-apoptotic acvtivity of *Hemidesmus* (Fig. 17E).

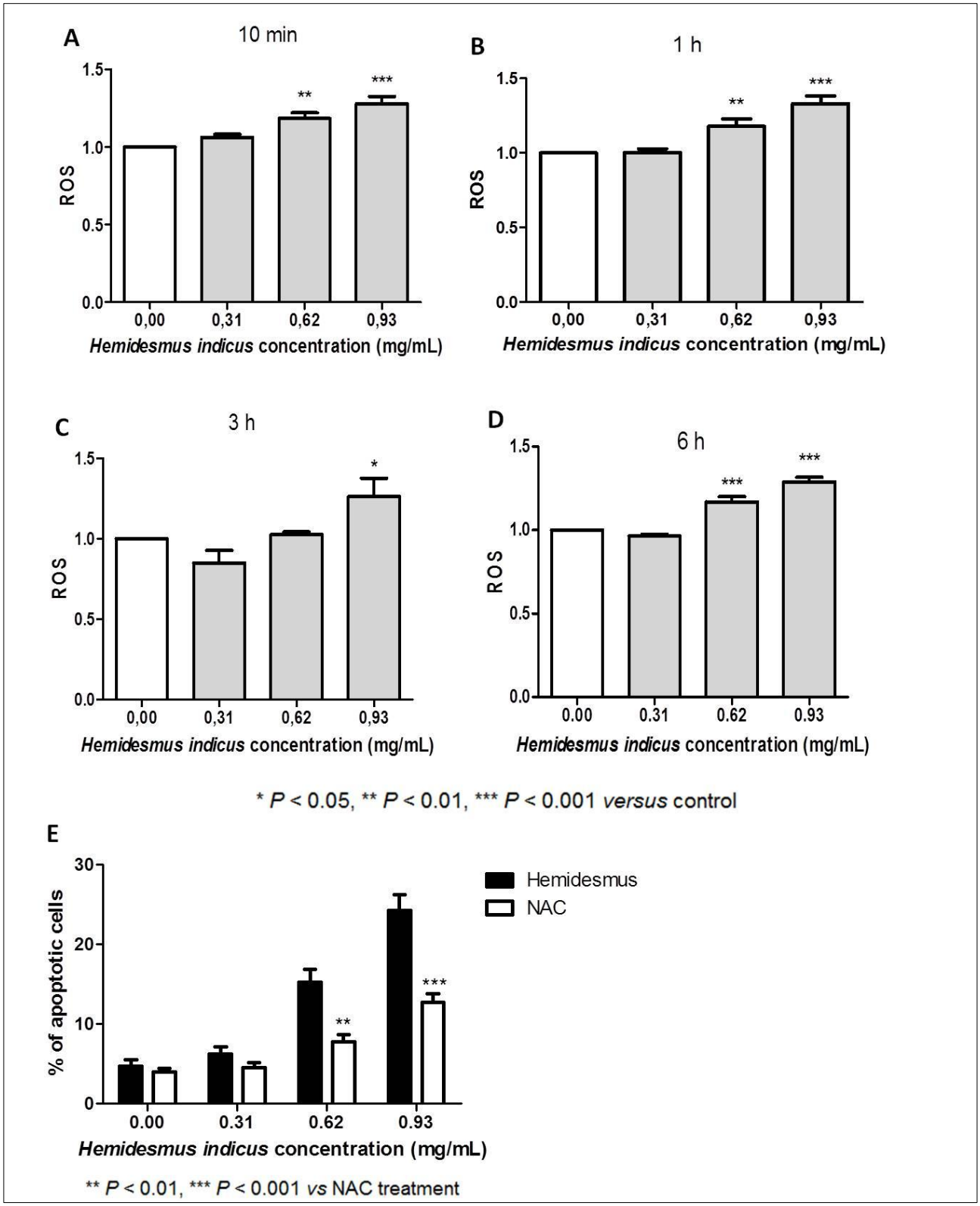

Figure 17: ROS relative expression after treatment of Jurkat cells for 10 min (A), 1h (B), 3h (C) and 6h (D) with Hemidesmus. Induction of apotptosis by Hemidesmus in absence and presence of NAC after treatment of Jurkat cells for 24h (E).

In order to define the mechanism of action whereby *Hemidesmus indicus* induces apoptosis in Jurkat cells, the pre- and post- transcriptional modulation of some proteins, involved in the regulation of the apoptotic intrinsic pathway, has been analyzed. The quality of the total RNA extracted, checked with the BioAnalyzer 2100, reported RIN values between 9 and 10, showing a good RNA integrity at all tested concentrations.

The p53 tumor suppressor promotes apoptosis through transcription-dependent and -independent mechanisms that act in concert to ensure that cell death program proceeds efficiently. Its inactivation can promote tumor progression and chemoresistance[174]. *Hemidesmus* did not induce significant variation in the expression of p53 (Fig. 18A), while showed a clear dose-dependent down-regulation of p53 mRNA (Fig. 18B). *Hemidesmus* 0.93 mg/mL induced the highest down-regulation in the p53 mRNA level after 6h of treatment (0.53±0.05).

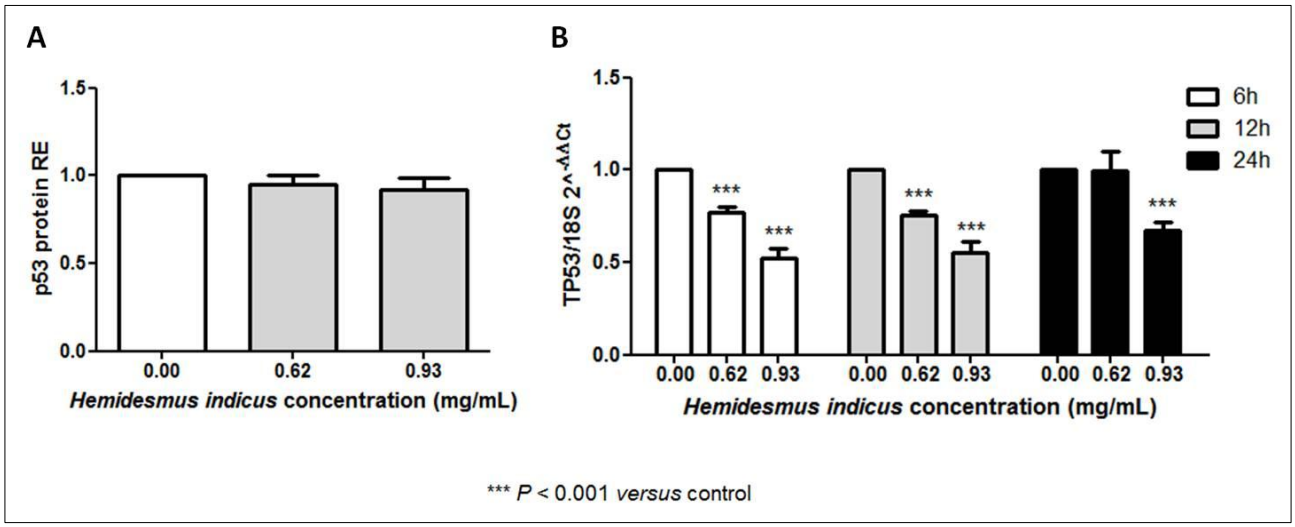

Figure 18: p53 protein relative expression after treatment of Jurkat cells with Hemidesmus for 24h. p53 mRNA relative expression following 6h, 12h and 24 h culture with Hemidesmus (B).

The study of the pro- and anti-apoptotic proteins modulated by *Hemidesmus* continued analyzing its ability to affect the expression of Noxa and Mcl-1 at protein and gene level and their ratio. *Hemidesmus* did not induce any modulation in the expression of Noxa (Fig. 19A). On the other hand, a clear, dose-dependent up-regulation of the gene expression of *PMAIP1* was induced by *Hemidesmus* at all treatment times (Fig. 19B). The highest expression of *PMAIP1* was reported after treatment of Jurkat cells for 6h with *Hemidesmus* 0.93 mg/mL (2.68±0.10). The ability of *Hemidesmus* to increase the mRNA levels of *PMAIP1* appeared time-dependent. Indeed, increasing the time of treatment reduced the induction of *PMAIP1* (Fig. 19B). Moreover, *Hemidesmus* reduced Mcl-1 protein expression after 6h treatment at all tested doses (Fig. 19C). The mRNA expression of

MCL1 was increased by treating cells with *Hemidesmus* at all time points and reached the highest effect after 6h treatment with *Hemidesmus* 0.93 mg/mL (1.99±0.20) (Fig. 19D). Noxa/Mcl.1 proteins ratio was determined by using the relative expression of both proteins normalized to the untreated sample (control) after 6h treatment with *Hemidesmus*. The Noxa/Mcl-1 ratio was significantly higher compared to the control group and reached its peak at the concentration 0.62 mg/mL (1.67±0.20) (Fig. 19E).

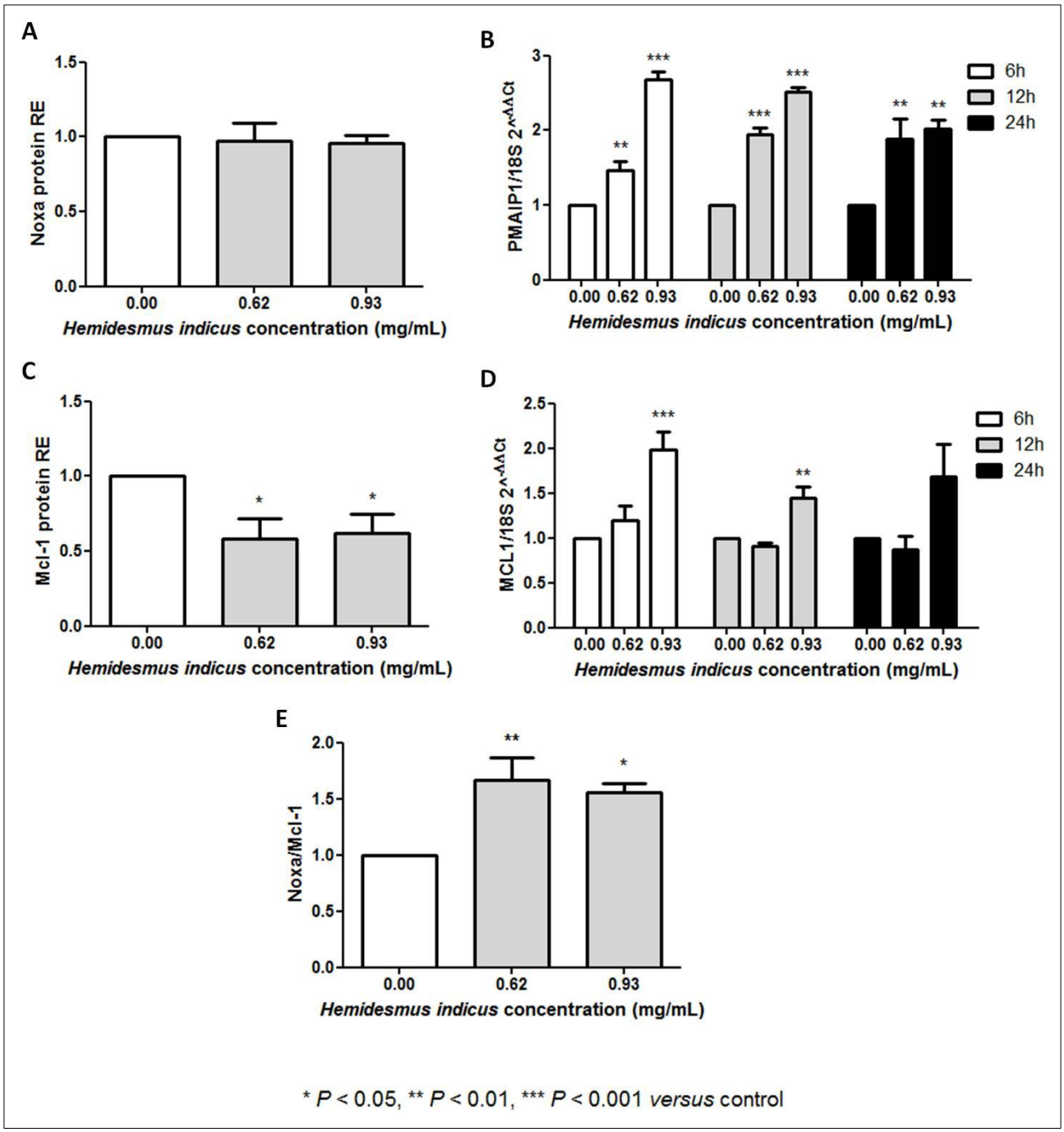

Figure 19: Relative expression of Noxa and Mcl-1 protein levels (A, C) and variation of Noxa/Mcl-1(E) after 6h treatment of Jurkat cells with Hemidesmus. Modulation of Noxa (B) and Mcl-1 (D) mRNA following 6h, 12h and 24h culture with Hemidesmus.

Furthermore, *Hemidesmus indicus* affected the expression of Bax and Bcl-2 protein levels. Both Bax (Fig. 20A) and Bcl-2 (Fig. 20B) expression was found to be significantly increased in treated cells. Bax-to-Bcl-2 ratio was determined by using the mean fluorescence intensity value of *Hemidesmus*-treated cells that was normalized to the mean fluorescence intensity of untreated (control) samples within each group (Fig. 20C). The Bax-to-Bcl-2 ratio was significantly higher than the control group. The expression levels of *BAX* and *BCL2* were strongly affected by the treatment with *Hemidesmus*. Both genes were down-regulated in a dose-dependent manner at all time points (6h, 12h and 24h) (Fig. 20D-E). Notably, the mRNA down-regulation of Bax was more pronounced in samples treated for 24h with *Hemidemsus* 0.93 mg/ml, while the expression of Bcl-2 was lowest after 12h treatment with the same concentration.

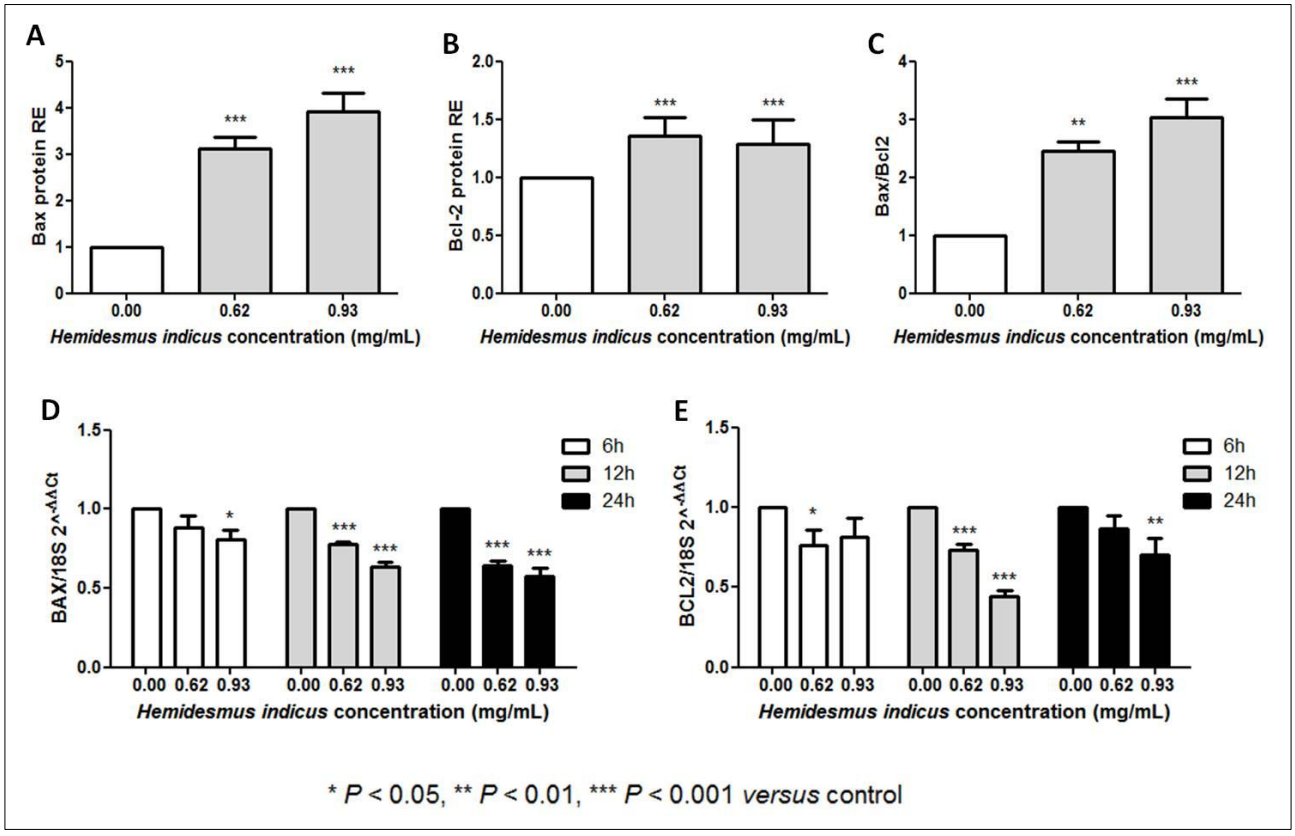

Figure 20: Relative expression of Bax and Bcl-2 protein levels (A, B) and variation of Bax-to-Bcl-2 ratio (C) after 24h treatment of Jurkat cells with Hemidesmus. Modulation of Bax (D) and Bcl-2 (E) gene expressions following 6h, 12h and 24h culture with Hemidesmus.

The differential regulation of Bax and Bcl-2 of mRNA and protein level observed for *Hemidesmus* encouraged specific studies to understand its ability of inhibiting proteasome. The ubiquitin-proteasome system is an important regulator of cell growth and apoptosis. Several proteasome inhibitors exert anti-tumor activity *in vivo* and potently induce apoptosis in tumor cells , including in those resistant to conventional chemotherapeutic agents[175]. The treatment of Jurkat cells with *Hemidesmus* caused a reduction in the protein expression of the 26S proteasome (0.53±0.02) (Fig. 21A). The proteasome inhibition evoked by *Hemidesmus* resulted comparable with that of two well-known proteasome inhibitors, like MG132 0.5 µM (0.48±0.02) and bortezomib 10µM (0.54±0.02) (Fig. 21A). Furthermore, *Hemidesmus* showed a dose-dependent inhibition of the proteasome (*PSMD11*) mRNA expression, after 12h and 24h treatment (Fig. 21B). *Hemidesmus* showed the highest inhibitory effect after 24h treatment and at 0.93 mg/mL induced a reduction in the gene expression of *PSMD11* of 0.52±0.04.

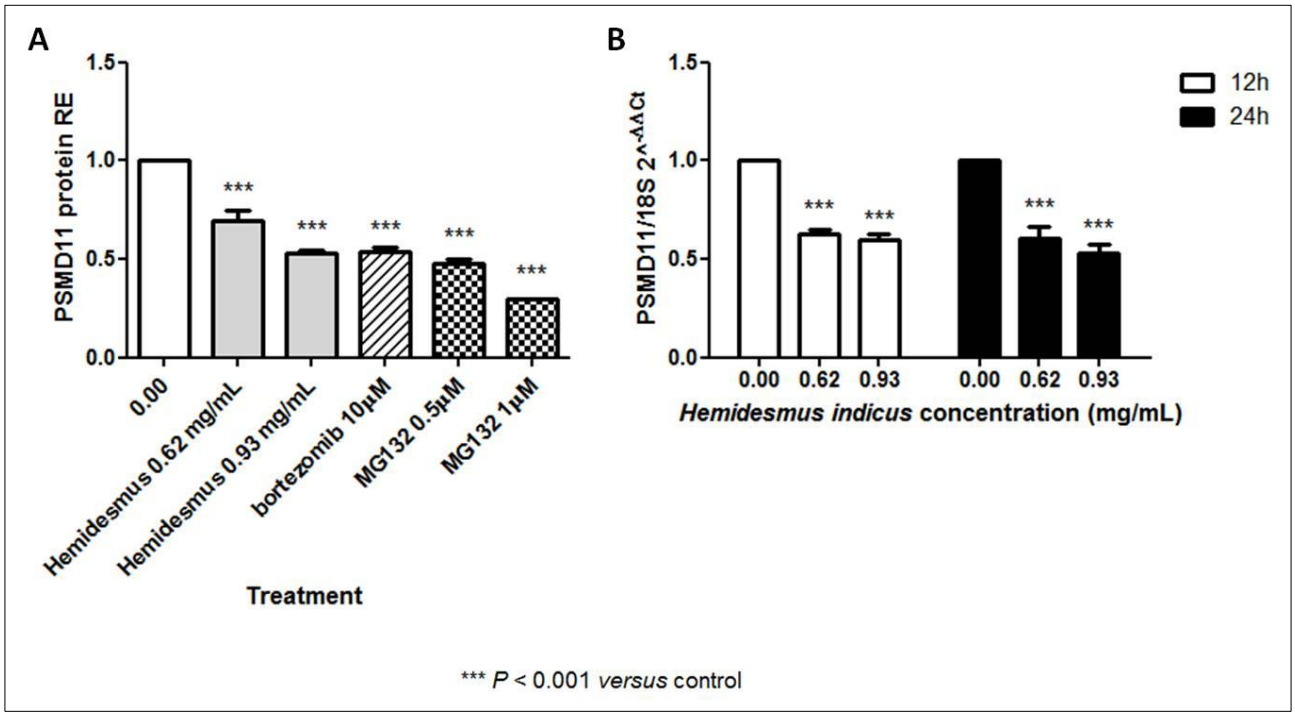

Figure 21: PSMD11 protein relative expression after treatment of Jurkat cells with Hemidesmus, bortezomib and MG132 (A) for 24h. Reduction of the PSMD11 mRNA relative expression following 12h and 24h culture in presence of Hemidesmus (B).

Hemidesmus indicus **perturbs Jurkat cell proliferation**

Hemidesmus significantly suppressed the progression of cells into the cell cycle (Fig. 22A). At 0.93 mg/mL, *Hemidesmus* suppressed Jurkat proliferation by 30% and at 1.9 mg/mL by 66%. At 3.1 mg/mL, cell-cycle progression was almost completely suppressed. By looking at the fraction of live and dead proliferated and unproliferated cells, we observed that more than 90% of the cells were proliferated and dead (propidium iodide-positive) at the highest concentration of *Hemidesmus* tested. These results indicate that the cytotoxicity of *Hemidesmus* against Jurkat cells was attributable to both the cytostatic effect causing the prevention of cell proliferation and the apoptotic and/or necrotic effect causing the loss of cell viability. At all concentrations, addition of *Hemidesmus* caused a dose-related accumulation of cells in the S phase (Fig. 22B-D). The immediate effects (8h) appeared primarily as an increase in the proportion of cells in the S phase of the cell cycle (from about 16% to 22%) accompanied by a slight compensatory decrease in G_1 phase cells. Longer exposure (24h) led to a further decrease in the proportion of G_1 cells, while the percentage of cells in S phase increased from 20% to 29%. Prolonged (48h) exposure appeared as a decrease in G_1 phase cells (from 62% to 43%), an unaffected fraction of G_2/M phase cells and a marked increase in the proportion of S cells (from 20 to 40%).

Since *Hemidesmus* was found to selectively alter the distribution of Jurkat cells in the cell cycle, we evaluated its effects on the expression of cell regulatory proteins including cyclins A2 and E, CDK2 and p21. As shown in Figure 22E, the proteins specific for CDK2, cyclin A2, cyclin E, and p21 were easily detectable in continuously growing Jurkat cells. Among the protein levels, those of cyclin A2 remained relatively constant, whereas those of both cyclin E and p21 significantly increased after treatment with *Hemidesmus indicus* for 24h (Fig. 22E). Moreover, treatment with *Hemidesmus* greatly decreased the expression of CDK2 (Fig. 22E).

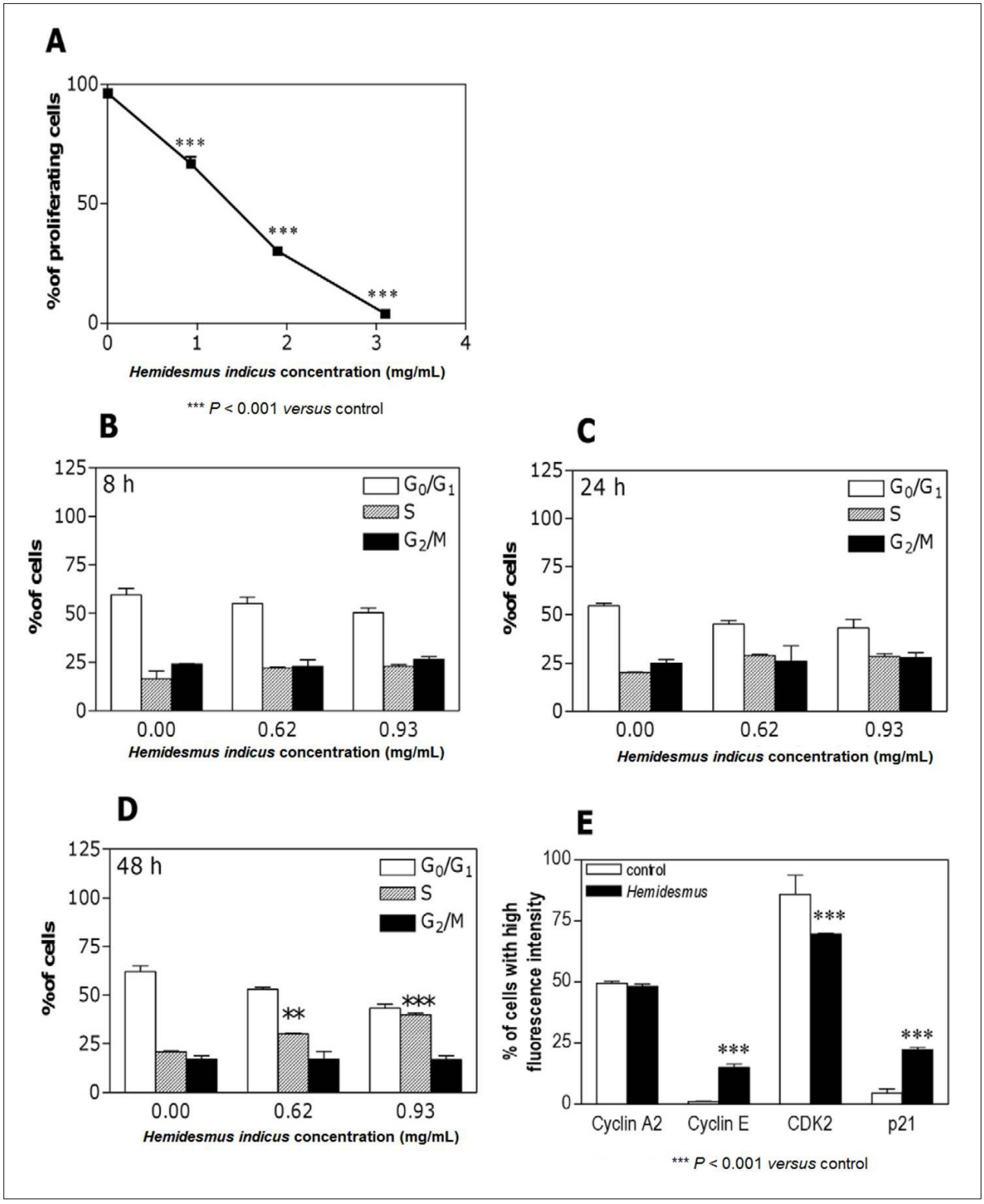

Figure 22: Cell proliferation (A), cell-cycle distribution (B-D), and cyclin A2, cyclin E, CDK2, and p21 protein levels (E) following 24h culture in the absence or presence of Hemidesmus.

Hemidesmus indicus increases the antitumor efficacy of 6-thioguanine, cytarabine and methotrexate

To investigate whether *Hemidesmus* could increase the cytotoxicity of some anticancer drugs, cells were treated with a combination of 6-thioguanine, cytarabine or methotrexate plus *Hemidesmus*. We measured the pro-apoptotic effect of the combination using doses of *Hemidesmus* that induced submaximal toxicity (0.31 mg/mL). This can allow observing potential additive or synergistic effects. Combination of *Hemidesmus* with 6-thioguanine, cytarabine or methotrexate had a synergistic or additive pro-apoptotic effect compared with each drug present alone (Fig. 23A-C). For instance, when 6-thioguanine was used alone, a 33% of apoptotic cells (versus 5% in the untreated cultures) was observed at the highest concentration tested. When it was used together with 0.31 mg/mL of *Hemidesmus*, a 51% of apoptotic cells was induced (Fig. 23A). Similarly, cytarabine alone at 1.25 mM induced a 35% of apoptotic cells (versus 4% in the untreated culture), but co-presence of *Hemidesmus* produced a 48% of apoptosis (Fig. 23B). The CI was found to be 0.6 for 6-thioguanine and 0.38 for cytarabine. The effect of *Hemidesmus* was also observed on cells treated with methotrexate. Treatment with methotrexate alone slightly affected cell viability. The % of apoptotic cells observed following treatment with methotrexate was similar to that of untreated cultures (Fig. 23C). Because of the relative insensitivity of Jurkat cells to methotrexate, we could not calculate a CI. In this case, the interaction between *Hemidesmus* and methotrexate was classified using the fractional inhibition method as follows: when expressed as the fractional inhibition of cell viability, additive inhibition produced by both inhibitors (*i*) occurs when $i_{1,2} = i_1 + i_2$; synergism when $i_{1,2} > i_1 + i_2$; antagonism when $i_{1,2} < i_1 + i_2$[176]. Using this method, the interaction between *Hemidesmus* and methotrexate was additive.

Hemidesmus indicus induces cytotoxic effects on mononuclear cells isolated from AML patients

We examined the effect of *Hemidesmus* on the viability of AML cells (Fig. 23D). *Hemidesmus* produced a cytotoxic effect in all samples tested. Viability of cells treated with *Hemidesmus* during 24h decreased from 97.5% in the control to 55.0% in the cells treated with *Hemidesmus* . To assess whether cell death induced by *Hemidesmus* was due to apoptosis, we measured the exposure of membrane phosphatidylserine by flow cytometry. As shown in Figure 23D, *Hemidesmus* at 0.93 mg/mL induced a 3-fold increase in apoptotic cell fraction in patients AML-1, AML-2 and AML-3,

and a 4-fold increase in AML-4 patient. Interestingly, the response to *Hemidesmus* was more pronounced on blasts obtained from a recidivant patient (AML4) (Fig. 23D).

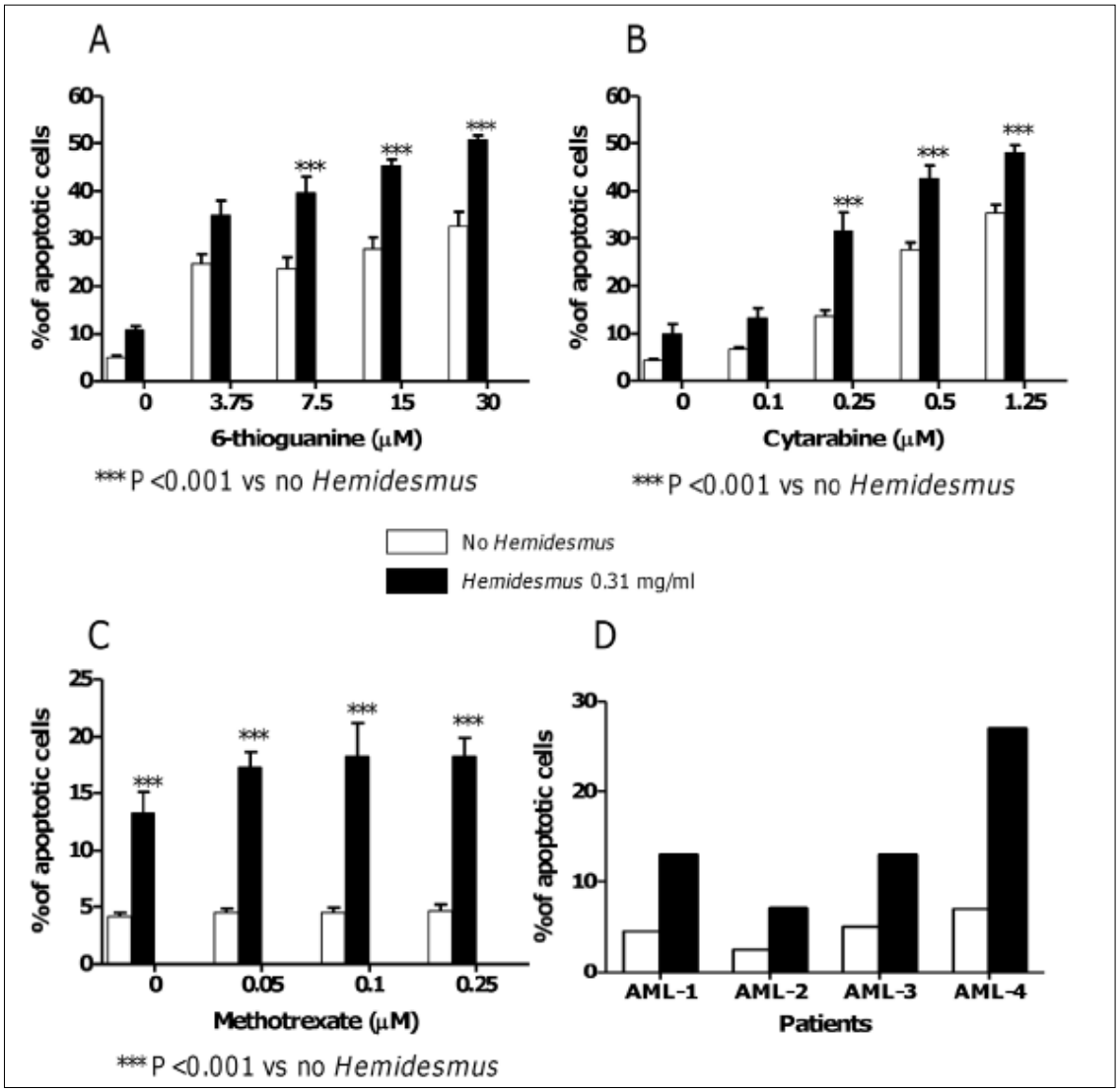

Figure 23: Fraction of apoptotic cells induced by 6-thioguanine (A), cytarabine (B) or methotrexate (C) following 24 h culture in the absence or presence of Hemidesmus (0.31 mg/mL) and fraction of apoptotic cells induced by Hemidesmus on mononuclear cells isolated from AML patients (D).

Hemidesmus indicus **induces apoptosis as well as differentiation of HL-60 cells**

Hemidesmus decreased HL-60 viability and the IC_{50} value calculated after 30h of treatment was 1.52 mg/mL (Fig. 24A). The induction of apoptosis was evaluated for concentrations similar or smaller than the IC_{50} (0.00–1.55 mg/mL). The incidence of apoptotic cells after 30h was statistically significant starting from the concentration of 0.62 mg/mL (11.6% *vs* 4.6% in the control). The

highest percentage of apoptotic cells (23.0%) was observed at the highest concentration tested, which resulted higher than that induced by cytarabine 0.5 µM. However, a significant fraction of necrotic cells was also recorded starting from the concentration 0.93 mg/mL (Fig. 24B).

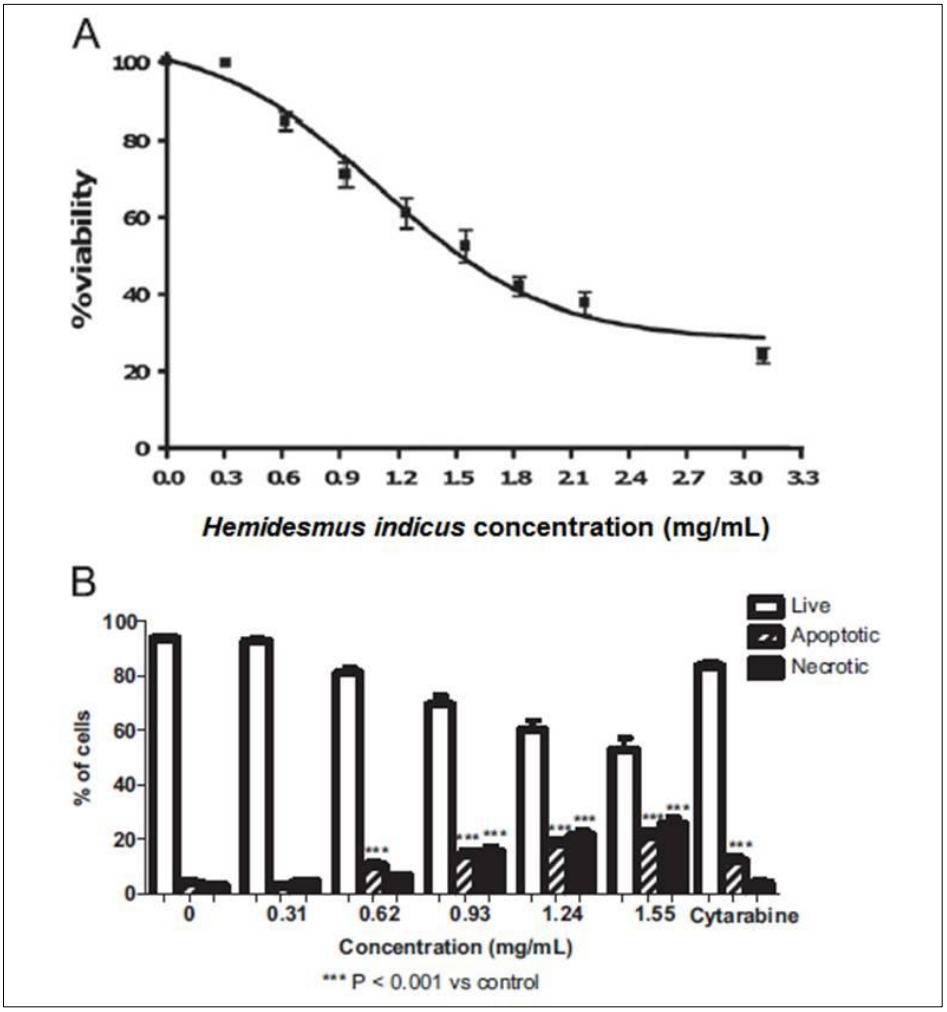

Figure 24: Cytotoxicity (A) and fraction of viable, apoptotic and necrotic cells (B) after treatment with Hemidesmus indicus at the indicated doses for 30h.

Hemidesmus is also able to alter cell-cycle progression. To define the rate at which *Hemidesmus* perturbed cell-cycle progression, cell cycle was evaluated at different time points. The effect of *Hemidesmus* was time-dependent. The early effect, observed at a concentration of 0.47–1.24 mg/mL, appeared as an increase in the percentage of cells in G_0/G_1 and S phases starting from the concentration 0.62 mg/mL, accompanied by a compensatory decrease in G_2/M phase cells. The highest effect was observed at the highest dose tested, where the percentage of cells in G_0/G_1 phase reached 23%, in S phase 31% and in G_2/M phase about -53% (Fig. 25). Longer exposure (30h) led to an increase of cells in the G_0/G_1 and S phases. The effect was significant starting from the concentration of 0.93 mg/mL *Hemidesmus* (G_0/G_1: 28%; S: 14%). A decrease of cells in G_2/M

phase starting from 0.62 mg/mL was also observed (from -15% to -59%) (Fig. 25). Prolonged exposure (48h) appeared as a marked increase in the proportion of cells in G_0/G_1 phase starting from 0.47 mg/mL (about 6%), that reached the highest level at 1.24 mg/mL (about 50%). A decrease in the percentage of cells in S and G_2/M phases was also recorded (Fig. 25).

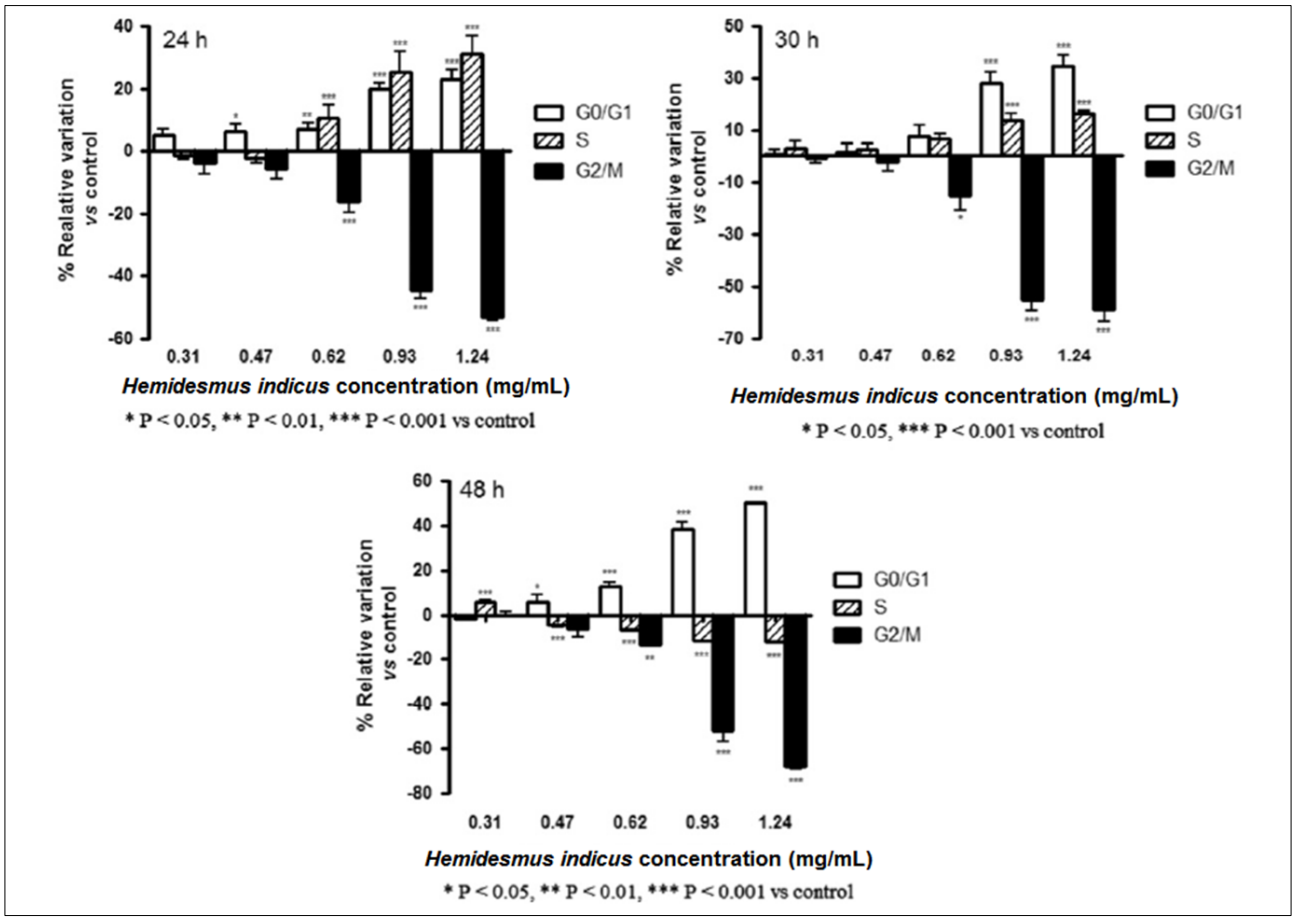

Figure 25: Effects of Hemidesmus indicus on cell-cycle distribution following 24h (A), 30h (B) and 48h (C) of treatment with Hemidesmus expressed as percentage of relative variation compared to untreated cells (control).

The analysis of cytodifferentiation has to be performed at concentrations where cell viability is higher than 80%[177]. For the analysis of cytodifferentiation induced by *Hemidesmus* after 72h of treatment, HL-60 cells were treated with up to 0.62 mg/mL of *Hemidesmus*, where we recorded a cell viability of 82%. At 0.93 mg/mL cell viability was 48%. NBT reduction, a marker for granulocyte/monocyte differentiation, revealed that *Hemidesmus* induced a dose-dependent differentiation of HL-60 cells (Fig. 26A). After treatment with *Hemidesmus* 0.62 mg/mL, the fraction of NBT-positive cells was 36.56%±0.78 compared to 5.62%±0.47 in the control, thus comparable to DMSO (43.88%±0.80), used as positive control (Fig. 26A). *Hemidesmus* 0.62

mg/mL also induced an increase in the number of adherent cells by over 8- fold (Fig. 26B). This suggests that *Hemidesmus* is able to stimulate differentiation into monocyte/macrophage. The increased number of α-naphthyl-acetate-esterase-positive cells confirmed the differentiation toward the monocyte/macrophage. The highest effect was observed at the highest concentration of *Hemidesmus* (23.50%±0.84 *vs* 3.00%±0.52 in the control) (Fig. 26C).

To confirm the ability of *Hemidesmus* to induce differentiation, the expression of two specific monocyte/granulocyte and monocyte/macrophage markers, CD15 and CD14 respectively, was analyzed. Cells treated with 0.62 mg/mL of *Hemidesmus* showed a CD15 mean fluorescence of 2.32-fold higher than untreated cells (Fig. 26D). The mean fluorescence of CD14 was 2.45-fold higher compared to the control at 0.62 mg/mL and 1.50-fold higher at 0.31 mg/mL (Fig. 26E). The cytodifferentiative potential of *Hemidesmus* was further detailed by TEM analysis. Figure 27 shows cell differentiation towards granulocyte and/or macrophage lineages. Myeloid cell granule maturation, at ultrastructural level, occurs through a progressive condensation of granule content from a loose, scarce electrondense substance, to a dense compact material. In *Hemidesmus*-treated HL60 cells, 0.2–0.5 mm immature granules, scattered throughout the cytoplasm and consistently absent in control cells, are clearly recognizable in A. Occasional 0.1–0.3 mm granules, containing a uniform, electron-dense material, can be also revealed and correspond to a further differentiated granule form (A, B). The presence of larger empty vacuoles (C), typical a phagocytic process, suggests a progressive macrophage differentiation, as also confirmed by the observation of large cells, with flattened polymorph nucleus, phagocyting necrotic ones (D).

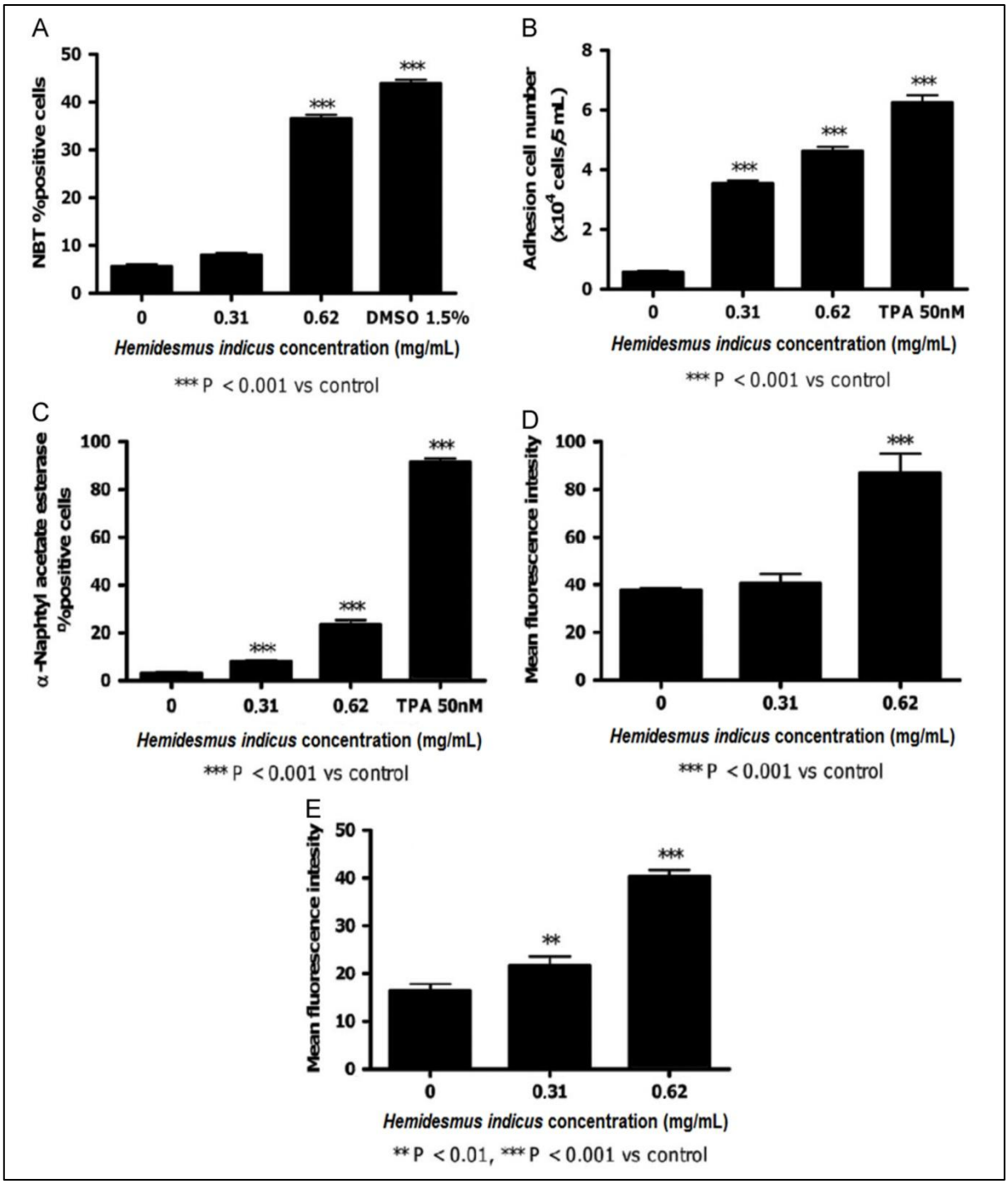

Figure 26: Dose-dependent effects of Hemidesmus indicus on HL-60 cell differentiation as evaluated by NBT-reducing ability (A), cell adhesion (B), a-naphthyl acetate esterase activity (C) and expression of CD15 (D) and CD14 (E) markers.

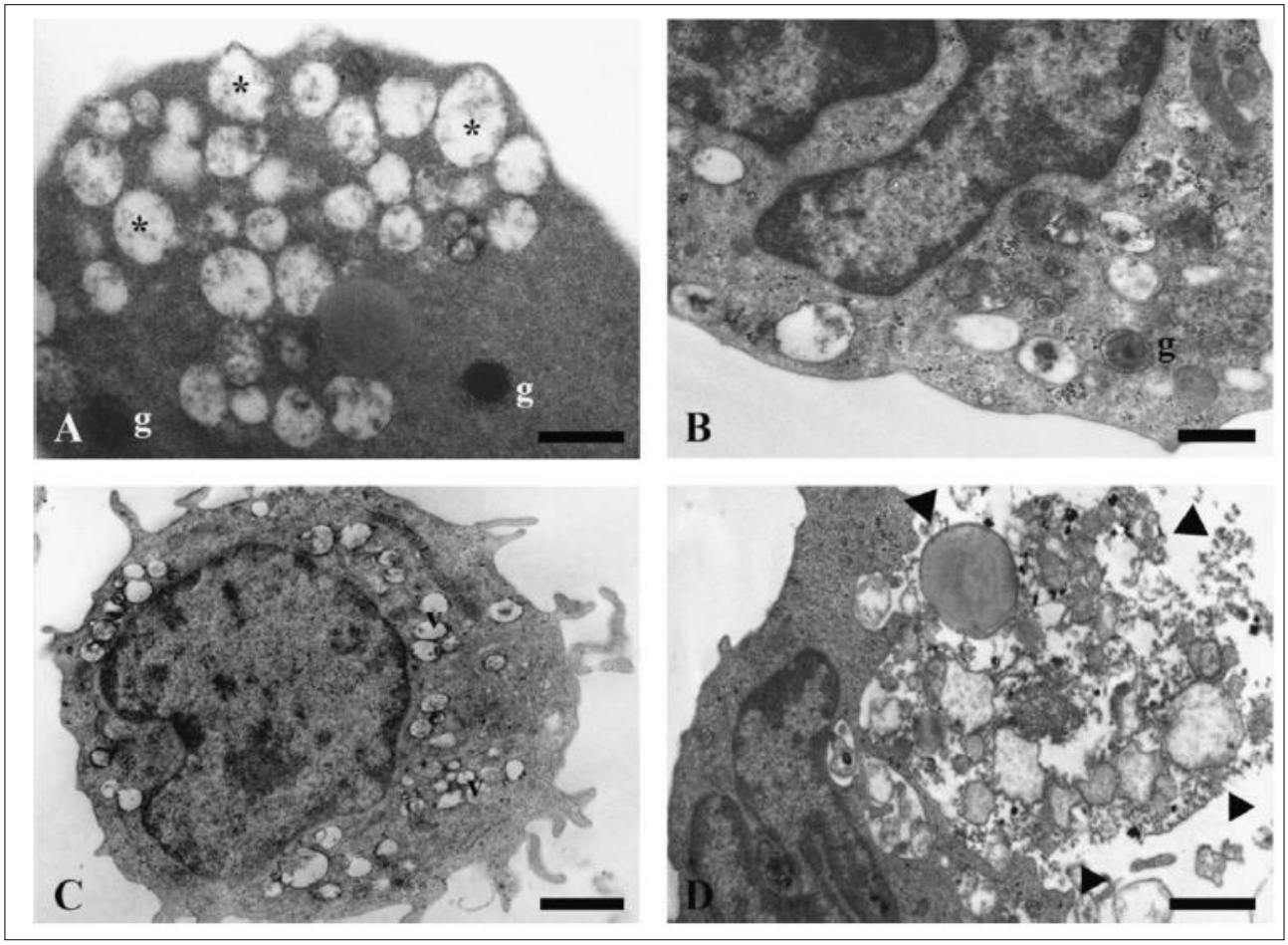

Figure 27: TEM of HL-60 cells after Hemidesmus indicus treatment. Forming (*) and mature (g) granules indicate the granulocytic differentiation (A, B). Cytoplasmic vacuoles (v) and phagocytosis patterns (c) evidentiate the macrophagic properties (C, D). A, B, bar=5 µm; C, D, bar=1 µm.

Hemidesmus indicus inhibits angiogenesis as well as reduces invasion and migration of HUVECs

In order to determine the effect of *Hemidesmus indicus* on the proliferation of HUVECs in normoxic (Fig. 28A) and hypoxic (Fig. 28B) conditions, these cells were treated with different concentration of *Hemidesmus* (0.00-0.93 mg/mL) for 6h and 24h. The treatment with *Hemidesmus* for 6h induced a significant reduction in cell proliferation only in normoxic condition and at the highest tested dose (68.7% proliferating cells). On the other hand, after 24h of treatment, in both O_2 conditions, a significant reduction of cell growth was induced by *Hemidesmus* 0.93 mg/mL (normoxia: 49.6%, hypoxia: 75.9% proliferating cells). To exclude any possible effect of

Hemidesmus on angiogenesis connected with the reduction of viability and induction of apoptosis, the pro-apoptotic potential of *Hemidesmus* on HUVECs was screened. In both normoxic (Fig. 28C) and hypoxic (Fig. 28D) conditions none of the *Hemidesmus* tested concentrations showed a significant increase in the fraction of apoptotic cells.

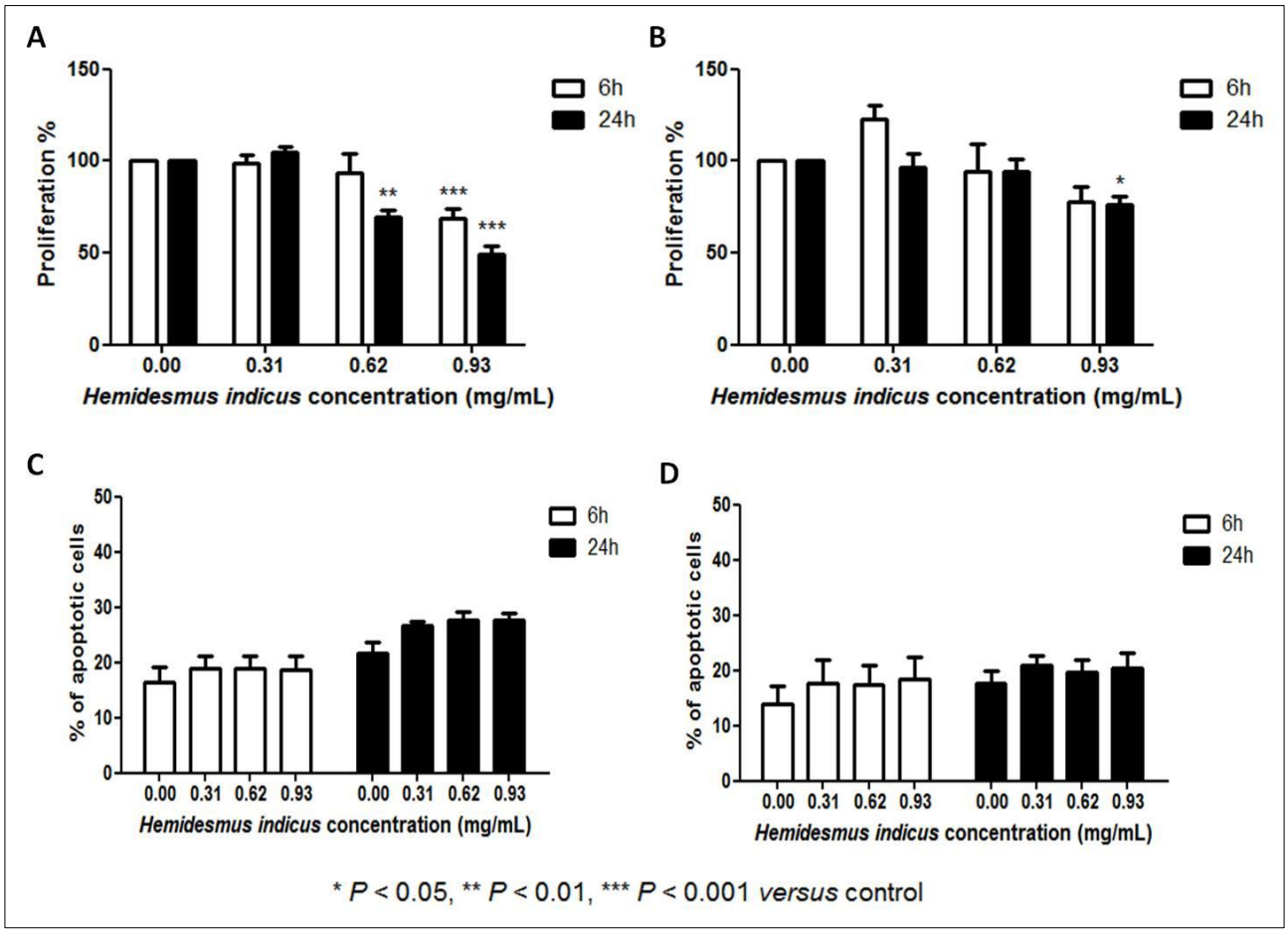

Figure 28: Cell proliferation (A-B) and induction of apoptosis (C-D) following 6h and 24h culture in normoxic (A, C) and hypoxic (B, D) conditions with Hemidesmus.

The ability of HUVECs, treated with *Hemidesmus* (0.00–0.93 mg/mL), VEGF 10µg/mL used as positive control, or their association, to migrate, attach each other, and form tube structure on ECMatrix™ are shown in the Figure 29A. This clearly demonstrates that *Hemidesmus* at the highest tested concentrations (0.62 and 0.93 mg/ml), in both hypoxic and normoxic conditions, strongly inhibits tube formation. The count of the tube branch points formed by HUVECs following different treatments showed the ability of *Hemidesmus* 0.62 mg/mL to reduce significantly the branch point number more in normoxic then in hypoxic conditions (0.17±0.07 *vs* 0.22±0.13) compared to the untreated sample (Fig. 29B). The association *Hemidesmus* 0.62 mg/mL-VEGF showed similar effects with a reduction of the branch point number in normoxia (0.21±0.06) and

hypoxia (0.24±0.20) compared to the VEGF control (Fig. 29C). Moreover, in samples treated with *Hemidesmus* 0.93 mg/mL in both normoxic and hypoxic conditions, HUVECs were not able to form hollow tube-like structures. Thus, branch point could not be determined (Fig. 29B-C).

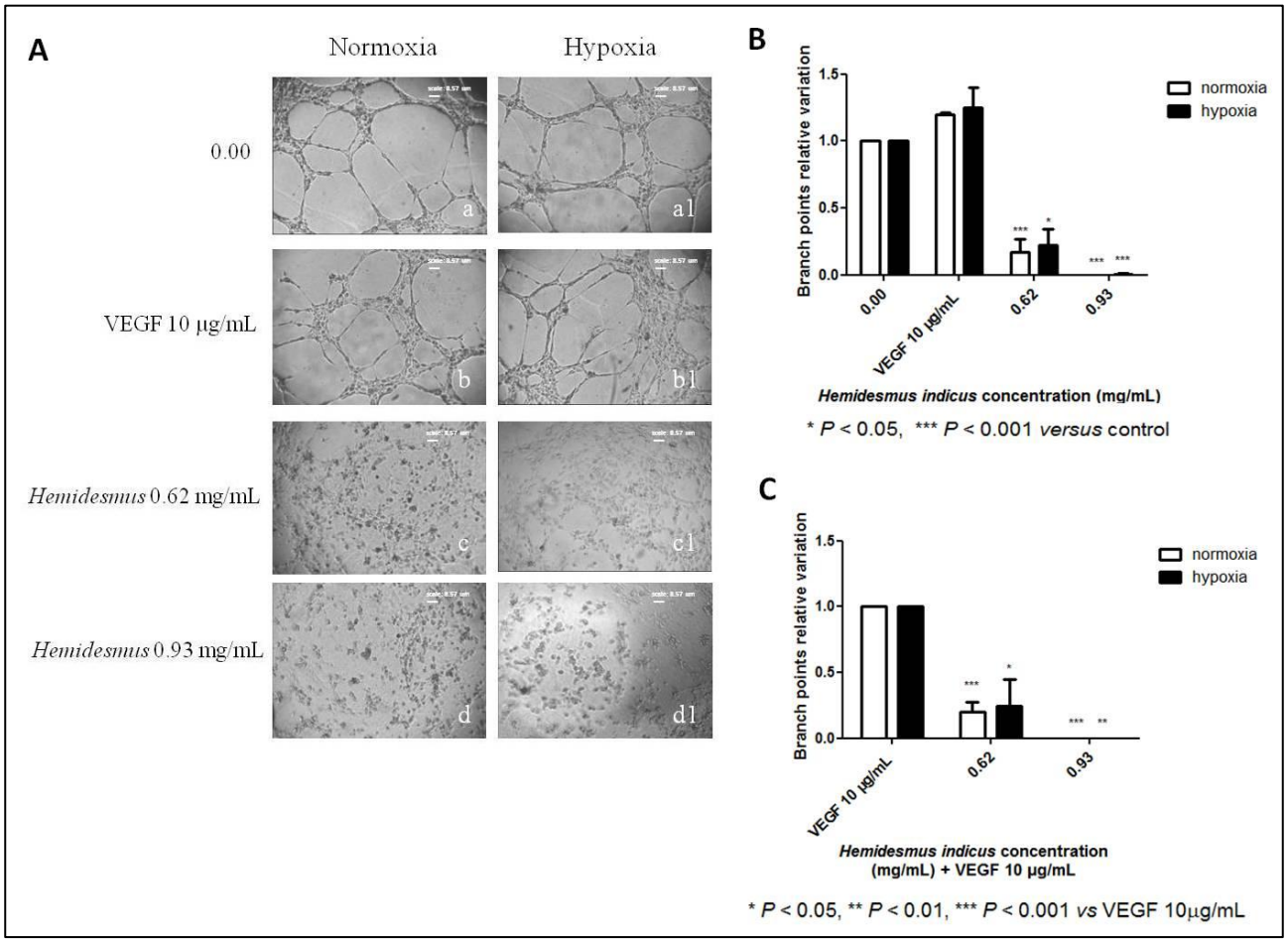

Figure 29: Microscopic photographs of tube formation on reconstituted basement membrane gel after 6h of incubation in normoxia and hypoxia. (A a, a1) untreated control; (A b, b1) VEGF 10 µg/mL control; (A c, c1) Hemidesmus 0.62 mg/mL; (A d, d1) Hemidesmus 0.93 mg/mL. Relative variation of the branch point number of HUVECs treated for 6h in normoxic and hypoxic conditions with Hemidesmus, VEGF (B) and their association (C).

The ability of *Hemidesmus* to inhibit angiogenesis was confirmed by checking its ability to induce a post-transcriptional and post-translational modulation of proteins involved in the regulation of the vessel formation process. The expression of VEGF, VEGFR2 and HIF-1α was quantified by mean fluorescence. Treatment with *Hemidesmus* showed, in hypoxic and normoxic conditions, a dose-dependent down-regulation of VEGF that reached the maximum effect at the highest tested

concentration with a decrease of its relative expression of 0.81±0.02 in normoxia and 0.77±0.11 in hypoxia (Fig. 30A). *Hemidesmus* did not show any effect in normoxic condition on the expression of VEGFR2 and HIF-1α (Fig. 30B-C). On the other hand, in hypoxic conditions, treatment with *Hemidesmus* down-regulated the expression of all three proteins at all tested doses. In particular, the highest effects on VEGFR2 and HIF-1α were observed after treatment with *Hemidesmus* 0.93 mg/mL that induced a reduction of their expressions of 0.60±0.07 and 0.83±0.03, respectively (Fig. 30B-C). Treatments with *Hemidesmus* in hypoxic conditions induced a significant reduction in the expression of VEGFR2 and HIF-1α compared to the same treatments conducted at normal O_2 pressure (Fig. 30B-C).

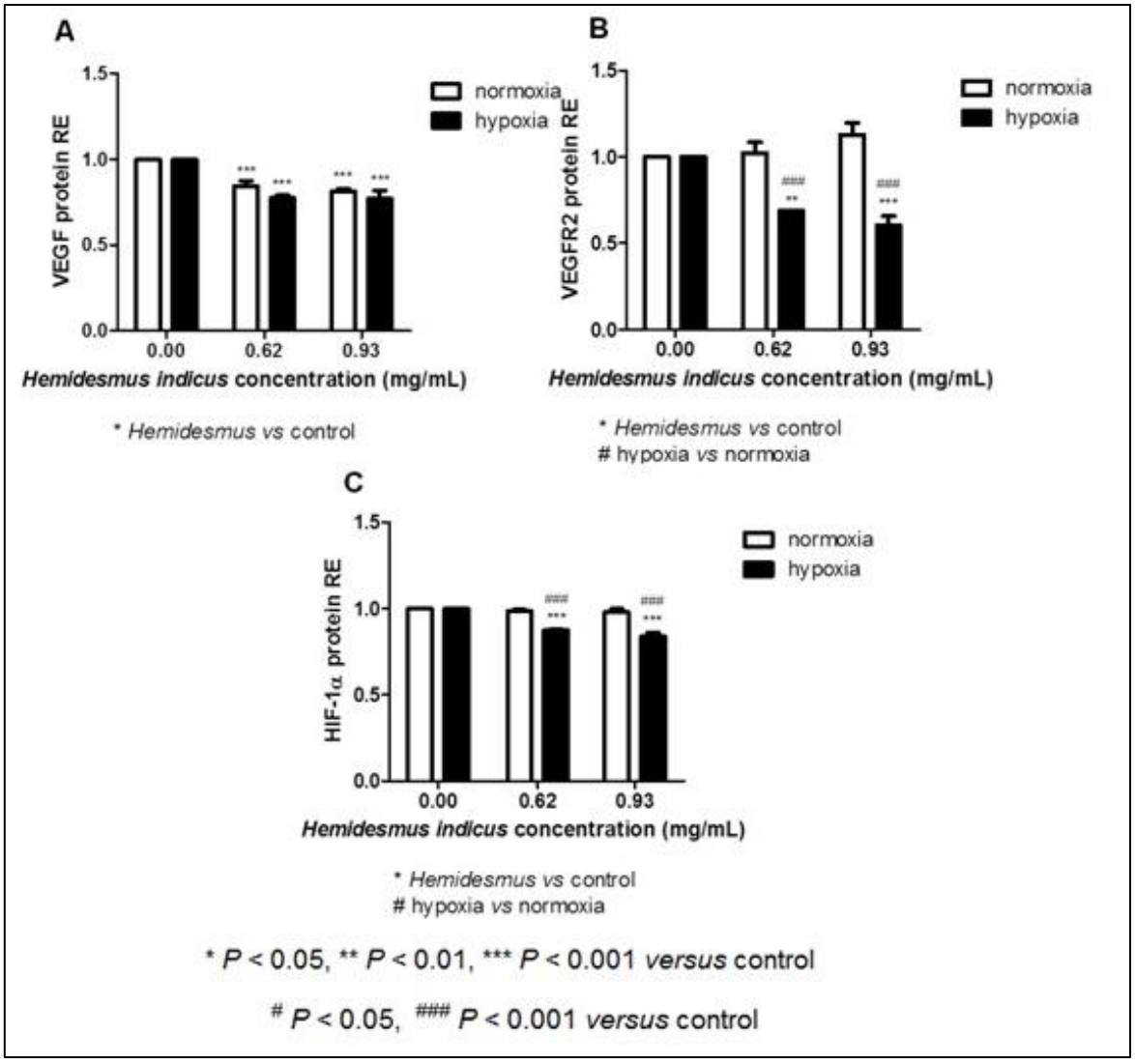

Figure 30: Relative protein expression of VEGF (A), VEGFR2 (B) and HIF-1α (C) after treatment of HUVECs for 6h with Hemidesmus.

Hemidesmus regulated *VEGF*, *KDR* and *HIF* expression. A dose-dependent down-regulation was observed, particularly marched for *HIF-1α* and *KDR* in hypoxic conditions (Fig. 31B-C). The highest inhibitory effect was observed after treatment of HUVECs with *Hemidesmus* 0.93 mg/mL, both in normoxic and hypoxic conditions. 0.93 mg/mL of *Hemidesmus* induced a stronger down-regulation on HIF-1α mRNA in hypoxia than in normoxia (0.07±0.04 *vs* 0.25±0.061, respectively) (Fig. 31C). With regard to VEGF mRNA, it was not possible to observe any significant modulation (Fig. 31A).

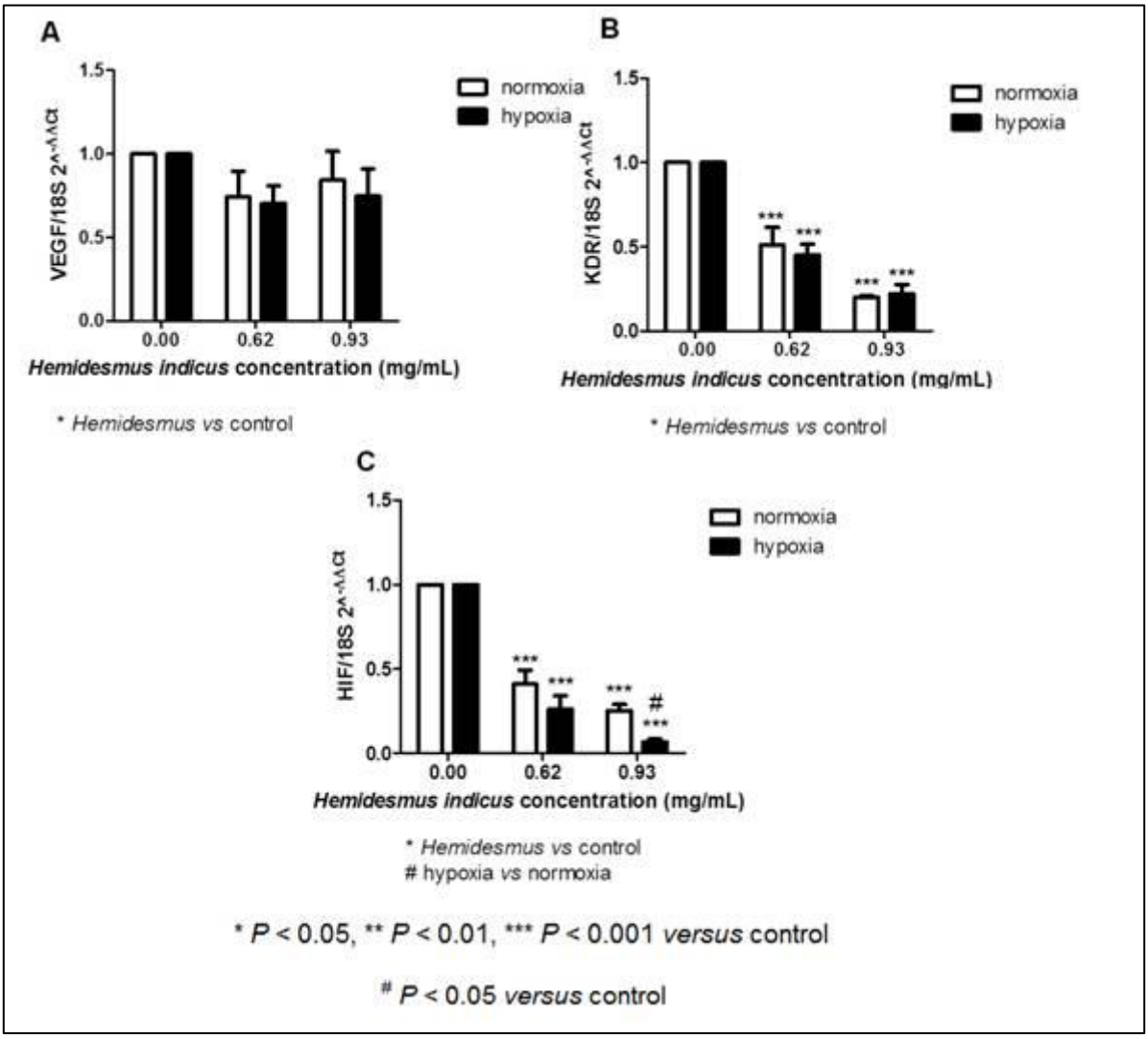

Figure 31: Relative mRNA expression of VEGF (A), KDR (B) and HIF (C) after treatment of HUVECs for 6h with Hemidesmus.

Migration plays an important role in angiogenesis and is a prerequisite for tumor-cell invasion and metastasis. We explored whether *Hemidesmus* was able to inhibit invasion and migration of HUVECs using a transwell chamber migration system with a polycarbonate membrane. In

normoxic conditions, the inhibition of migration and invasion was more pronounced than in hypoxia (Fig. 32A-B). The migrated and invaded cell number relative variation was obtained from the comparison between their fluorescence signal in treated samples and the untreated control. Actually, at normal oxygen concentration conditions, *Hemidesmus* 0.93 mg/mL after 6h of treatment led to a reduction of the migrated cell number relative variation to 0.65±0.01. The invaded cell number relative variation was 0.50±0.03. The same treatment conduced in hypoxic conditions showed a reduction of the capability of migration (0.789±0.003) and invasion (0.63±0.07) (Fig. 32A-B). Notably, the ability of *Hemidesmus* to inhibit cellular invasion was more pronounced in normoxia rather than hypoxia. This effect was particularly pronounced at the lowest treatment dose of *Hemidesmus*.

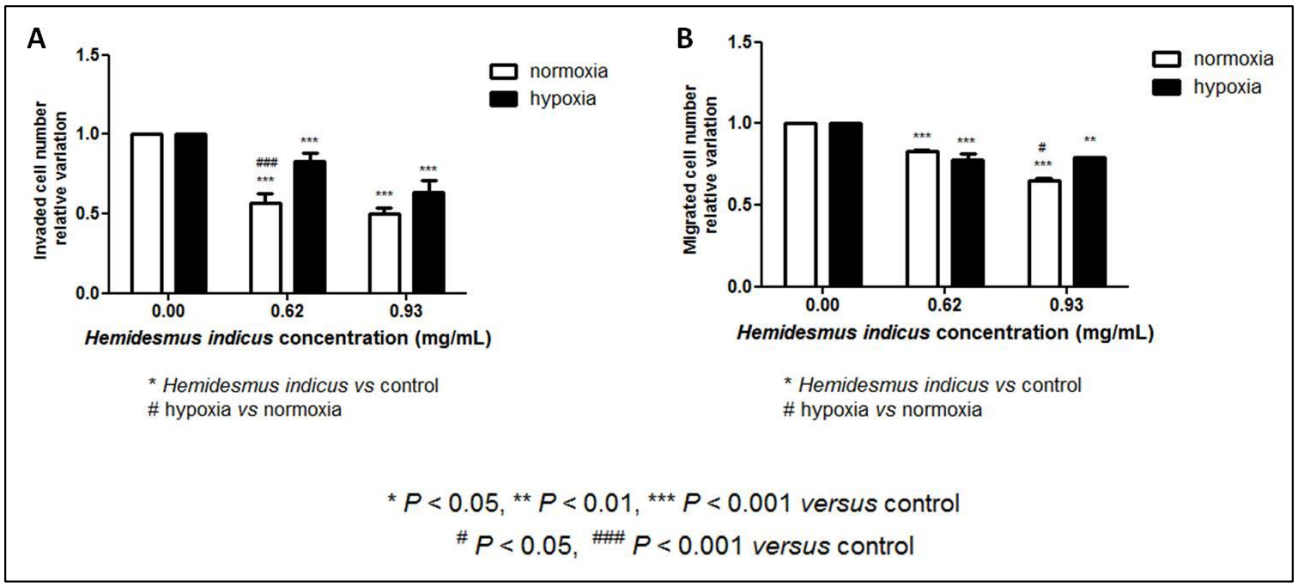

Figure 32: Relative variation of migrated (A) and invaded (B) cell number following culture of HUVECs in normoxic and hypoxic conditions with Hemidesmus.

Hemidesmus indicus **and piperlongumine have a selective action toward LSC**

The selectivity of action of *Hemidesmus* and piperlongumine in the eradication of LSC was evaluated in terms of pro-apoptotic potential and inhibition of the colony formation capability. After treatment for 24h of the CD34+ subpopulation of 6 AML patients, *Hemidesmus* (Fig. 33A-B) and piperlongumine (Fig. 34A-B) showed the ability to reduce cell viability and induce apoptosis. This effect reached the peak at the highest tested doses. The sample PB2585 appeared to be the most sensible to the pro-apoptotic effect of both drugs. The fraction of apoptotic cells induced by

Hemidesmus 1.55 mg/mL was 36.7% *vs* 14.4% in the control, and by piperlongumine 14 µM was 79.1 % *vs* 20.4% in the control.

Furthermore, *Hemidesmus* and piperlongumine inhibited the colony formation capability of CD34+ leukemic cells. Only in 3 out of 6 AML samples the formation of colonies was observed in the control. In these patient samples, *Hemidesmus* 0.93 and 1.55 mg/mL induced a reduction in the number of CFU-GM and clusters (Fig. 35A). Moreover, after treatment with piperlongumine 14 µM it was not possible to observe any colony in all AML samples (Fig. 35B). In order to demonstrate the selectivity of action of piperlongumine and *Hemidesmus* toward LSC, their ability to induce apoptosis on CD34+ cells separated from the cord blood of healthy donors was evaluated. *Hemidesmus* did not show any increase in the apoptotic cell fraction of the CB19 sample (Fig. 33C). On the other hand, the pro-apoptotic potential of piperlongumine was tested on 3 cord blood samples. Piperlongumine, at the highest tested dose, induced a reduction of the viability associated with an increase in the apoptotic fraction (Fig. 34C). CB10 appeared to be the most sensible sample to the pro-apoptotic effect induced by piperlongumine (14 µM) with a 34.4% of apoptotic cells (*vs* 2.3% of the DMSO solvent control).

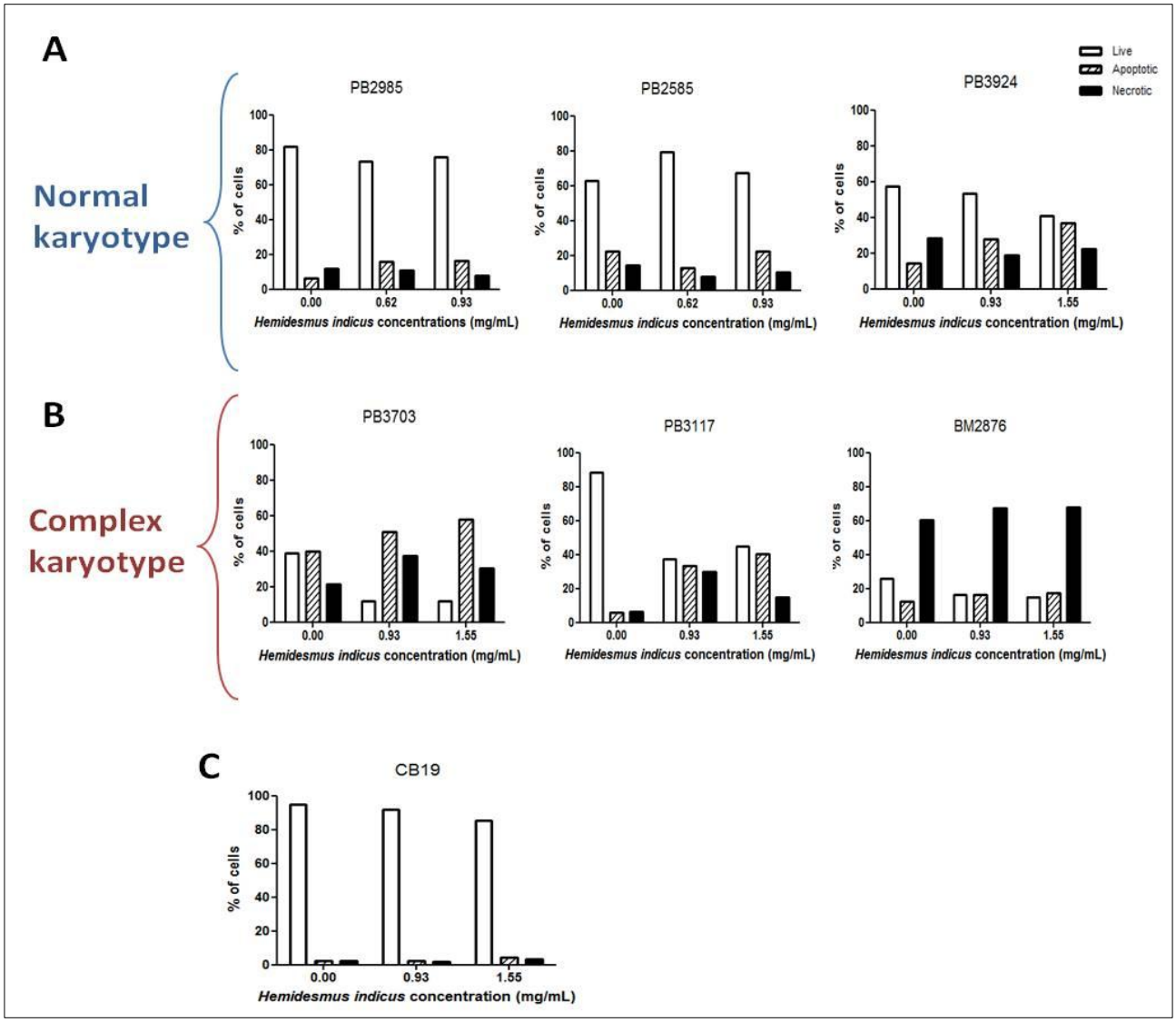

Figure 33: Fraction of viable, apoptotic and necrotic CD34+ cells, isolated from PB and BM samples of AML patients (A,B) and cord blood sample from healthy donors (C), after treatment for 24h with Hemidesmus. Patient samples are divided in two groups based on their kariotype: normal (A) or complex (B).

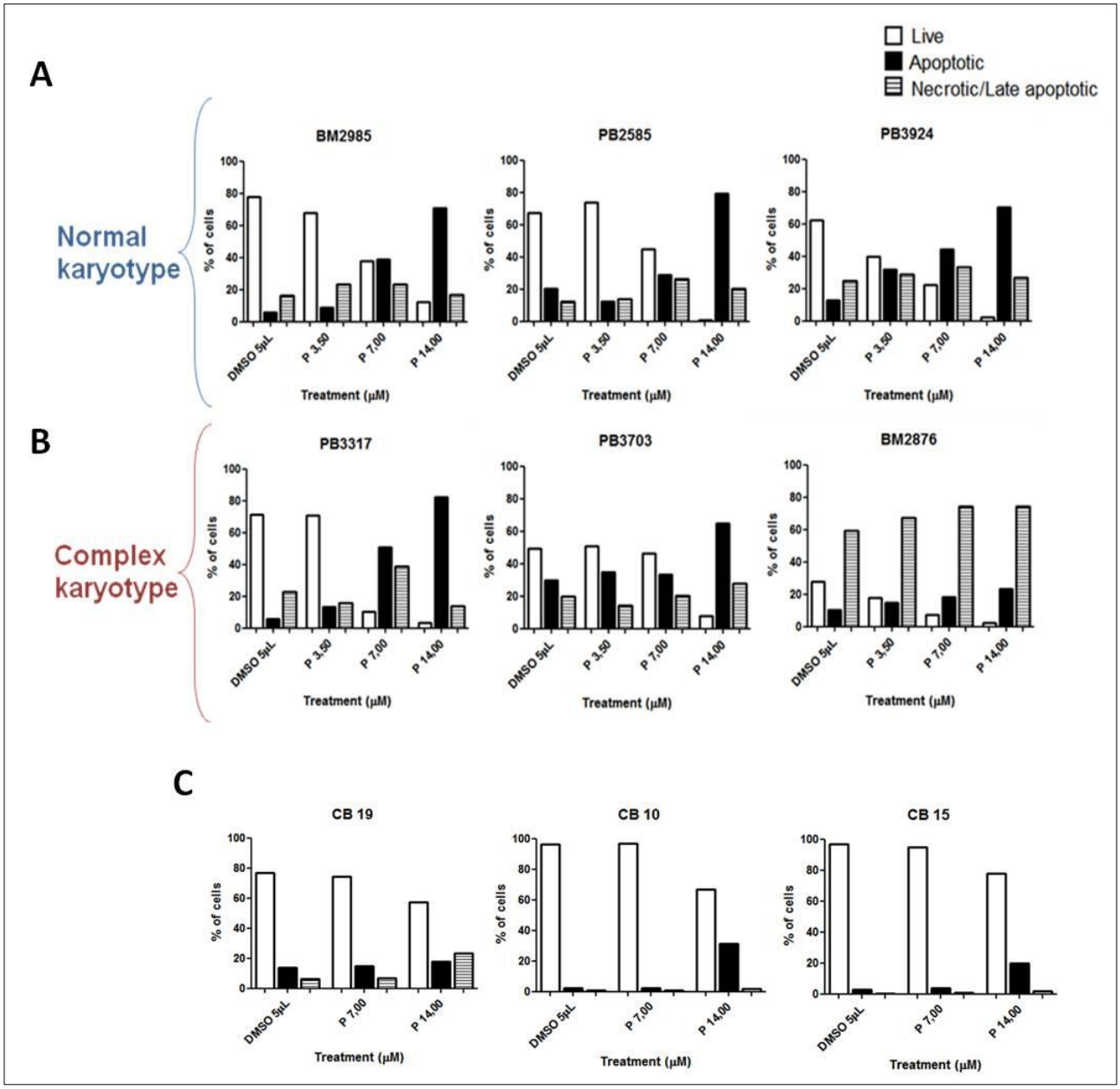

Figure 34: Fraction of viable, apoptotic and necrotic CD34+ cells, isolated from PB and BM samples of AML patients (A,B) and cord blood samples from healthy donors (C), after treatment for 24h with piperlongumine. Patient samples are divided in two groups based on their kariotype: normal (A) or complex (B).

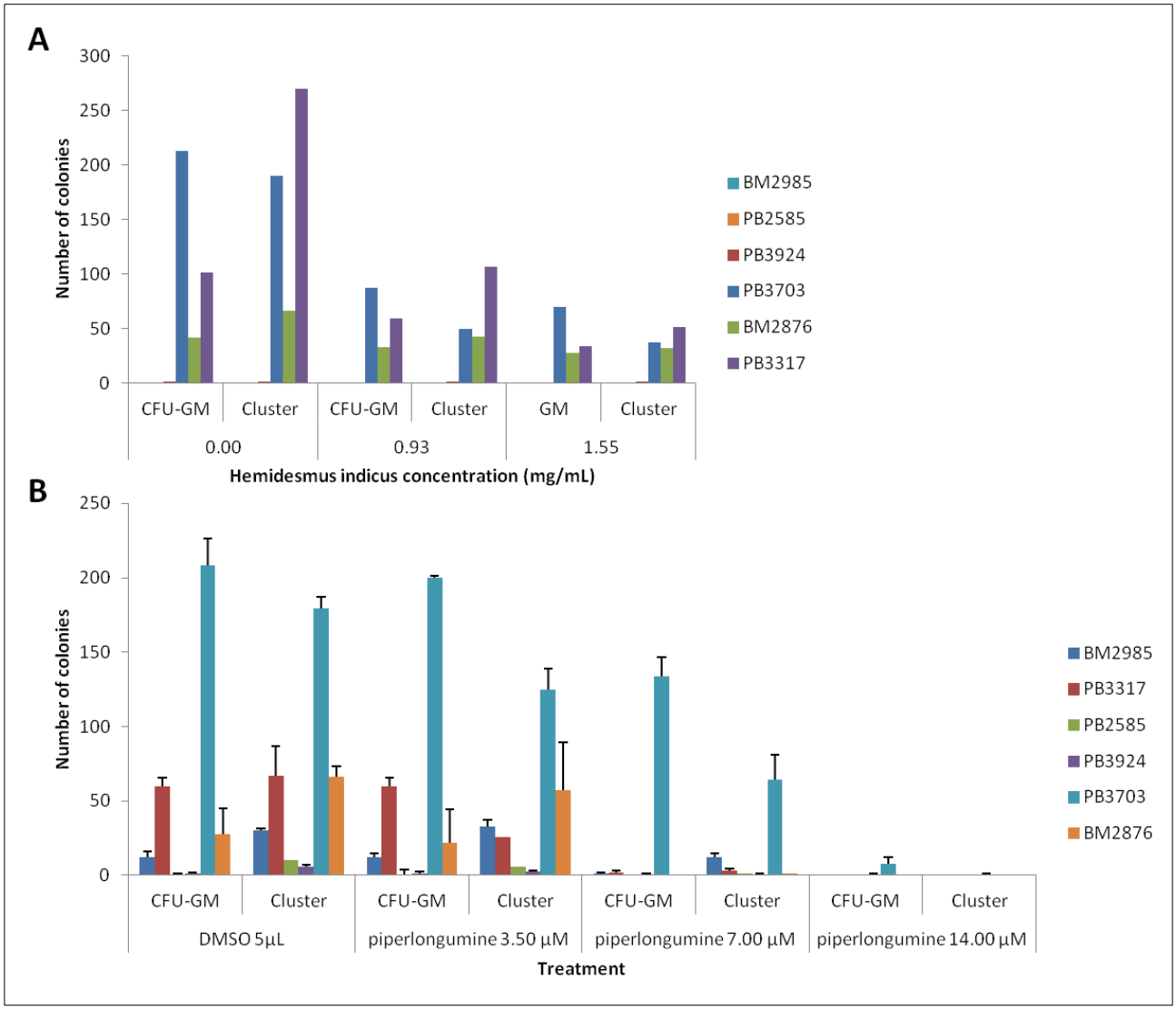

Figure 35: Colony-forming capability of CD34+ cells, sorted from AML patient samples, treated with Hemidesmus (A) or piperlongumine (B) for 24h and kept in culture for 14 days.

Chapter 5

Discussion

In this study, we show that *Hemidesmus indicus*, a traditionally used medicinal plant, exerts potent anti-leukemic effects through the modulation of different critical targets. *Hemidesmus* was subjected to an HPLC analysis to quantify its main phytomarkers, namely 2H4MBAL, 3H4MBAL and 2H4MBAC.

We then examined its effect on human T-leukemia cell proliferation by focusing on cell-cycle regulation. According to our flow cytometry data, treatment of Jurkat cells with *Hemidesmus* resulted in a potent inhibition of cell growth, due to the block of cells in the S phase.

Many stimuli can induce cell arrest at different phases. Agents that cause damage to DNA or spindle apparatus will cause either apoptosis or cell-cycle arrest, which usually occurs at the G_1/S or G_2/M boundaries[178]. Moreover, certain taxanes and vinca alkaloids that cause G_2/M arrest by damaging microtubules have proven clinically successful for cancer treatment[179]. Consequently, cell-cycle arrest at the G_1/S and G_2/M transitions has been intensively investigated in mammalian cells. In contrast, relatively little is known about mechanisms that control progress within the S phase. S-phase arrest has been observed in mammalian cells with prolonged arrest at the G_1/S boundary[180]; Rb(+/+) mouse embryo fibroblasts treated with cisplatin, etoposide or mitomycin[181]; human melanocytes treated with thymidine dinucleotides[182]; and human osteosarcoma cells transduced with the p21 gene[183].

Because our study demonstrated that *Hemidesmus* treatment of Jurkat cells resulted in an S-phase delay, we examined the changes of some regulators associated with cell cycle in order to further elucidate its cytostatic mechanism. The activation of preassembled replication complexes and initiation of DNA synthesis is mediated by cyclin A2/CDK2 complex and cyclin

E/CDK2 complex. Cyclin A2 promotes both G_1/S and G_2/M transitions[184]. Cyclin A2/CDK2 activity is first evident in late G_1, persists through S phase and peaks at G_2 phase until prometaphase[185]. Cyclin E/CDK2 activity increases in late G_1 and peaks in early S phase[186]. p21 is a CDK inhibitor that directly inhibits the activity of CDK2 activity[187].

Hemidesmus treatment resulted in a significant down-modulation of CDK2, whereas the expression of cyclin E was increased. Although *Hemidesmus* caused an increase in cyclin E levels, the global cellular response was a block of the cell cycle. In this situation, an important role can be played by p21, whose over-expression results in S-phase arrest and senescence[188]. *Hemidesmus* did not modulate the expression of cyclin A2. Since cyclin A2 is mainly involved in S progression and its

expression peaks at G_2 phase[184], this differential regulation suggests that the effect of *Hemidesmus* resides in early S phase.

Hemidesmus-treated cultures revealed a dose-dependent increase in the percentage of apoptotic cells. Apoptosis is primarily mediated through two pathways: the death receptor pathway and the mitochondrial pathway. In the death receptor pathway, a death receptor ligand, such as Fas ligand, binds to its receptor, such as Fas, triggering aggregation of the death receptor, recruitment of an adaptor molecule, such as FADD, as well as pro-caspase-8 or -10 forming a complex named the death inducing signaling complex. This results in the autocatalytic cleavage and activation of caspase-8 or caspase-10, leading to activation of caspase-3 or -7 and induction of apoptosis[189].

In the mitochondrial pathway, multidomain pro-apoptotic proteins, excessive mitochondrial calcium and reactive oxygen species induce the opening of the mitochondrial pore, with loss of mitochondrial integrity and transmembrane potential ($D\Psi_m$)[190].

Cytochrome c is released from the mitochondria to form the apoptosome. The apoptosome then activates caspase-9, which in turn activates caspase-3, thereby inducing apoptosis. Many protein targets of active caspases are biologically important apoptotic indicators of morphological and biochemical changes associated with apoptosis[189]. One of the essential substrates cleaved by caspase-3 is PARP, an abundant DNA-binding enzyme that detects and signals DNA strand breaks[191]. In our system, *Hemidesmus* activated caspase-3 and induced PARP cleavage and cytochrome c release. The death receptor pathway was not induced by *Hemidesmus*, as indicated by the lack of activation of caspase-8. Thus, for the specific measurement of $D\Psi_m$, Jurkat cells were loaded with the fluorochrome JC-1, a cationic probe that distributes passively between media, the cytosol and the mitochondria according to the Nernst's equation, where the final distribution of the fluorochrome depends mainly on the transmembrane potential[192]. Compared to control cells, *Hemidesmus*-treated cells had drop in $D\Psi_m$. During the effector phase of mitochondria-dependent apoptosis, the inner transmembrane potential of the mitochondria collapses, indicating the opening of mitochondrial permeability transition pores. Mitochondrial permeability transition activation compromises the normal integrity of the mitochondrial inner membrane resulting into uncoupled oxidative phosphorylation, ATP decay, mitochondrial swelling and release of apoptogenic factors. The structure and composition of the transition pore includes inner membrane proteins, such as adenine nucleotide translocator, outer membrane proteins, such as the voltage-dependent anion channel, and cyclophilin D at contact sites between the mitochondrial outer and inner membranes[161]. The inner and outer membrane proteins operate in concert to create the conductance channels[189]. The adenine nucleotide translocator is an ADP-ATP antiporter that imports ADP to the matrix and

exports ATP to the cytosol[193]. The adenine nucleotide translocator alternates between two distinct conformations in which adenine nucleotides are either bound to the cytosolic side (c-state) or to the matrix side (m-state) of the inner mitochondrial membrane[193]. CATR binds to adenine nucleotide translocator in the c-state. CATR binding occurs at a site similar to the ADP-binding site, thus preventing ADP/ATP transport. BA binds to adenine nucleotide translocator in the m-state. The two ligands are known to be adenine nucleotide translocator specific inhibitors[193]. The third putative component of the mitochondrial permeability transition is cyclophilin D, which binds to complexes of voltage-dependent anion channel and adenine nucleotide translocator in order to form the mitochondrial permeability transition complex. Cyc A was shown to block the binding of cyclophilin D[194]. To further elucidate the significance of mitochondria in *Hemidesmus*-induced Jurkat cell death, we investigated the effects of different inhibitors. *Hemidesmus* did not interact with adenine nucleotide translocator and did not disturb the effect of BA, CATR and Cyc A. The effect of *Hemidesmus* on mitochondrial depolarization was not even modulated by ADP. Because ADP is a potent ligand of the adenine nucleotide translocator[195], the results confirm that *Hemidesmus* does not stimulate the mitochondrial permeability transition through an interaction with the adenine nucleotide translocator but to an unrelated mechanism.

Numerous data have shown the pro-apoptotic effects of elevated concentrations of intracellular calcium[196] and, accordingly, many calcium ionophores are also apoptotic inductors in some cell types[192]. Since *Hemidesmus* possesses a strong pro-apoptotic effect in Jurkat cells, we were interested in studying its calcium mobilization activity. The major pathways of $[Ca^{2+}]_i$ increase are Ca_{2+} influx from extracellular space and Ca^{2+} release from internal Ca^{2+} stores. Numerous studies have demonstrated that both pathways appear to be involved in the $[Ca^{2+}]_i$ increase associated with apoptosis[197]. Our study demonstrated that *Hemidesmus* induced $[Ca^{2+}]_i$ rise and explored the underlying mechanisms. Removal of extracellular Ca^{2+} did not abolish the $[Ca^{2+}]_i$ raise induced by *Hemidesmus*. Moreover, our results suggest that *Hemidesmus* did not cause Ca^{2+} influx via stimulating store operated Ca^{2+} entry or voltage-gated Ca^{2+} channels because nifedipine (a blocker of L-type voltage-gated Ca^{2+} channels)[198] and econazole (an inhibitor of store-operated Ca_{2+} channels)[199] failed to inhibit the $[Ca^{2+}]_i$ raise. Aristolochic acid, a phospholipase A2 inhibitor, increased *Hemidesmus*-induced $[Ca^{2+}]_i$ raise. These findings indicate that phospholipase A2 could be not required for *Hemidesmus*-induced Ca^{2+} signal in our experimental model. However, aristolochic acid is able to induce a rapid rise in $[Ca^{2+}]_i$ through both release of endoplasmic reticulum stores and influx of extracellular Ca^{2+} [200]. To better understand the mechanism of *Hemidesmus*, we used thapsigargin, a compound that induces the release of intracellular endoplasmic reticulum Ca^{2+} stores and prevents refilling by inhibition of the endoplasmic reticulum

Ca^{2+}-ATPase[201]. Thapsigargin significantly increased *Hemidesmus*-induced $[Ca^{2+}]_i$ raise. On the whole, our results suggest that *Hemidesmus* may cause $[Ca^{2+}]_i$ raise through the mobilization of intracellular Ca^{2+} stores.

Moreover, the intrinsic pathway is strongly regulated by interactions between members of the Bcl-2 family. This family of proteins is composed of three groups defined according to their function and content of Bcl-2 homology (BH) domains. Bcl-2, the oncoprotein activated by chromosome translocation in follicular lymphoma[202], inhibits apoptosis[203], as do four of its homologues Bcl-XL, Bcl-w, Mcl-1 and A1, which share four BH domains. Within the Bcl-2 family, there are also pro-apoptotic effectors like Bax and Bak that share three BH domains, as well as a C-terminal transmembrane segment that selectively targets these proteins to the membranes of mitochondria and endoplasmic reticulum. Lastly, a large and diverse pro-apoptotic group within this family, named BH3-only proteins, contains only a single BH3 domain, such as Bim, Puma, Bid, and Noxa. Induction of apoptosis requires the activation of members of both of these death-promoting families[204, 205]. The induction of BH3-only proteins results in the neutralization of pro-survival proteins, and in the subsequent activation of Bax and Bak. The activation of the two pro-apoptotic effectors involves their conformational change and homo-oligomerisation on the mitochondrial outer membrane, which leads to its permeabilization. It has been shown that the Bcl-2 protein physically interacts with several of its homologous proteins. The most important interactions are considered to lie in Bcl-2/Bax dimerization. Thus, we studied the profile of Bcl-2 and Bax gene products in terms of protein and gene expressions. Our results showed that Bax protein expression was markedly induced, suggesting that Bax was up-regulated and played an important role in the induction of apoptosis after *Hemidesmus* exposure. However, in contrast to the Bcl-2 inhibiting apoptotic cell death, the present study found that Bcl-2 expression was also increased after *Hemidesmus* exposure compared to control. The increase in anti-apoptotic Bcl-2 protein may serve as a compensatory protection of the leukemia cells upon *Hemidesmus* insult. Although the expressions of Bcl-2 and Bax, both of them, were increased, the ratio of Bax/Bcl-2 (pro- to anti-apoptotic proteins) was also increased after *Hemidesmus* treatment. The findings support the notion that the relative concentrations of pro-apoptotic and anti-apoptotic proteins may act as a rheostat for the cell death program[206]. Notably, the mRNA expression of *BCL2* and *BAX* was reduced by *Hemidesmus* treatment. This result was in conflict to what demonstrated at post-transcriptional level with the overexpression of the two Bcl-2 family proteins. Since both proteins are degraded through an ubiquitin-proteasome dependent pathway, we studied the ability of *Hemidesmus* to modulate this pathway. The 26S proteasome is critical for the maintenance of homeostasis of most intracellular proteins[207]. A large number of proteins involved in cell cycle progression and apoptosis are

regulated by ubiquitinylation and proteasome-mediated degradation. Therefore, targeting proteasome pathway has emerged as a promising approach to cancer therapy[208]. Bortezomib, a cell-permeable dipeptidyl boronic acid, is a specific and selective inhibitor of 26S proteasome and was the first proteasome inhibitor used for the treatment of relapsed or refractory multiple myeloma[209]. In our experimental model, *Hemidesmus* reduced the 26S proteasome expression. Its ability was comparable with that expressed by bortezomib 10 μM and MG132 0.5 μM. Furthermore, *Hemidesmus* induced a post-transcriptional down-regulation of the proteasome mRNA. These results partially justify the differential post-transcriptional and post-translational regulation of Bax and Bcl-2 evoked by *Hemidesmus*.

Among the pro-survival Bcl-2 family members, Mcl-1 is essential for the survival of multiple cell lineages in the adult, including lymphocytes[210, 211], HSCs[212], neutrophils[213, 214], neurons[215], and for embryonic development[216]. Moreover, Mcl-1 is frequently over-expressed in human cancers[217] representing a key factor in the resistance of leukemia to conventional anti-cancer therapy[218]. Mcl-1 is localized to distinct mitochondrial sub-compartments, with differential functions that affect mitochondrial activity and integrity. On the outer mitochondrial membrane, Mcl-1 exerts its anti-apoptotic activity where it antagonizes Bax and Bak activation, maintaining mitochondrial integrity, and inhibits mitochondrial calcium signals following an apoptotic stimulus[219]. In contrast, Mcl-1 localized in the mitochondrial matrix is unable to inhibit apoptosis, but maintains normal inner mitochondrial membrane structure, regulates fusion and promotes the assembly of ATP synthase oligomers; thereby, it facilitates mitochondrial homeostasis and supports mitochondrial bioenergetic function[220]. A down-regulation of Mcl-1 is often sufficient to promote apoptosis in leukemic cells, suggesting that Mcl-1 can be a potential therapeutic target in the treatment of several human leukemias[218, 221-223]. To date, numerous strategies, including small molecule BH3 mimetics, stapled BH3 peptides, and down-regulation of Mcl-1 by kinase inhibitors, deubiquitinase inhibitors, and antisense oligonucleotides, have been attempted to target Mcl- 1 for cancer treatment[224]. However, none of the Mcl-1 specific inhibitors are in clinic. Our study revealed that *Hemidesmus* induces a rapid decrease in Mcl-1 protein levels. This regulation appeared to be essentially post-translational because Mcl-1 mRNA was up-regulated at all treatment times. The increased gene expression of Mcl-1 may represent as a mechanism of leukemic cells protection against the degradation of the anti-apoptotic protein induced by *Hemidesmus*. At post-translational level, Mcl-1 can be cleaved by caspases, specifically caspase-3, at Asp127 and Asp157. This results in the removal of a large part of the N-terminus of Mcl-1, leaving the BH1-3 and the C-terminal transmembrane domain intact. The caspase-dependent cleavage of Mcl-1 suggests that the cleavage products become pro-death apoptosis[225-228]. Since *Hemidesmus* stimulate caspase-3 activity, its induction may be responsible

for the post-translational down-regulation of Mcl-1. Furthermore, Mcl-1 is subject to a rapid turnover through ubiquitin-dependent protein degradation by the 26S proteasome. One of E3 ligases of the proteasome, MULE/LASU1, is a BH3-only Hect E3-ligase whose BH3 domain interacts with the hydrophobic BH3 binding pocket of Mcl-1, and not with other pro-survival Bcl-2 family members[229, 230]. Noxa has been shown to associate mainly with Mcl-1, and induce ubiquitin-proteasome-mediated degradation of Mcl-1[231]. In our study, despite the clear post-transcriptional stimulation of Noxa induced by *Hemidesmus*, the protein levels were not modulated, even if the proteasome inhibition ability exerted by *Hemidesmus* should have led to an accumulation of the BH3-only family protein[232]. Reasonable explanations for this phenomenon could be the lack of a specific antibody able to recognize the epitope of Noxa in dimmer with Mcl-1[233], or the high physiological level of Noxa in Jurkat cells that could make the detection of alterations in protein expression difficult[234]. The importance of the Noxa/Mcl-1 balance has been recently proved to play an important role in the intrinsic apoptotic pathway[234, 235]. Treatments with *Hemidesmus* caused a variation in the Noxa/Mcl-1 ratio in favor of Noxa. These results showed how much the down-regulation of Mcl-1 and its close relation with Noxa are crucial for the pro-apoptotic activity exerted by *Hemidesmus*.

Senescence is an established cellular pathway involved in all aspects of cancer biology from carcinogenesis to tumor proliferation and appears to be a major obstacle for cancer progression[236]. Senescence appears to be controlled by distinct pathways, but in general it is initiated by tumor suppressors like p53. Thus, without the loss of tumor suppressor genes like p53, cells expressing or even over-expressing oncosuppressors fail to become cancerous due to senescence[237]. Bolesta et al. showed that Mcl-1 plays an important role in preventing chemotherapy-induced senescence in both a p53-dependent and -independent manner and that Mcl-1-mediated inhibition can enhance tumor growth *in vivo*. Moreover, they observed an increased p21 expression in all cases where senescence can be induced[238]. This allows to speculate that Mcl-1 down-regulation represents a key step not only in the induction of apoptosis but also in the inhibition of the cell cycle progression induced by *Hemidesmus*. This result was supported by the fact that *Hemidesmus* did not show any modulation of p53 in our experimental setting.

Other key factors in the regulation of cellular apoptosis pathway, in both physiological and pathological conditions, are ROS. The level of ROS influences several proteins involved in the apoptotic and cell-cycle regulation. Mitochondria are strictly correlated with ROS as their source and target. As an example, the release of cytochrome c and then the activation of caspases are directly and indirectly regulated by ROS[239]. Furthermore, several studies reported that p21 expression during senescence is dependent on the production of ROS[240, 241]. *Hemidesmus* showed

the ability to increase the production of ROS starting after short-term treatments. The association with NAC resulted in a significant reduction of the pro-apoptotic capability of *Hemidesmus*.
Altogether, our results suggest that the growth inhibition of Jurkat cells produced by *Hemidesmus* results from a combination of apoptosis and of cell-cycle derangements in which S accumulation, p21 increase, down-regulation of Mcl-1, and induction of ROS are key events.

The *Hemidesmus*-induced S accumulation could have potentially important clinical implications. This factor made evaluation of the pro-apoptotic effects of *Hemidesmus* together with anticancer agents an important focus of our pre-clinical experiments. Cells which are synthesizing DNA usually display increased susceptibility to most anticancer drugs (e.g. antimetabolites or intercalating agents)[242]. The anticancer agents tested in this study in association with *Hemidesmus* included 6-thioguanine, cytarabine and methotrexate. Their inclusion was important for determining whether *Hemidesmus* can enhance the anticancer efficacy of chemotherapeutic agents. Accordingly, the ability of *Hemidesmus* to increase the fraction of cells engaged in the S-phase of the cell-cycle was useful in potentiating the efficacy of 6-thioguanine, cytarabine and methotrexate.

The research continued with the study of the pro-differentiating ability of *Hemidesmus*. The stimulation of differentiation is a recognized alternative in the treatment of cancer, by generating cells with limited or no replicative capability able to enter in the apoptotic pathways[243]. It is well known that the only successful differentiation therapy in the clinic still remains treatment with all-trans retinoic acid plus arsenic trioxide[244]. At molecular level, all-trans retinoic acid and arsenic trioxide are able to modulate synergistically multiple downstream pathways/cascades. This combination therapy, compared to the traditional anthracycline-based regimen, results in lower toxicity, improvement of long-term outcome, higher survival rates, with >90% patients disease-free after 5 years by the end of treatment[244, 245].

The ability of *Hemidesmus* to induce cytodifferentiation was screened on HL-60 cells that have the potential to differentiate into macrophages or granulocytes[246]. Treatment of HL-60 cultures with *Hemidesmus* caused apoptosis and cell-cycle inhibition, which may represent an event only partly dependent on cytodifferentiation in our experimental conditions. In fact, the induction of apoptosis and the inhibition of cell-cycle were almost simultaneous. The early appearance of cell-cycle-inhibition and apoptosis compared with cytodifferentiation clearly indicates that cytotoxicity and cytostasis events are primary direct effects due to *Hemidesmus* and are not due to activation of apoptosis and/or inhibition of cell proliferation as a consequence of cell's differentiation. Although reported *in vitro*, those effects are worthy of comparing with the effects recorded for all-trans retinoic acid on the same cell line. No induction of apoptosis was observed on HL-60 cells after 48h

of treatment with all-trans retinoic acid. By 72h, a modest fraction of cells incubated with all-trans retinoic acid became apoptotic[247]. These results are consistent with the evidence that apoptosis induced by all-trans retinoic acid is a consequence of its cytodifferentiative potential[248] and does not represent an independent event. The treatment of HL-60 with *Hemidesmus* altered cell-cycle progression though the induction of a dose- and time-dependent accumulation of cells in the G_0/G_1 phase evident after 24h of treatment. This is a critical point because cells need to exit from cell cycle before differentiating and this decision is commonly made in G_1 phase[249]. By comparing our results with those obtained with all-trans retinoic acid and arsenic trioxide on the same cell line, we observe that the antiproliferative effects of *Hemidesmus* are much earlier than those of all-trans retinoic acid and arsenic trioxide, evident after 4 and 5 days of incubation, respectively[250].

Our biological data support the conclusion that *Hemidesmus* significantly induced HL-60 to differentiate along the macrophage and granulocyte lineage. The subsequent morphological analysis by TEM confirmed the cytodifferentiation ability of this traditional plant. The ability of *Hemidesmus* to induce differentiation into granulocytes resulted in a less extent compared to the data concerning the differentiation induced by all-trans retinoic acid, but in a greater extent compared to arsenic trioxide[250].

Taken together, these results evidence the ability of *Hemidesmus* to induce a plethora of effects, all contributing to its anti-leukemic effect. This aspect appears important because the therapeutic success of drugs used in the acute promyelocytic leukemia results from the balance of self renewal, apoptosis and differentiation. Indeed, in clinical practice, retinoic acid by itself only rarely yields prolonged remission, even thought it induce massive differentiation. Otherwise, *in vivo* studies on arsenic trioxide reported an initial induction of apoptosis followed by slow blast differentiation[245].

The study continued investigating the ability of *Hemidesmus* to modulate new blood vessels formation. Angiogenesis plays a crucial role in the development and spread of tumor[251]. Cancer cells are not able to grow in diameter more than 1-2 mm^3 and metastasis without blood circulation. To spread, they need to be supplied by blood vessels that bring oxygen and nutrients and remove metabolic wastes. In absence of vascular support, tumors may become necrotic or even apoptotic[252]. Angiogenesis has been identified as a hallmark of tumor progression[253] and therefore anti-angiogenic therapy has become a new promising anticancer strategy. Nowadays, numerous anti-angiogenic therapeutics are used alone in maintenance treatment[254] or in polytherapy regimens against cancer[255].

Hypoxia has a strong influence in the biology of tumors and in their response to treatments. In particular, hypoxia plays a central role in the induction of angiogenesis. Limitation of oxygen diffusion in vascular primary tumor arise hypoxic conditions and stimulates the formation of tumor

abnormal microvasculature[256]. The master regulator of cellular adaptation in response to oxygen deprivation is HIF. HIF is a heterodimer and its subunit HIF-1α is involved in the initiation of a transcriptional program that promotes an aggressive tumor phenotype leading to metastasis and tissue invasion[257]. The hypoxic condition enhances the transcription of VEGF, by HIF-1α. Among the few growth factors that regulate angiogenesis, VEGF has a pivotal role. An increased activity of VEGF has been reported in the most aggressive cancers[258] and it is related with a poor prognosis[259], also in hematological malignancies[260].

For several years angiogenesis has been correctly attributed only to solid tumor. Nonetheless, several *in vitro*[261, 262], *in vivo*[263, 264], and clinical studies[265, 266] strongly suggest that induction of angiogenesis in hematological tumors has a pathophysiological relevance for disease progression and represents a valid pharmacological target. As an example, Kopp et al. showed how the BM vasculature plays an important role in hematopoiesis in health and disease. Kopp demonstrated the role of mural cells (pericytes and smooth muscle cells) in providing a specialized vascular "niche" for HSCs[267]. Therefore, development of pharmacological strategies that target both the stromal and tumor compartments, such as the combination between the traditional cytotoxic chemotherapy and anti-angiogenic agents, may conduce to an improvement of cancer treatment.

In this context, *Hemidesmus* represents an interesting strategy due to its capability to contemporary modulate several targets. We have already demonstrated its ability to induce apoptosis, interfere with cell-cycle progression and induce differentiation in leukemic cell lines. An *in vitro* model of angiogenesis was used and it focused on endothelial cell proliferation, formation of capillary-like structures in matrigel, quantification of the sprouting, migration, and invasion[268]. Treatment with *Hemidesmus* inhibited angiogenesis in normoxia and hypoxia through the regulation of key factors of the neovascularization process. Endothelial cell proliferation is strictly correlated with the angiogenic and metastatic process[269]. In both O_2 conditions, *Hemidesmus* reduced proliferation without showing any appreciable effect in the induction of apoptosis on HUVECs. Using the *in vitro* angiogenesis assay, we found that *Hemidesmus* was able to inhibit microvessels outgrowth in a dose-dependent manner, also in association with VEGF, a well-know angiogenesis inducer. The expression levels of the principal proteins involved in the regulation of angiogenesis (HIF-1α, VEGF and VEGFR-2) and their mRNAs have been analyzed after treatment with *Hemidesmus*. A down-regulation of HIF-1α protein level was reported after treating HUVECs in hypoxic condition, while in normoxia no modulation was reported. At gene level, *Hemidesmus* induced a dose-dependent reduction in the expression of HIF-1α, both in normoxic and hypoxic conditions, but the major down-regulation was observed in the low oxygen condition. This result is partially justified by the fact that the hypoxic microenvironment stimulates tumor angiogenesis more than in normal

O_2 pressure condition[270]. Moreover, the down-regulation of HIF-1α induced by *Hemidesmus* demonstrates its ability to overcome the accumulation of the protein that typically appears in hypoxic condition due to the inhibition of its degradation[271]. Additionally, *Hemidesmus* down-regulated the VEGF protein expression in both O_2 conditions. This result clearly demonstrates the role of HIF-1α in the modulation of VEGF in hypoxic conditions. Between the two VEGF receptors, VEGFR-2 appears to be the major transducer of VEGF signals in endothelial cells, leading to cell proliferation, migration, differentiation, capillary-like formation and vascular permeability. In the light of these considerations, inhibition of VEGFR-2 might represent an interesting approach for an anti-angiogenic intervention[272]. The protein expression of VEGFR-2 was reduced by *Hemidesmus* only in condition of low oxygen, while, a modulation of the gene appeared in both O_2 conditions. Taken together our results suggest that the inhibition of angiogenesis induced by *Hemidesmus* is mediated through two distinct mechanisms according to the oxygen availability. In normoxic condition, the reduced expression of VEGF induced by the decoction seems to be the main cause for the inhibition of angiogenesis, while the inhibition of angiogenesis induced by *Hemidesmus* in hypoxic condition is regulated by a more complex mechanism, which involves the inhibition of HIF-1α first, VEGF and its receptor VEGFR-2.

Neovascularization influences the dissemination of cancer cells throughout the entire body eventually leading to metastasis formation. The vascularization level of a solid tumor is thought to be an excellent indicator of its metastatic potential[273]. In this context, *Hemidesmus* suppressed significantly invasion and migration of endothelial cells. These results demonstrate that *Hemidesmus indicus* modulates angiogenesis by the inhibition of new vessel formation and migration/invasion. Indeed, it down-regulates key proteins and genes involved in neoangiogenesis, such as HIF-1α, VEGF, and VEGFR-2. Based on these data, the use of *Hemidesmus* might be promoted as a therapeutic agent for diseases in which the inhibition of angiogenesis could be beneficial, in particular in anticancer therapy.

In the final part of this study we explored the ability of *Hemidesmus* to induce apoptosis in fresh AML cells. *Ex vivo* samples represent a good surrogate for determining patient's cellular response to treatment and predicting clinical outcome. This can not be realized by using cell lines, which markedly differ from blasts in terms of growth kinetics and pharmacological determinants[35, 274-276]. We observed that *Hemidesmus* was a potent inducer of apoptosis in AML cells. Its pro-apoptotic activity was particularly marked on blasts obtained from a recidivant patient (AML4), characterized by a genomic alteration of the *FLT3* gene, including FLT3/ITD. This observation is particularly interesting because *FLT3/ITD*s are predictive of relapse and poor outcome in the chemotherapy setting[277].

The characterization of stem cells in different leukemic processes led to the conclusion that these cells can actively contribute to the failure of therapies focalized on the eradication of leukemic blasts. CSCs are naturally resistant to chemotherapy through their quiescence, their ability for DNA repair, and ABC transporter expression. As a result, LSCs that survive from traditional anti-leukemic chemotherapy can support the regrowth and the relapse of leukemia[7]. Moreover, LSCs play a pivotal role in the process of leukemia initiation and progression. For these reasons, LSCs represent a potential and promising pharmacological target for the treatment of leukemia[278].

We investigated the effect of *Hemidesmus* and piperlongumine on CD34+ sorted subpopulation from 6 primary human AML and healthy cord blood samples. Both drugs induced apoptosis and inhibited the colony formation in CD34+ AML patient samples, regardless of their karyotype. This evidence is extremely important since complex karyotype AML is strongly associated with poor prognosis[279]. The effect of piperlongumine in the inhibition of colony formation resulted more pronounced at the highest tested concentration and brought to a complete lack of colonies. Of note, *Hemidesmus* did not show any effect on healthy CD34+ cells at all tested concentrations, while piperlongumine induced a low induction of apoptosis at the concentration 14 μM. Since LSCs plays key role in the initiation and development of leukemia, the selectivity of action toward them expressed by both *Hemidesmus* and piperlongumine outlines their interesting pharmacological profile in the treatment of leukemia.

Chapter 6

Conclusions

On the whole, our results indicate that the traditional preparation of *Hemidesmus indicus* could be a promising botanical drug in the oncologic area. The simultaneous modulation of several key processes in cancer development like apoptosis, ROS formation, cytodifferentiation and angiogenesis makes *Hemidesmus indicus* a promising botanical drug in the treatment of leukemia. Furthermore, *Hemidesmus* showed a selective action toward LSCs that are viewed as the origin of the hierarchy of tumor cells. Since selective targeting and low toxicity for normal host tissues are fundamental requisites for anticancer drugs, it is also interesting to note that the cytotoxic activity of *Hemidesmus* on nontransformed cells was significantly lower than that observed in cancer cells (data not shown) and absent on healthy CD34+ cells. This could allow the definition of a range of concentrations potentially active only on cancer cells.

Hemidesmus contains a mixture of known and possibly active compounds and this aspect poses many challenging issues. However, it is a relatively simple botanical product (single part of single plant). As a naturally occurring mixture from a single part of a single plant, it is not considered a combination product[115]. Of note, FDA demonstrated that therapeutic consistency of the commercial batches of simple botanical preparations (single part of single plant) can be assured. Although the chemical constituents of a botanical drug are not always well defined and in many cases the active constituent is not identified nor is its biological activity characterized[116], variations in raw material quality can be minimized by restricting the cultivars, the composition of the preparation can be equivalent by robust chemistry, manufacturing and control measures, 'fingerprinting', and conducting chromatographic analyses of marker compounds[115]. Our HPLC phytochemical analysis of *Hemidesmus indicus* demonstrated the presence of 2H4MBAC, 2H4MBAL and 3H4MBAL, which can be used as fingerprint. Of note in this context, the phytochemical analysis performed on different batches of *Hemidesmus* demonstrated that the levels of the above reported phytomarkers were not statistically different among batches. The above reported phytomarkers lacked pro-apoptotic activities, while their association induced apoptosis in Jurkat cells. Although relatively high doses of single bioactive agents may show potent anticarcinogenic effects, the antitumor properties of interactions among various ingredients that potentiate the activities of any single constituent may better explain the observed pharmacological effect of whole plant, as evidenced for other plants in many *in vitro* and *in vivo* studies[170, 280, 281]. On these bases, we conclude that *Hemidesmus* can represent a valuable strategy in the anticancer pharmacology, and should be considered for further investigations.

As regards piperlongumine, many studies reported its ability to eradicate cancer cells. Through our study we expanded the knowledge about this promising natural agent by the demonstration of its selective action toward LSCs. Through its anti-leukemic effects that include induction of apoptosis, cell-cycle arrest, ROS induction, inhibition of angiogenesis/metastasis and LSCs elimination, piperlongumine represents an example of multi-target drug and could lead to treatment and long-term remission of cancer.

Chapter 8

Reference list

1. Siegel, R., Ma, J., Zou, Z., & Jemal, A. Cancer statistics, 2014. *CA Cancer J. Clin. 2014; 64: 9-29.*
2. Estey, E. & Dohner, H. Acute myeloid leukaemia. *Lancet 2006; 368: 1894-1907.*
3. Brown, C.M., Larsen, S.R., Iland, H.J., Joshua, D.E., & Gibson, J. Leukaemias into the 21st century: part 1: the acute leukaemias. *Intern. Med. J. 2012; 42: 1179-86.*
4. Doulatov, S., Notta, F., Laurenti, E., & Dick, J.E. Hematopoiesis: a human perspective. *Cell Stem Cell. 2012; 10: 120-36.*
5. Akashi, K., Traver, D., Miyamoto, T., & Weissman, I.L. A clonogenic common myeloid progenitor that gives rise to all myeloid lineages. *Nature. 2000; 404: 193-7.*
6. Kondo, M., Weissman, I.L., & Akashi, K. Identification of clonogenic common lymphoid progenitors in mouse bone marrow. *Cell. 1997; 91: 661-72.*
7. Reya, T., Morrison, S.J., Clarke, M. F., & Weissman, I. L. Stem cells, cancer, and cancer stem cells. *Nature. 2001; 414: 105-11.*
8. Adolfsson, J. *et al.* Upregulation of Flt3 expression within the bone marrow Lin(-)Sca1(+)c-kit(+) stem cell compartment is accompanied by loss of self-renewal capacity. *Immunity. 2001; 15: 659-69.*
9. Morrison, S.J., Wandycz, A.M., Hemmati, H.D., Wright, D.E., & Weissman, I.L. Identification of a lineage of multipotent hematopoietic progenitors. *Development. 1997; 124: 1929-39.*
10. Katsura, Y. & Kawamoto, H. Stepwise lineage restriction of progenitors in lympho-myelopoiesis. *Int. Rev. Immunol. 2001; 20: 1-20.*
11. Katsura, Y. Redefinition of lymphoid progenitors. *Nat. Rev. Immunol. 2002; 2: 127-32.*
12. Kawamoto, H.A close developmental relationship between the lymphoid and myeloid lineages. *Trends Immunol. 2006: 27: 169-75.*
13. Kawamoto, H., Ikawa, T., Masuda, K., Wada, H., & Katsura, Y. A map for lineage restriction of progenitors during hematopoiesis: the essence of the myeloid-based model. *Immunol. Rev. 2010; 238: 23-36.*
14. Adolfsson, J. *et al.* Identification of Flt3+ lympho-myeloid stem cells lacking erythro-megakaryocytic potential a revised road map for adult blood lineage commitment. *Cell. 2005; 121: 295-306.*
15. Boyer, S.W., Schroeder, A.V., Smith-Berdan, S., & Forsberg, E.C. All hematopoietic cells develop from hematopoietic stem cells through Flk2/Flt3-positive progenitor cells. *Cell Stem Cell. 2011; 9: 64-73.*
16. Buza-Vidas, N. *et al.* FLT3 expression initiates in fully multipotent mouse hematopoietic progenitor cells. *Blood. 2011; 118: 1544-8.*
17. Rinkevich, Y., Lindau, P., Ueno, H., Longaker, M.T., & Weissman, I.L. Germ-layer and lineage-restricted stem/progenitors regenerate the mouse digit tip. *Nature. 2011; 476: 409-13.*
18. Nguyen, L.V., Vanner, R., Dirks, P., & Eaves, C.J. Cancer stem cells: an evolving concept. *Nat. Rev. Cancer. 2012; 12: 133-43.*
19. Bosma, G.C., Custer, R.P., & Bosma, M.J. A severe combined immunodeficiency mutation in the mouse. *Nature. 1983; 301: 527-30.*
20. Bhatia, M., Wang, J.C., Kapp, U., Bonnet, D., & Dick, J.E. Purification of primitive human hematopoietic cells capable of repopulating immune-deficient mice. *Proc. Natl. Acad. Sci. U. S. A. 1997; 94: 5320-5.*
21. Civin, C.I. *et al.* Sustained, retransplantable, multilineage engraftment of highly purified adult human bone marrow stem cells in vivo. *Blood. 1996; 88: 4102-9.*
22. Kimura, T. *et al.* In vivo dynamics of human cord blood-derived CD34(-) SCID-repopulating cells using intra-bone marrow injection. *Leukemia. 2010; 24: 162-8.*
23. Wang, J. *et al.* SCID-repopulating cell activity of human cord blood-derived CD34- cells assured by intra-bone marrow injection. *Blood. 2003; 101: 2924-31*
24. Hogan, C.J., Shpall, E.J., & Keller, G. Differential long-term and multilineage engraftment potential from subfractions of human CD34+ cord blood cells transplanted into NOD/SCID mice. *Proc. Natl. Acad. Sci. U. S. A. 2002; 99: 413-8.*
25. McKenzie, J.L., Gan, O.I., Doedens, M., Wang, J.C., & Dick, J.E. Individual stem cells with highly variable proliferation and self-renewal properties comprise the human hematopoietic stem cell compartment. *Nat. Immunol. 2006; 7: 1225-33.*

26. Benveniste, P. *et al.* Intermediate-term hematopoietic stem cells with extended but time-limited reconstitution potential. *Cell Stem Cell. 2010; 6: 48-58.*

27. Challen, G.A., Boles, N.C., Chambers, S.M., & Goodell, M.A. Distinct hematopoietic stem cell subtypes are differentially regulated by TGF-beta1. *Cell Stem Cell. 2010; 6: 265-78.*

28. Omatsu, Y. *et al.* The essential functions of adipo-osteogenic progenitors as the hematopoietic stem and progenitor cell niche. *Immunity. 2010; 33: 387-99.*

29. Himburg, H. A. *et al.* Pleiotrophin regulates the expansion and regeneration of hematopoietic stem cells. *Nat. Med. 2010; 16: 475-82.*

30. Mohyeldin, A., Garzon-Muvdi, T., & Quinones-Hinojosa, A. Oxygen in stem cell biology: a critical component of the stem cell niche. *Cell Stem Cell. 2010; 7: 150-61.*

31. Takubo, K. *et al.* Regulation of the HIF-1alpha level is essential for hematopoietic stem cells. *Cell Stem Cell. 2010; 7: 391-402.*

32. Orford, K.W. & Scadden, D. T. Deconstructing stem cell self-renewal: genetic insights into cell-cycle regulation. *Nat. Rev. Genet. 2008; 9: 115-28.*

33. Mohrin, M. *et al.* Hematopoietic stem cell quiescence promotes error-prone DNA repair and mutagenesis. *Cell Stem Cell. 2010; 7: 174-85.*

34. Pui, C.H. *et al.* Acute myeloid leukemia in children treated with epipodophyllotoxins for acute lymphoblastic leukemia. *N. Engl. J. Med. 1991; 325: 1682-7.*

35. Larson, R.A. Cytogenetics, not just previous therapy, determines the course of therapy-related myeloid neoplasms. *J. Clin. Oncol. 2012; 30: 2300-2*

36. Bacher, U., Schnittger, S., & Haferlach, T. Molecular genetics in acute myeloid leukemia. *Curr. Opin. Oncol. 2010; 22.: 646-55.*

37. Gilliland, D.G., Jordan, C.T., & Felix, C.A. The molecular basis of leukemia. *Hematology. Am. Soc. Hematol. Educ. Program. 2004; 80-97.*

38. Falini, B. *et al.* Cytoplasmic nucleophosmin in acute myelogenous leukemia with a normal karyotype. *N. Engl. J. Med. 2005; 352: 254-66.*

39. Gale, R.E. *et al.* The impact of FLT3 internal tandem duplication mutant level, number, size, and interaction with NPM1 mutations in a large cohort of young adult patients with acute myeloid leukemia. *Blood. 2008; 111: 2776-84.*

40. Schnittger, S. *et al.* Analysis of FLT3 length mutations in 1003 patients with acute myeloid leukemia: correlation to cytogenetics, FAB subtype, and prognosis in the AMLCG study and usefulness as a marker for the detection of minimal residual disease. *Blood. 2002; 100: 59-66.*

41. Thiede, C. *et al.* Analysis of FLT3-activating mutations in 979 patients with acute myelogenous leukemia: association with FAB subtypes and identification of subgroups with poor prognosis. *Blood. 2002; 99: 4326-35.*

42. Whitman, S.P. *et al.* Absence of the wild-type allele predicts poor prognosis in adult de novo acute myeloid leukemia with normal cytogenetics and the internal tandem duplication of FLT3: a cancer and leukemia group B study. *Cancer Res. 2001; 61: 7233-9.*

43. Burnett, A.K. *et al.* The impact on outcome of the addition of all-trans retinoic acid to intensive chemotherapy in younger patients with nonacute promyelocytic acute myeloid leukemia: overall results and results in genotypic subgroups defined by mutations in NPM1, FLT3, and CEBPA. *Blood. 2010; 115: 948-56.*

44. Dohner, K. *et al.* Mutant nucleophosmin (NPM1) predicts favorable prognosis in younger adults with acute myeloid leukemia and normal cytogenetics: interaction with other gene mutations. *Blood. 2005; 106: 3740-6.*

45. Schlenk, R.F. *et al.* Mutations and treatment outcome in cytogenetically normal acute myeloid leukemia. *N. Engl. J. Med. 2008; 358: 1909-18*

46. Lowenberg, B. *et al.* High-dose daunorubicin in older patients with acute myeloid leukemia. *N. Engl. J. Med. 2009; 361: 1235-48.*

47. Yates, J.W., Wallace, H.J., Jr., Ellison, R.R., & Holland, J.F. Cytosine arabinoside (NSC-63878) and daunorubicin (NSC-83142) therapy in acute nonlymphocytic leukemia. *Cancer Chemother. Rep. 1973; 57: 485-8.*

48. Arlin, Z. *et al.* Randomized multicenter trial of cytosine arabinoside with mitoxantrone or daunorubicin in previously untreated adult patients with acute nonlymphocytic leukemia (ANLL). Lederle Cooperative Group. *Leukemia. 1990; 4: 177-83.*

49. Berman, E. *et al.* Results of a randomized trial comparing idarubicin and cytosine arabinoside with daunorubicin and cytosine arabinoside in adult patients with newly diagnosed acute myelogenous leukemia. *Blood. 1991; 77: 1666-74.*

50. Wiernik, P.H. *et al.* Cytarabine plus idarubicin or daunorubicin as induction and consolidation therapy for previously untreated adult patients with acute myeloid leukemia. *Blood. 1992; 79: 313-9.*

51. Bishop, J.F. *et al.* A randomized study of high-dose cytarabine in induction in acute myeloid leukemia. *Blood. 1996; 87: 1710-7.*

52. Estey, E.H. *et al.* Comparison of idarubicin + ara-C-, fludarabine + ara-C-, and topotecan + ara-C-based regimens in treatment of newly diagnosed acute myeloid leukemia, refractory anemia with excess blasts in transformation, or refractory anemia with excess blasts. *Blood. 2001; 98: 3575-83.*

53. Appelbaum, F.R. Haematological cancer: The rule of three in AML induction--is cladribine the answer? *Nat. Rev. Clin. Oncol. 2012; 9: 376-7.*

54. Lyman, G.H. *et al.* Acute myeloid leukemia or myelodysplastic syndrome in randomized controlled clinical trials of cancer chemotherapy with granulocyte colony-stimulating factor: a systematic review. *J. Clin. Oncol. 2010; 28: 2914-24.*

55. Knapper, S. The clinical development of FLT3 inhibitors in acute myeloid leukemia. *Expert. Opin. Investig. Drugs. 2011; 20: 1377-95.*

56. Rowe, J.M. Consolidation therapy: what should be the standard of care? *Best. Pract. Res. Clin. Haematol. 2008; 21: 53-60.*

57. Ferrara, F. New agents for acute myeloid leukemia: is it time for targeted therapies? *Expert. Opin. Investig. Drugs. 2012; 21: 179-89.*

58. Burnett, A.K. *et al.* Attempts to optimize induction and consolidation treatment in acute myeloid leukemia: results of the MRC AML12 trial. *J. Clin. Oncol. 2010; 28: 586-95.*

59. Cassileth, P.A. *et al.* Chemotherapy compared with autologous or allogeneic bone marrow transplantation in the management of acute myeloid leukemia in first remission. *N. Engl. J. Med. 1998; 339: 1649-56.*

60. Zittoun, R.A. *et al.* Autologous or allogeneic bone marrow transplantation compared with intensive chemotherapy in acute myelogenous leukemia. European Organization for Research and Treatment of Cancer (EORTC) and the Gruppo Italiano Malattie Ematologiche Maligne dell'Adulto (GIMEMA) Leukemia Cooperative Groups. *N. Engl. J. Med. 1995; 332: 217-23.*

61. Burnett, A.K. *et al.* The value of allogeneic bone marrow transplant in patients with acute myeloid leukaemia at differing risk of relapse: results of the UK MRC AML 10 trial. *Br. J. Haematol. 2002; 118: 385-400.*

62. Sanz, M.A. & Lo-Coco, F. Modern approaches to treating acute promyelocytic leukemia. *J. Clin. Oncol. 2011; 29: 495-503.*

63. Hu, J. *et al.* Long-term efficacy and safety of all-trans retinoic acid/arsenic trioxide-based therapy in newly diagnosed acute promyelocytic leukemia. *Proc. Natl. Acad. Sci. U. S. A. 2009; 106: 3342-7 .*

64. Estey, E. *et al.* Potential curability of newly diagnosed acute promyelocytic leukemia without use of chemotherapy: the example of liposomal all-trans retinoic acid. *Blood. 2005; 105: 1366-7.*

65. Mathews, V. *et al.* Single-agent arsenic trioxide in the treatment of newly diagnosed acute promyelocytic leukemia: long-term follow-up data. *J. Clin. Oncol. 2010; 28: 3866-71.*

66. Lapidot, T. *et al.* A cell initiating human acute myeloid leukaemia after transplantation into SCID mice. *Nature. 1994; 367: 645-8.*

67. Bonnet, D. & Dick, J.E. Human acute myeloid leukemia is organized as a hierarchy that originates from a primitive hematopoietic cell. *Nat. Med. 1997; 3: 730-7.*

68. Ailles, L.E., Gerhard, B., Kawagoe, H., & Hogge, D.E. Growth characteristics of acute myelogenous leukemia progenitors that initiate malignant hematopoiesis in nonobese diabetic/severe combined immunodeficient mice. *Blood. 1999; 94: 1761-72.*

69. Rombouts, W.J., Martens, A.C., & Ploemacher, R.E. Identification of variables determining the engraftment potential of human acute myeloid leukemia in the immunodeficient NOD/SCID human chimera model. *Leukemia. 2000; 14: 889-97.*

70. Taussig, D.C. *et al.* Anti-CD38 antibody-mediated clearance of human repopulating cells masks the heterogeneity of leukemia-initiating cells. *Blood. 2008; 112: 568-75.*

71. Ferrara, F. & Schiffer, C.A. Acute myeloid leukaemia in adults. *Lancet. 2013; 381: 484-95.*

72. Wojiski, S. *et al.* PML-RARalpha initiates leukemia by conferring properties of self-renewal to committed promyelocytic progenitors. *Leukemia. 2009; 23: 1462-71.*

73. Guibal, F.C. *et al.* Identification of a myeloid committed progenitor as the cancer-initiating cell in acute promyelocytic leukemia. *Blood. 2009; 114: 5415-25.*

74. Hunger, S.P. *et al.* Improved survival for children and adolescents with acute lymphoblastic leukemia between 1990 and 2005: a report from the children's oncology group. *J. Clin. Oncol. 2012; 30: 1663-9.*

75. Pui, C.H., Robison, L.L., & Look, A.T. Acute lymphoblastic leukaemia. *Lancet. 2008; 371: 1030-43.*

76. Preston, D.L. *et al.* Cancer incidence in atomic bomb survivors. Part III. Leukemia, lymphoma

and multiple myeloma, 1950-1987. *Radiat. Res. 1994; 137: 68-97.*

77. Doll, R. & Wakeford, R. Risk of childhood cancer from fetal irradiation. *Br. J. Radiol. 1997; 70: 130-9.*

78. Kroll, M.E., Draper, G.J., Stiller, C.A., & Murphy, M.F. Childhood leukemia incidence in Britain, 1974-2000: time trends and possible relation to influenza epidemics. *J. Natl. Cancer Inst. 2006; 98: 417-20.*

79. Hasle, H., Clemmensen, I.H., & Mikkelsen, M. Risks of leukaemia and solid tumours in individuals with Down's syndrome. *Lancet. 2000; 355: 165-9.*

80. Papaemmanuil, E. *et al.* Loci on 7p12. 2, 10q21.2 and 14q11.2 are associated with risk of childhood acute lymphoblastic leukemia. *Nat. Genet. 2009; 41: 1006-10.*

81. Trevino, L.R. *et al.* Germline genomic variants associated with childhood acute lymphoblastic leukemia. *Nat. Genet. 2009; 41: 1001-5.*

82. Sherborne, A.L. *et al.* Variation in CDKN2A at 9p21. 3 influences childhood acute lymphoblastic leukemia risk. *Nat. Genet. 2010; 42: 492-4.*

83. Inaba, H., Greaves, M., & Mullighan, C.G. Acute lymphoblastic leukaemia. *Lancet. 2013; 381: 1943-55.*

84. Greaves, M.F. & Wiemels, J. Origins of chromosome translocations in childhood leukaemia. *Nat. Rev. Cancer. 2003; 3: 639-49.*

85. Greaves, M.F. Aetiology of acute leukaemia. *Lancet. 1997; 349: 344-9.*

86. http: //www. cancer. org/cancer. 2014.

87. Mullighan, C.G. *et al.* BCR-ABL1 lymphoblastic leukaemia is characterized by the deletion of Ikaros. *Nature. 2008; 453: 110-4.*

88. Mullighan, C.G. *et al.* Genome-wide analysis of genetic alterations in acute lymphoblastic leukaemia. *Nature. 2007; 446: 758-64.*

89. Schafer, E.S. & Hunger, S.P. Optimal therapy for acute lymphoblastic leukemia in adolescents and young adults. *Nat. Rev. Clin. Oncol. 2011; 8: 417-24.*

90. Stanulla, M. & Schrappe, M. Treatment of childhood acute lymphoblastic leukemia. *Semin. Hematol. 2009; 46: 52-63.*

91. Inaba, H. & Pui, C.H. Glucocorticoid use in acute lymphoblastic leukaemia. *Lancet Oncol. 2010; 11: 1096-106.*

92. Ravandi, F. *et al.* First report of phase 2 study of dasatinib with hyper-CVAD for the frontline treatment of patients with Philadelphia chromosome-positive (Ph+) acute lymphoblastic leukemia. *Blood. 2010; 116: 2070-7.*

93. Seibel, N.L. *et al.* Early postinduction intensification therapy improves survival for children and adolescents with high-risk acute lymphoblastic leukemia: a report from the Children's Oncology Group. *Blood. 2008; 111: 2548-55.*

94. Mattano, L.A., Jr. *et al.* Effect of alternate-week versus continuous dexamethasone scheduling on the risk of osteonecrosis in paediatric patients with acute lymphoblastic leukaemia: results from the CCG-1961 randomised cohort trial. *Lancet Oncol. 2012; 13: 906-15.*

95. Bhatia, S. *et al.* Nonadherence to oral mercaptopurine and risk of relapse in Hispanic and non-Hispanic white children with acute lymphoblastic leukemia: a report from the children's oncology group. *J. Clin. Oncol. 2012; 30: 2094-101.*

96. Balduzzi, A. *et al.* Chemotherapy versus allogeneic transplantation for very-high-risk childhood acute lymphoblastic leukaemia in first complete remission: comparison by genetic randomisation in an international prospective study. *Lancet. 2005; 366: 635-42.*

97. Hong, D. *et al.* Initiating and cancer-propagating cells in TEL-AML1-associated childhood leukemia. *Science. 2008; 319: 336-9.*

98. Cox, C.V., Diamanti, P., Evely, R.S., Kearns, P.R., & Blair, A. Expression of CD133 on leukemia-initiating cells in childhood ALL. *Blood. 2009; 113: 3287-96.*

99. Le, V.C. *et al.* In childhood acute lymphoblastic leukemia, blasts at different stages of immunophenotypic maturation have stem cell properties. *Cancer Cell. 2008; 14: 47-58.*

100. Jimeno, A. & Hidalgo, M. Multitargeted therapy: can promiscuity be praised in an era of political correctness? *Crit Rev. Oncol. Hematol. 2006; 59: 150-8.*

101. Voltz, E. & Gronemeyer, H. A new era of cancer therapy: cancer cell targeted therapies are coming of age. *Int. J. Biochem. Cell Biol. 2008; 40: 1-8.*

102. Hashida, M., Kawakami, S., & Yamashita, F. Lipid carrier systems for targeted drug and gene delivery. *Chem. Pharm. Bull. 2005; 53: 871-80.*

103. Houghton, P.J. *et al.* Imatinib mesylate is a potent inhibitor of the ABCG2 (BCRP) transporter and reverses resistance to topotecan and SN-38 in vitro. *Cancer Res. 2004; 64: 2333-7.*

104. Ozvegy-Laczka, C. *et al.* High-affinity interaction of tyrosine kinase inhibitors with the ABCG2 multidrug transporter. *Mol. Pharmacol. 2004; 65: 1485-95.*

105. Burger, H. *et al.* Imatinib mesylate (STI571) is a substrate for the breast cancer resistance protein (BCRP)/ABCG2 drug pump. *Blood. 2004; 104: 2940-2.*

106. Gottesman, M.M., Fojo, T., & Bates, S.E. Multidrug resistance in cancer: role of ATP-dependent transporters. *Nat. Rev. Cancer. 2002; 2: 48-58.*

107. Seemann, S., Maurici, D., Olivier, M., Caron de, F.C., & Hainaut, P. The tumor suppressor gene TP53: implications for cancer management and therapy. *Crit Rev. Clin. Lab Sci. 2004; 41: 551-83.*

108. Knutsen, T. *et al.* Cytogenetic and molecular characterization of random chromosomal rearrangements activating the drug resistance gene, MDR1/P-glycoprotein, in drug-selected cell lines and patients with drug refractory ALL. *Genes Chromosomes. Cancer. 1998; 23: 44-54.*

109. Anand, P., Sundaram, C., Jhurani, S., Kunnumakkara, A.B., & Aggarwal, B.B. Curcumin and cancer: an "old-age" disease with an "age-old" solution. *Cancer Lett. 2008; 267: 133-64.*

110. Aggarwal, B.B., Danda, D., Gupta, S., & Gehlot, P. Models for prevention and treatment of cancer: problems vs promises. *Biochem. Pharmacol. 2009; 78: 1083-94.*

111. Petrelli, A. & Giordano, S. From single- to multi-target drugs in cancer therapy: when aspecificity becomes an advantage. *Curr. Med. Chem. 2008; 15: 422-32.*

112. Gertsch, J. Botanical drugs, synergy, and network pharmacology: forth and back to intelligent mixtures. *Planta Med. 2011; 77: 1086-98.*

113. Efferth, T. & Koch, E. Complex interactions between phytochemicals. The multi-target therapeutic concept of phytotherapy. *Curr. Drug Targets. 2011; 12: 122-32.*

114. Fimognari, C. *et al.* Metabolic and toxicological considerations of botanicals in anticancer therapy. *Expert. Opin. Drug Metab Toxicol. 2012; 8: 819-32.*

115. Chen, S.T. *et al.* New therapies from old medicines. *Nat. Biotechnol. 2008; 26: 1077-83.*

116. US Department of Health and Human Services FaDACfDEaR. Guidance for Industry. Botanical Drug Product US Department of Health and Human Services FaDACfDEaR. *2004*.

117. Ichikawa, H., Nakamura, Y., Kashiwada, Y., & Aggarwal, B.B. Anticancer drugs designed by mother nature: ancient drugs but modern targets. *Curr. Pharm. Des. 2007; 13: 3400-16.*

118. Dash, S. & Padhy, S.N. Ethnomedicinal information from the tribals of Orissa state-review. J. *Human Ecology. 2003; 14: 165-227.*

119. Satoskar, R.S., Shah, L.G., Bhatt, K., & Sheth, U.K. Preliminary study of pharmacologic properties of Anantmul (Hemidesmus indicus). *Indian J. Physiol Pharmacol. 1962; 6: 68-76.*

120. Aneja, V., Suthar, A., Verma, S., & Kalkunte, S. Phyto-pharmacology of *Hemidesmus indicus*. *Pharmacog Rev. 2008; 2: 143-150.*

121. Austin, A.A review on Indian Sarsaparilla, *Hemidesmus indicus* (L.) R. Br. *J. Biol. Sci.2008; 8: 1-12.*

122. George, S., Tushar, K. V., Unnikrishnan, K.P., Hasim, K.M., & Balachandran, I. *Hemidesmus indicus* (L.) R. Br. A Review. *J. Plant. Sci. 2008; 3: 146-156.*

123. Nagarajan, S., Mohan Rao, L.J., & Gurudutt, K.N. Chemical composition of the volatiles of *Hemidesmus indicus* R. Br. Flan. *Fragran. 2001; 16: 212-214*.

124. Ananthi, R., Chandra, N., & Santhiya, S.T. Protective effect of Hemidesmus indicus R. Br. root extract against cisplatin-induced cytogenetic damage in mouse bone marrow cells. *Genet. Mol. Biol. 2010; 33: 182-5.*

125. Mandal, S., Das, P.C., Joshi, P.C., Das, A., & Chatterjee, A. Hemidesmine, a new coumarino-lignoid from *Hemidesmus indicus* R. Br. *Indian. J. Chem. 1991;* 30: 712-713.

126. Zhao, Z. *et al.* A condensed phenylpropanoid glucoside and pregnane saponins from the roots of Hemidesmus indicus. *J. Nat. Med. 2013; 67: 137-42.*

127. Das, S. & Bisht, S.S. The bioactive and therapeutic potential of Hemidesmus indicus R. Br. (Indian Sarsaparilla) root. *Phytother. Res. 2013; 27: 791-801.*

128. Das, S. & Devaraj, S.N. Antienterobacterial activity of Hemidesmus indicus R. Br. root extract. *Phytother. Res. 2006; 20: 416-21.*

129. Das, S. & Devaraj, S.N. Glycosides derived from Hemidesmus indicus R. Br. root inhibit adherence of Salmonella typhimurium to host cells: receptor mimicry. *Phytother. Res. 2006; 20: 784-93.*

130. Kotnis, M.S., Patel, P., Menon, S.N., & Sane, R.T. Renoprotective effect of Hemidesmus indicus, a herbal drug used in gentamicin-induced renal toxicity. *Nephrology. 2004; 9: 142-52.*

131. Evans, D.A., Rajasekharan, S., & Subramoniam, A. Enhancement in the absorption of water and electrolytes from rat intestine by Hemidesmus indicus R. Br. root (water extract). *Phytother. Res. 2004; 18: 511-5.*

132. Bezerra, D.P. *et al.* Overview of the therapeutic potential of piplartine (piperlongumine). *Eur. J. Pharm. Sci. 2012; 48: 453-463.*

133. Kumar, S., Kamboj, J., Sharma, S., & Sharma, S. Overview for various aspects of the health benefits of Piper longum linn. fruit. *J. Acupunct. Meridian. Stud. 2011; 4: 134-40.*

134. Adams, D.J. *et al.* Synthesis, cellular evaluation, and mechanism of action of piperlongumine analogs. *Proc. Natl. Acad. Sci. U. S. A. 2012; 109: 15115-20.*

135. Bezerra, D.P. *et al.* Piplartine induces inhibition of leukemia cell proliferation triggering both apoptosis and necrosis pathways. *Toxicol. In Vitro. 2007; 21: 1-8.*

136. Bezerra, D.P. *et al.* Antiproliferative effects of two amides, piperine and piplartine, from Piper species. *Z. Naturforsch. C. 2005; 60: 539-43.*

137. Bokesch, H.R. *et al.* A new hypoxia inducible factor-2 inhibitory pyrrolinone alkaloid from roots and stems of Piper sarmentosum. *Chem. Pharm. Bull. 2011; 59: 1178-9.*

138. Duh, C.Y., Wu, Y.C., & Wang, S.K. Cytotoxic pyridone alkaloids from the leaves of Piper aborescens. *J. Nat. Prod. 1990; 53: 1575-7.*

139. Golovine, K.V. *et al.* Piperlongumine induces rapid depletion of the androgen receptor in human prostate cancer cells. *Prostate. 2013; 73: 23-30.*

140. Jyothi, D. *et al.* Diferuloylmethane augments the cytotoxic effects of piplartine isolated from Piper chaba. *Toxicol. In Vitro. 2009; 23: 1085-91.*

141. Lin, Z., Liao, Y., Venkatasamy, R., Hider, R.C., & Soumyanath, A. Amides from Piper nigrum L. with dissimilar effects on melanocyte proliferation in-vitro. *J. Pharm. Pharmacol. 2007; 59: 529-36.*

142. Raj, L. *et al.* Selective killing of cancer cells by a small molecule targeting the stress response to ROS. *Nature. 2011; 475: 231-4.*

143. Tsai, I.L. *et al.* New cytotoxic cyclobutanoid amides, a new furanoid lignan and anti-platelet aggregation constituents from Piper arborescens. *Planta Med. 2005; 71: 535-42.*

144. Fontenele, J.B. *et al.* Antiplatelet effects of piplartine, an alkamide isolated from Piper tuberculatum: possible involvement of cyclooxygenase blockade and antioxidant activity. *J. Pharm. Pharmacol. 2009; 61: 511-5.*

145. Iwashita, M., Oka, N., Ohkubo, S., Saito, M., & Nakahata, N. Piperlongumine, a constituent of Piper longum L., inhibits rabbit platelet aggregation as a thromboxane A(2) receptor antagonist. *Eur. J. Pharmacol. 2007; 570: 38-42.*

146. Lee, S.E. *et al.* Suppression of ochratoxin biosynthesis by naturally occurring alkaloids. *Food Addit. Contam. 2007; 24: 391-7.*

147. Park, B.S. *et al.* Antiplatelet activities of newly synthesized derivatives of piperlongumine. *Phytother. Res. 2008; 22: 1195-9.*

148. Park, B.S., Son, D.J., Park, Y.H., Kim, T.W., & Lee, S.E. Antiplatelet effects of acidamides isolated from the fruits of Piper longum L. *Phytomedicine. 2007; 14: 853-5.*

149. Son, D.J. *et al.* Piperlongumine inhibits atherosclerotic plaque formation and vascular smooth muscle cell proliferation by suppressing PDGF receptor signaling. *Biochem. Biophys. Res. Commun. 2012; 427: 349-54.*

150. Rao, V.R. *et al.* Synthesis and biological evaluation of new piplartine analogues as potent aldose reductase inhibitors (ARIs). *Eur. J. Med. Chem. 2012; 57: 344-61.*

151. Navickiene, H.M. *et al.* Antifungal amides from Piper hispidum and Piper tuberculatum. *Phytochemistry. 2000; 55: 621-6.*

152. de, M.J., Nascimento, C., Yamaguchi, L.F., Kato, M.J., & Nakano, E. Schistosoma mansoni: in vitro schistosomicidal activity and tegumental alterations induced by piplartine on schistosomula. *Exp. Parasitol. 2012; 132: 222-7.*

153. Moraes, J. *et al.* Schistosoma mansoni: In vitro schistosomicidal activity of piplartine. *Exp. Parasitol. 2011; 127: 357-64.*

154. Lee, S.W. & Mandinova, A. Patent application title: Methods for the treatment of cancer using piperlongumine and piperlongumine Analogs. [WO20090312373.]. *2009.*

155. Bezerra, D.P. *et al.* Evaluation of the genotoxicity of piplartine, an alkamide of Piper tuberculatum, in yeast and mammalian V79 cells. *Mutat. Res. 2008; 652: 164-74.*

156. Bezerra, D.P. *et al.* In vitro and in vivo antitumor effect of 5-FU combined with piplartine and piperine. *J. Appl. Toxicol. 2008; 28: 156-63.*

157. Kong, E.H. *et al.* Piplartine induces caspase-mediated apoptosis in PC-3 human prostate cancer cells. *Oncol. Rep. 2008; 20: 785-92.*

158. Bezerra, D.P. *et al.* Piplartine induces genotoxicity in eukaryotic but not in prokaryotic model systems. *Mutat. Res. 2009; 677: 8-13.*

159. Government of India, M. o. H. &. F. W. D. o. *The Ayurvedic Pharmacopoeia of India. 1989.*

160. Eppert, K. *et al.* Stem cell gene expression programs influence clinical outcome in human leukemia. *Nat. Med. 2011; 17: 1086-93.*

161. Macho, A. *et al.* Calcium ionophoretic and apoptotic effects of ferutinin in the human Jurkat T-cell line. *Biochem. Pharmacol. 2004; 68: 875-83.*

162. Baou, M. *et al.* Role of NOXA and its ubiquitination in proteasome inhibitor-induced apoptosis in chronic lymphocytic leukemia cells. *Haematologica. 2010; 95: 1510-8.*

163. Gores, G.J. & Kaufmann, S.H. Selectively targeting Mcl-1 for the treatment of acute myelogenous leukemia and solid tumors. *Genes Dev. 2012; 26: 305-11.*

164. Chomczynski, P. & Sacchi, N. Single-step method of RNA isolation by acid guanidinium thiocyanate-phenol-chloroform extraction. *Anal. Biochem. 1987; 162: 156-9.*

165. Mueller, O. *et al.* A microfluidic system for high-speed reproducible DNA sizing and quantitation. *Electrophoresis. 2000; 21: 128-34.*

166. Schroeder, A. *et al.* The RIN: an RNA integrity number for assigning integrity values to RNA measurements. *BMC. Mol. Biol. 2006; 7: 3.*

167. Myhre, O., Andersen, J.M., Aarnes, H., & Fonnum, F. Evaluation of the probes 2', 7'-dichlorofluorescin diacetate, luminol, and lucigenin as indicators of reactive species formation. *Biochem. Pharmacol. 2003; 65: 1575-82.*

168. Catino, J.J. & Miceli, L.A. Microtiter assay useful for screening of cell-differentiation agents. *J. Natl. Cancer Inst. 1988; 80: 962-6.*

169. Ahmed, N., Williams, J.F., & Weidemann, M.J. The human promyelocytic HL60 cell line: a model of myeloid cell differentiation using dimethylsulphoxide, phorbol ester and butyrate. *Biochem. Int. 1991; 23: 591-602.*

170. Zhou, J.R., Yu, L., Zhong, Y., & Blackburn, G.L. Soy phytochemicals and tea bioactive components synergistically inhibit androgen-sensitive human prostate tumors in mice. *J. Nutr. 2003; 133: 516-21.*

171. Burattini, S., Battistelli, M., & Falcieri, E. Morpho-functional features of in-vitro cell death induced by physical agents. *Curr. Pharm. Des. 2010; 16: 1376-86.*

172. Yamaguchi, H., Wyckoff, J., & Condeelis, J. Cell migration in tumors. *Curr. Opin. Cell Biol. 2005; 17: 559-64.*

173. Zhao, L., Wientjes, M.G., & Au, J.L. Evaluation of combination chemotherapy: integration of nonlinear regression, curve shift, isobologram, and combination index analyses. *Clin. Cancer Res. 2004; 10: 7994-8004.*

174. Vousden, K.H. & Lane, D.P. p53 in health and disease. *Nat. Rev. Mol. Cell Biol. 2007; 8: 275-83.*

175. Almond, J.B. & Cohen, G.M. The proteasome: a novel target for cancer chemotherapy. *Leukemia. 2002; 16: 433-43.*

176. Cuello, M., Ettenberg, S.A., Nau, M.M., & Lipkowitz, S. Synergistic induction of apoptosis by the combination of trail and chemotherapy in chemoresistant ovarian cancer cells. *Gynecol. Oncol. 2001; 81: 380-90.*

177. Kong, G., Lee, S.J., Kim, H.J., Surh, Y.J., & Kim, N.D. Induction of granulocytic differentiation in acute promyelocytic leukemia cells (HL-60) by 2-(allylthio) pyrazine. *Cancer Lett. 1999; 144: 1-8.*

178. Shapiro, G.I. & Harper, J.W. Anticancer drug targets: cell cycle and checkpoint control. *J. Clin. Invest. 1999; 104: 1645-53.*

179. Toogood, P.L. Progress toward the development of agents to modulate the cell cycle. *Curr. Opin. Chem. Biol. 2002; 6: 472-8.*

180. Borel, F., Lacroix, F.B., & Margolis, R.L. Prolonged arrest of mammalian cells at the G1/S boundary results in permanent S phase stasis. *J. Cell Sci. 2002; 115: 2829-38.*

181. Knudsen, K.E. *et al.* RB-dependent S-phase response to DNA damage. *Mol. Cell Biol. 2000; 20: 7751-63.*

182. Pedeux, R. *et al.* Thymidine dinucleotides induce S phase cell cycle arrest in addition to increased melanogenesis in human melanocytes. *J. Invest Dermatol. 1998; 111: 472-7.*

183. Ogryzko, V.V., Wong, P., & Howard, B.H. WAF1 retards S-phase progression primarily by inhibition of cyclin-dependent kinases. *Mol. Cell Biol. 1997; 17: 4877-82.*

184. Tsang, W.Y., Wang, L., Chen, Z., Sanchez, I., & Dynlacht, B.D. SCAPER, a novel cyclin A-interacting protein that regulates cell cycle progression. *J. Cell Biol. 2007; 178: 621-33.*

185. Geley, S. *et al.* Anaphase-promoting complex/cyclosome-dependent proteolysis of human cyclin A starts at the beginning of mitosis and is not subject to the spindle assembly checkpoint. *J. Cell Biol. 2001; 153: 137-48.*

186. Koff, A. *et al.* Formation and activation of a cyclin E-cdk2 complex during the G1 phase of the human cell cycle. *Science. 1992; 257: 1689-94.*

187. Gartel, A.L. & Radhakrishnan, S.K. Lost in transcription: p21 repression, mechanisms, and consequences. *Cancer Res. 2005; 65: 3980-5.*

188. Radhakrishnan, S.K. *et al.* Constitutive expression of E2F-1 leads to p21-dependent cell

cycle arrest in S phase of the cell cycle. *Oncogene. 2004; 23: 4173-6.*

189. Khan, N., Afaq, F., & Mukhtar, H. Apoptosis by dietary factors: the suicide solution for delaying cancer growth. *Carcinogenesis. 2007; 28: 233-9.*

190. Moncada, S. Mitochondria as pharmacological targets. *Br. J. Pharmacol. 2010; 160: 217-9.*

191. Koh, D.W., Dawson, T.M., & Dawson, V.L. Mediation of cell death by poly(ADP-ribose) polymerase-1. *Pharmacol. Res. 2005; 52: 5-14.*

192. Salvioli, S., Ardizzoni, A., Franceschi, C., & Cossarizza, A. JC-1, but not DiOC6(3) or rhodamine 123, is a reliable fluorescent probe to assess delta psi changes in intact cells: implications for studies on mitochondrial functionality during apoptosis. *Febs Lett. 1997; 411: 77-82.*

193. Armstrong, J.S. The role of the mitochondrial permeability transition in cell death. *Mitochondrion. 2006; 6: 225-34.*

194. Qanungo, S., Das, M., Haldar, S., & Basu, A. Epigallocatechin-3-gallate induces mitochondrial membrane depolarization and caspase-dependent apoptosis in pancreatic cancer cells. *Carcinogenesis. 2005; 26: 958-67.*

195. Crompton, M. The mitochondrial permeability transition pore and its role in cell death. *Biochem. J. 1999; 341: 233-49.*

196. Nicotera, P. & Orrenius, S. The role of calcium in apoptosis. *Cell Calcium. 1998; 23: 173-80.*

197. Choi, J.H., Lee, H.W., Park, H.J., Kim, S.H., & Lee, K.T. Kalopanaxsaponin A induces apoptosis in human leukemia U937 cells through extracellular Ca2+ influx and caspase-8 dependent pathways. *Food Chem. Toxicol. 2008; 46: 3486-92.*

198. Harper, J.L. *et al.* Dihydropyridines as inhibitors of capacitative calcium entry in leukemic HL-60 cells. *Biochem. Pharmacol. 2003; 65: 329-38.*

199. Jiang, N. *et al.* Effects of Ca2+ channel blockers on store-operated Ca2+ channel currents of Kupffer cells after hepatic ischemia/reperfusion injury in rats. *World J. Gastroenterol. 2006; 12: 4694-8.*

200. Hsin, Y.H. *et al.* Effect of aristolochic acid on intracellular calcium concentration and its links with apoptosis in renal tubular cells. *Apoptosis. 2006; 11: 2167-77.*

201. Thastrup, O., Cullen, P.J., Drobak, B.K., Hanley, M.R., & Dawson, A.P. Thapsigargin, a tumor promoter, discharges intracellular Ca2+ stores by specific inhibition of the endoplasmic reticulum Ca2(+)-ATPase. *Proc. Natl. Acad. Sci. U. S. A. 1990; 87: 2466-70.*

202. Tsujimoto, Y., Cossman, J., Jaffe, E., & Croce, C.M. Involvement of the bcl-2 gene in human follicular lymphoma. *Science. 1985; 228: 1440-3.*

203. Vaux, D.L., Cory, S., & Adams, J.M. Bcl-2 gene promotes haemopoietic cell survival and cooperates with c-myc to immortalize pre-B cells. *Nature. 1988; 335: 440-2.*

204. Cheng, E.H. *et al.* BCL-2, BCL-X(L) sequester BH3 domain-only molecules preventing BAX- and BAK-mediated mitochondrial apoptosis. *Mol. Cell. 2001; 8: 705-11.*

205. Zong, W.X., Lindsten, T., Ross, A.J., MacGregor, G.R., & Thompson, C.B. BH3-only proteins that bind pro-survival Bcl-2 family members fail to induce apoptosis in the absence of Bax and Bak. *Genes Dev. 2001; 15: 1481-6.*

206. Adams, J.M. & Cory, S. The Bcl-2 protein family: arbiters of cell survival. *Science. 1998; 281: 1322-6.*

207. Adams, J. The development of proteasome inhibitors as anticancer drugs. *Cancer Cell. 2004; 5: 417-21.*

208. Richardson, P.G., Mitsiades, C., Hideshima, T., & Anderson, K.C. Bortezomib: proteasome inhibition as an effective anticancer therapy. *Annu. Rev. Med. 2006; 57: 33-47.*

209. Cavo, M. Proteasome inhibitor bortezomib for the treatment of multiple myeloma. *Leukemia. 2006; 20: 1341-52.*

210. Opferman, J.T. *et al.* Development and maintenance of B and T lymphocytes requires antiapoptotic MCL-1. *Nature. 2003; 426: 671-6.*

211. Dzhagalov, I., Dunkle, A., & He, Y.W. The anti-apoptotic Bcl-2 family member Mcl-1 promotes T lymphocyte survival at multiple stages. *J. Immunol. 2008; 181: 521-8.*

212. Opferman, J.T. *et al.* Obligate role of anti-apoptotic MCL-1 in the survival of hematopoietic stem cells. *Science. 2005; 307: 1101-4.*

213. Dzhagalov, I., St, J.A., & He, Y.W. The antiapoptotic protein Mcl-1 is essential for the survival of neutrophils but not macrophages. *Blood. 2007; 109: 1620-6.*

214. Steimer, D.A. *et al.* Selective roles for antiapoptotic MCL-1 during granulocyte development and macrophage effector function. *Blood. 2009; 113: 2805-15.*

215. Arbour, N. *et al.* Mcl-1 is a key regulator of apoptosis during CNS development and after DNA damage. *J. Neurosci. 2008; 28: 6068-78.*

216. Rinkenberger, J.L., Horning, S., Klocke, B., Roth, K., & Korsmeyer, S.J. Mcl-1 deficiency results in peri-implantation embryonic lethality. *Genes Dev. 2000; 14: 23-7.*

217. Beroukhim, R. *et al.* The landscape of somatic copy-number alteration across human cancers. *Nature. 2010; 463: 899-905.*

218. Hussain, S.R. *et al.* Mcl-1 is a relevant therapeutic target in acute and chronic lymphoid malignancies: down-regulation enhances rituximab-mediated apoptosis and complement-dependent cytotoxicity. *Clin. Cancer Res. 2007; 13: 2144-50.*

219. Minagawa, N. *et al.* The anti-apoptotic protein Mcl-1 inhibits mitochondrial Ca2+ signals. *J. Biol. Chem. 2005; 280: 33637-44.*

220. Perciavalle, R.M. *et al.* Anti-apoptotic MCL-1 localizes to the mitochondrial matrix and couples mitochondrial fusion to respiration. *Nat. Cell Biol. 2012; 14: 575-83.*

221. Moulding, D.A. *et al.* Apoptosis is rapidly triggered by antisense depletion of MCL-1 in differentiating U937 cells. *Blood. 2000; 96: 1756-63.*

222. Opferman, J.T. *et al.* Obligate role of anti-apoptotic MCL-1 in the survival of hematopoietic stem cells. *Science. 2005; 307: 1101-4.*

223. Opferman, J.T. *et al.* Development and maintenance of B and T lymphocytes requires antiapoptotic MCL-1. *Nature. 2003; 426: 671-6.*

224. Quinn, B.A. *et al.* Targeting Mcl-1 for the therapy of cancer. *Expert. Opin. Investig. Drugs. 2011; 20: 1397-411.*

225. Weng, C., Li, Y., Xu, D., Shi, Y., & Tang, H. Specific cleavage of Mcl-1 by caspase-3 in tumor necrosis factor-related apoptosis-inducing ligand (TRAIL)-induced apoptosis in Jurkat leukemia T cells. *J. Biol. Chem. 2005; 280: 10491-500.*

226. Clohessy, J.G., Zhuang, J., & Brady, H.J. Characterisation of Mcl-1 cleavage during apoptosis of haematopoietic cells. *Br. J. Haematol. 2004; 125: 655-65.*

227. Herrant, M. *et al.* Cleavage of Mcl-1 by caspases impaired its ability to counteract Bim-induced apoptosis. *Oncogene. 2004; 23: 7863-73.*

228. Michels, J. *et al.* Mcl-1 is required for Akata6 B-lymphoma cell survival and is converted to a cell death molecule by efficient caspase-mediated cleavage. *Oncogene. 2004; 23: 4818-27.*

229. Warr, M.R. *et al.* BH3-ligand regulates access of MCL-1 to its E3 ligase. *FEBS Lett. 2005; 579: 5603-8.*

230. Zhong, Q., Gao, W., Du, F., & Wang, X. Mule/ARF-BP1, a BH3-only E3 ubiquitin ligase, catalyzes the polyubiquitination of Mcl-1 and regulates apoptosis. *Cell. 2005; 121: 1085-95.*

231. Willis, S.N. *et al.* Proapoptotic Bak is sequestered by Mcl-1 and Bcl-xL, but not Bcl-2, until displaced by BH3-only proteins. *Genes Dev. 2005; 19: 1294-305.*

232. Craxton, A. *et al.* NOXA, a sensor of proteasome integrity, is degraded by 26S proteasomes by an ubiquitin-independent pathway that is blocked by MCL-1. *Cell Death. Differ. 2012; 19: 1424-34.*

233. Lowman, X.H. *et al.* The proapoptotic function of Noxa in human leukemia cells is regulated by the kinase Cdk5 and by glucose. *Mol. Cell. 2010; 40: 823-33.*

234. Alves, N.L. *et al.* The Noxa/Mcl-1 axis regulates susceptibility to apoptosis under glucose limitation in dividing T cells. *Immunity. 2006; 24: 703-16.*

235. Mei, Y. *et al.* Noxa/Mcl-1 balance regulates susceptibility of cells to camptothecin-induced apoptosis. *Neoplasia. 2007; 9: 871-81.*

236. Collado, M. & Serrano, M. Senescence in tumours: evidence from mice and humans. *Nat. Rev. Cancer. 2010; 10: 51-7.*

237. Beausejour, C.M. *et al.* Reversal of human cellular senescence: roles of the p53 and p16 pathways. *Embo J. 2003; 22: 4212-22.*

238. Bolesta, E. *et al.* Inhibition of Mcl-1 promotes senescence in cancer cells: implications for preventing tumor growth and chemotherapy resistance. *Mol. Cell Biol. 2012; 32: 1879-92.*

239. Simon, H.U., Haj-Yehia, A., & Levi-Schaffer, F. Role of reactive oxygen species (ROS) in apoptosis induction. *Apoptosis. 2000; 5: 415-8.*

240. Passos, J.F. *et al.* Feedback between p21 and reactive oxygen production is necessary for cell senescence. *Mol. Syst. Biol. 2010; 6: 347.*

241. Weyemi, U. *et al.* ROS-generating NADPH oxidase NOX4 is a critical mediator in oncogenic H-Ras-induced DNA damage and subsequent senescence. *Oncogene. 2012; 31: 1117-29.*

242. Levi, F. *et al.* Implications of circadian clocks for the rhythmic delivery of cancer therapeutics. *Adv. Drug Deliv. Rev. 2007; 59: 1015-35.*

243. Nowak, D., Stewart, D., & Koeffler, H.P. Differentiation therapy of leukemia: 3 decades of development. *Blood. 2009; 113: 3655-65.*

244. Mi, J. Q., Li, J. M., Shen, Z.X., Chen, S.J., & Chen, Z. How to manage acute promyelocytic leukemia. *Leukemia. 2012; 26: 1743-51.*

245. Ablain, J. & de, T.H. Revisiting the differentiation paradigm in acute promyelocytic leukemia. *Blood. 2011; 117: 5795-802.*

246. Birnie, G.D. The HL60 cell line: a model system for studying human myeloid cell differentiation. *Br. J. Cancer Suppl. 1988; 9: 41-5.*

247. Otake, Y., Sengupta, T.K., Bandyopadhyay, S., Spicer, E.K., & Fernandes, D.J. Retinoid-induced apoptosis in HL-60 cells is associated with nucleolin down-regulation and destabilization of Bcl-2 mRNA. *Mol. Pharmacol. 2005; 67: 319-26.*

248. Lawson, N.D. & Berliner, N. Neutrophil maturation and the role of retinoic acid. *Exp. Hematol. 1999; 27: 1355-67.*

249. Wang, J.G. *et al.* Retinoic acid induces leukemia cell G1 arrest and transition into differentiation by inhibiting cyclin-dependent kinase-activating kinase binding and phosphorylation of PML/RARalpha. *Faseb J. 2006; 20: 2142-4.*

250. Jiang, G., Albihn, A., Tang, T., Tian, Z., & Henriksson, M. Role of Myc in differentiation and apoptosis in HL60 cells after exposure to arsenic trioxide or all-trans retinoic acid. *Leuk. Res. 2008; 32: 297-307.*

251. Folkman, J. Angiogenesis in cancer, vascular, rheumatoid and other disease. *Nat. Med. 1995; 1: 27-31.*

252. Parangi, S. *et al.* Antiangiogenic therapy of transgenic mice impairs de novo tumor growth. *Proc. Natl. Acad. Sci. U. S. A. 1996; 93: 2002-7.*

253. Hanahan, D. & Weinberg, R.A. Hallmarks of cancer: the next generation. *Cell. 2011; 144: 646-74.*

254. Johnsson, A. *et al.* A randomized phase III trial on maintenance treatment with bevacizumab alone or in combination with erlotinib after chemotherapy and bevacizumab in metastatic colorectal cancer: the Nordic ACT Trial. *Ann. Oncol. 2013; 24: 2335-41.*

255. Cesca, M., Bizzaro, F., Zucchetti, M., & Giavazzi, R. Tumor Delivery of Chemotherapy Combined with Inhibitors of Angiogenesis and Vascular Targeting Agents. *Front Oncol. 2013; 3: 259.*

256. Jain, R.K. Normalization of tumor vasculature: an emerging concept in antiangiogenic therapy. *Science. 2005; 307: 58-62.*

257. Semenza, G.L. Hypoxia-inducible factors: mediators of cancer progression and targets for cancer therapy. *Trends Pharmacol. Sci. 2012; 33: 207-14.*

258. Balbay, M.D. *et al.* Highly metastatic human prostate cancer growing within the prostate of athymic mice overexpresses vascular endothelial growth factor. *Clin. Cancer Res. 1999; 5: 783-9.*

259. Foekens, J.A. *et al.* High tumor levels of vascular endothelial growth factor predict poor response to systemic therapy in advanced breast cancer. *Cancer Res. 2001; 61: 5407-14.*

260. Li, W.W., Hutnik, M., & Gehr, G. Antiangiogenesis in haematological malignancies. *Br. J. Haematol. 2008; 143: 622-31.*

261. Dias, S., Shmelkov, S.V., Lam, G., & Rafii, S. VEGF(165) promotes survival of leukemic cells by Hsp90-mediated induction of Bcl-2 expression and apoptosis inhibition. *Blood. 2002; 99: 2532-40.*

262. Mayerhofer, M., Valent, P., Sperr, W.R., Griffin, J.D., & Sillaber, C. BCR/ABL induces expression of vascular endothelial growth factor and its transcriptional activator, hypoxia inducible factor-1alpha, through a pathway involving phosphoinositide 3-kinase and the mammalian target of rapamycin. *Blood. 2002; 100: 3767-75.*

263. He, R. *et al.* Inhibition of K562 leukemia angiogenesis and growth by expression of antisense vascular endothelial growth factor (VEGF) sequence. *Cancer Gene Ther. 2003; 10: 879-86.*

264. Madlambayan, G.J. *et al.* Leukemia regression by vascular disruption and antiangiogenic therapy. *Blood. 2010; 116: 1539-47.*

265. Karp, J.E. *et al.* Targeting vascular endothelial growth factor for relapsed and refractory adult acute myelogenous leukemias: therapy with sequential 1-beta-d-arabinofuranosylcytosine, mitoxantrone, and bevacizumab. *Clin. Cancer Res. 2004; 10: 3577-85.*

266. Rodriguez-Ariza, A., Lopez-Pedrera, C., Aranda, E., & Barbarroja, N. VEGF targeted therapy in acute myeloid leukemia. *Crit Rev. Oncol. Hematol. 2011; 80: 241-56.*

267. Kopp, H.G., Avecilla, S.T., Hooper, A.T., & Rafii, S. The bone marrow vascular niche: home of HSC differentiation and mobilization. *Physiology. 2005; 20: 349-56.*

268. Staton, C.A. *et al.* Current methods for assaying angiogenesis in vitro and in vivo. *Int. J. Exp. Pathol. 2004; 85: 233-48.*

269. Browne, C.D., Hindmarsh, E.J., & Smith, J.W. Inhibition of endothelial cell proliferation and angiogenesis by orlistat, a fatty acid synthase inhibitor. *Faseb J. 2006; 20: 2027-35.*

270. Shweiki, D., Itin, A., Soffer, D., & Keshet, E. Vascular endothelial growth factor induced by hypoxia may mediate hypoxia-initiated angiogenesis. *Nature. 1992; 359: 843-5.*

271. Semenza, G.L. Targeting HIF-1 for cancer therapy. *Nat. Rev. Cancer. 2003; 3: 721-32.*

272. Jung, M.H., Lee, S.H., Ahn, E.M., & Lee, Y.M. Decursin and decursinol angelate inhibit VEGF-induced angiogenesis via suppression of the

VEGFR-2-signaling pathway. *Carcinogenesis. 2009; 30: 655-61.*

273. Nishida, N., Yano, H., Nishida, T., Kamura, T., & Kojiro, M. Angiogenesis in cancer. *Vasc. Health Risk Manag. 2006; 2: 213-9.*

274. Cree, I.A. Chemosensitivity and chemoresistance testing in ovarian cancer. *Curr. Opin. Obstet. Gynecol. 2009; 21: 39-43.*

275. Nagourney, R.A. Ex vivo programmed cell death and the prediction of response to chemotherapy. *Curr. Treat. Options. Oncol. 2006; 7: 103-10.*

276. Nygren, P. & Larsson, R. Predictive tests for individualization of pharmacological cancer treatment. *Expert. Opin. Med. Diagn. 2008; 2: 349-60.*

277. Meshinchi, S. & Appelbaum, F.R. Structural and functional alterations of FLT3 in acute myeloid leukemia. *Clin. Cancer Res. 2009; 15: 4263-9.*

278. Zhang, H. *et al.* Preferential eradication of acute myelogenous leukemia stem cells by fenretinide. *Proc. Natl. Acad. Sci. U. S. A. 2013; 110: 5606-11.*

279. Gohring, G. *et al.* Complex karyotype newly defined: the strongest prognostic factor in advanced childhood myelodysplastic syndrome. *Blood. 2010; 116: 3766-9.*

280. de Kok, T.M., van Breda, S.G., & Manson, M.M. Mechanisms of combined action of different chemopreventive dietary compounds: a review. *Eur. J. Nutr. 2008; 47: 51-9.*

281. Williams, S.N. *et al.* Comparative studies on the effects of green tea extracts and individual tea catechins on human CYP1A gene expression. *Chem. Biol. Interact. 2000; 128: 211-29.*